



Dissertation submitted to the University of Hamburg

The Role of Centrosomal Microtubules in F-actin Dynamics during Neuronal Polarization

By Bing Zhao, born in Baoding, China

Group of Neuronal development, Center for Molecular neurobiology (ZMNH) at University
Medical Center Hamburg-Eppendorf

&

Department of Chemistry, Faculty of Mathematics, Informatics and Natural Sciences,
University of Hamburg

Hamburg 2017

Thesis evaluators:

Prof. Dr. Wolfram Brune

Prof. Dr. Matthias Kneussel

Date of disputation: 1st Sep., 2017

The work involved in this dissertation is mainly conducted in the Center for molecular neurobiology (ZMNH) under the supervision of Dr. Froylan Calderón de Anda from 12.2013 to 01.2017.

Dedicated to my fiancée Bin and my parents

Contents

1. Abstract	1
2. Zusammenfassung	3
3. Introduction	5
3.1 Neuronal polarity.....	5
3.1.1 Axon and dendrite differentiation <i>in vivo</i>	5
3.1.1.1 Retinal bipolar cells and ganglion cells	7
3.1.1.2 Cerebellar granule cell	7
3.1.1.3 Cortical pyramidal cell	8
3.1.2 Neuronal polarization <i>in vitro</i>	8
3.1.2.1 Hippocampal neuron culture	8
3.1.2.2 Cerebellar granule neuron <i>in vitro</i>	9
3.2 Growth cone structure and function	10
3.2.1 Structure	10
3.2.2 Function	12
3.3 Role of cytoskeleton in neuronal polarization	13
3.3.1 Basics of the two cytoskeletal components	13
3.3.1.1 Dynamics of actin.....	13
3.3.1.2 Dynamics of microtubule.....	14
3.3.2 MT and actin in axon fate decision	16
3.3.2.1 The role of actin	16
3.3.2.2 The role of MT	17
3.4 Centrosome in neuronal polarization	21
3.4.1 Centrosome as MT organizing center.....	21
3.4.2 Centrosome & axon specification	23
3.5 MT-actin interaction	25
3.5.1 Direct protein crosslinker	25
3.5.2 +TIP-associated interaction	26

Contents

3.5.3	Interaction mediated by motor proteins	28
3.6	Drebrin-mediated MT and F-actin interaction	29
3.6.1	Drebrin	29
3.6.2	EB3	31
3.6.3	Drebrin and EB3 link MT and F-actin.....	31
4.	Aim of the work	33
5.	Results	35
5.1.	LifeAct labeling unveils F-actin dynamic puncta structure in neuronal soma.....	35
5.2.	Actin dots preferentially behave over centrosome	38
5.3.	Super resolution microscopy exposes fine actin puncta structure surrounding centrosome	39
5.4.	Centrosome inactivation leads to puncta distribution alteration and overall actin dynamic change.....	40
5.5.	Acute centrosome inactivation alters MT organization	43
5.6.	Global MT disruption severely undermine actin dynamics.....	45
5.7.	MT stabilization favors F-actin dynamics	47
5.8.	The MT and F-actin linker drebrin E is actively involved in overall actin dynamics..	49
5.9.	Enriched drebrin leads the path of axon extension.....	53
5.10.	Disruption of MT-actin interaction impairs actin dynamics	54
5.11.	Breaking of MT-actin interaction stalls growth cone formation	60
6.	Discussion.....	63
6.1	Somatic dots, the presence form of dynamic F-actin in neuronal cell body.....	64
6.2	F-actin dots are distributed preferentially around centrosome	66
6.3	Centrosomal MT is involved in neuronal F-actin dynamics.....	66
6.4	Centrosomal MT instructs global F-actin dynamics	67
6.4.1	Role of centrosomal MT on peripheral actin dynamics	67
6.4.2	Modulation of centrosomal MT on somatic actin dynamics	69
6.5	Drebrin-dependent MT-actin interaction is essential for normal F-actin dynamics ..	70

6.6	Drebrin-mediated MT-dependent actin dynamics is essential for neuronal polarization	72
6.7	Concluding remarks	73
7.	Materials and Methods	75
7.1	Materials	75
7.1.1	Plasmids	75
7.1.2	Staining reagents.....	75
7.1.3	Culture reagents	76
7.1.4	Chemicals	76
7.1.5	MEM-HS formula	77
7.1.6	Kit.....	77
7.2	Methods	77
7.2.1	Pre-treatment of coverslips or culture chambers	77
7.2.2	Poly-L-lysine or Poly-D-lysine coating	78
7.2.3	Primary hippocampi neurons preparation.....	78
7.2.4	Hippocampi neuronal transfections	79
7.2.5	Pharmacological treatments	79
7.2.6	Immunocytochemistry.....	80
7.2.7	Epi-fluorescence imaging	80
7.2.8	Chromophore-assisted light inactivation of Centrosome	81
7.2.9	STED microscopy	81
7.2.10	Analysis of somatic F-actin dots distribution.....	82
7.2.11	Analysis of blinking duration and total number of somatic F-actin dots.....	82
7.2.12	Analysis of F-actin retrograde flow in growth cones	83
7.2.13	EB3 comets quantifications	83
7.2.14	Drebrin fluorescence intensity measurement in the growth cones	84
7.2.15	Neurite and growth cone number quantifications	85
7.2.16	Image processing	85
7.2.17	Statistical analysis	85

Contents

8. References.....87

9. Appendix.....105

 9.1 Abbreviation List 105

 9.2 List of hazardous substances 108

 9.3 List of publications 109

Acknowledgement.....111

Declaration on oath.....113

1. Abstract

Neurons are a highly polarized cell type, with morphologically and functionally distinct cellular compartments: axon and dendrites, which endow neurons the ability of integrating and transmitting information in the brain. Neurites, the precursor of dendrites and the axon, exhibit relatively uniform morphology until one of them elongates preferentially more than the others and acquires the axonal identity. This process is referred to as neuronal polarization. Both actin and microtubule (MT) cytoskeleton have been shown to play an indispensable role in axon formation. However, whether a functional interplay exists between microtubules and actin dynamics in growing axons and whether this is instrumental to neuronal polarization remain elusive.

In the present study, I first characterized the actin dynamics in developing neurons during the time of axon formation. The growth cone is a cellular domain present at the neurite tip and is enriched with dynamic actin. Actin dynamics in growth cones has long been studied. Here I also found that in the neuronal soma, actin is present as puncta, which appear and disappear with different lifetimes, suggesting a very dynamical organization of somatic actin. Analysis of actin dot distribution and ultrastructural imaging reveal that these dots preferentially distribute near the centrosome, the MT organization center. Pharmacological manipulations of MT unveil a negative correlation between MT and actin dynamics, suggesting that MT modulate actin dynamics and a functional crosstalk exists between these two.

Next I also studied the role of drebrin, a known MT-actin crosslinker together with MT plus end binding protein EB3. Drebrin is found to be strongly correlated with actin dynamics and involved in axon elongation. Disruption of the interaction between MT and actin via mutated drebrin and truncated EB3 leads to the attenuated actin dynamics and impaired growth cone formation. Previous studies have shown that actin dynamics in the growth cone is crucial for

Abstract

axon formation; therefore my data highlights the essentiality of drebrin-and-EB3-mediated interaction in axon development.

Taken together I have shown that MTs instruct global actin dynamics via drebrin and EB3 and this instruction is critical for neuronal polarization.

2. Zusammenfassung

Neuronen sind hochpolarisierte Zellen mit morphologisch und funktionell distinkten Bereichen, dem Axon und den Dendriten. Diese verleihen den Neuronen die Fähigkeit zur Integration und Übertragung von Informationen im Gehirn. Neuriten, die Vorläufer der Dendriten und des Axons, zeigen zunächst eine relativ einheitliche Morphologie, bis sich einer von ihnen verlängert und seine axonale Identität erhält. Dieser Vorgang wird als neuronale Polarisation bezeichnet. Sowohl das Aktin- als auch das Mikrotubuli (MT)-Zytoskelett spielen eine unentbehrliche Rolle bei der Axonbildung. Jedoch, ob ein funktionelles Zusammenspiel zwischen Mikrotubuli und Aktindynamik in auswachsenden Axonen besteht und ob dies an der neuronalen Polarisation maßgeblich beteiligt ist, bleibt unklar.

In der vorliegenden Studie habe ich zuerst die Aktin-Dynamik während der Entwicklung von Neuronen in der Zeit der Axonbildung charakterisiert. Der Wachstumskegel ist eine zelluläre Domäne an der Spitze der Neuriten, die mit dynamischem Aktin angereichert ist. Die Aktin-Dynamik in Wachstumskegeln wurde seit langem untersucht. Mit dieser Studie konnte ich zeigen, dass im neuronalen Soma Aktin als punktförmige Struktur vorliegt und dass diese eine sehr variable Lebensdauer haben: Die Aktinpunkte erscheinen und verschwinden, was auf eine sehr dynamische Organisation des somatischen Aktins hindeutet. Die Analyse der Verteilung der Aktinpunkte und die ultrastrukturellen Bildanalysen zeigen, dass sich diese Aktinpunkte vorzugsweise in der Nähe des Zentrosoms, dem MT-Organisationszentrum, aufhalten. Pharmakologische Manipulation der MT enthüllen eine negative Korrelation zwischen MT- und Aktin-Dynamik, was darauf hindeutet, dass MT die Aktin-Dynamik modulieren und dass ein funktionelles Zusammenspiel zwischen diesen beiden besteht.

Als nächstes habe ich die Rolle von Drebrin, einem bekannten MT-Aktin-Vernetzer, zusammen mit dem MT Plus-Ende-bindenden Protein EB3 untersucht. Drebrin korreliert stark mit der Aktin-Dynamik und ist an der Axon-Verlängerung beteiligt. Eine Störung der

Zusammenfassung

Wechselwirkung zwischen MT und Actin mittels mutiertem Drebrin oder verkürztem EB3 führt zu einer verstärkten Aktin-Dynamik und einer eingeschränkten Bildung der Wachstumskegel. Frühere Studien haben gezeigt, dass die Aktin-Dynamik im Wachstumskegel für die Ausbildung des Axons entscheidend ist. Meine Ergebnisse unterstreichen die Bedeutung der Drebrin-und-EB3-vermittelten Interaktion während der Axonentwicklung.

Zusammen genommen konnte ich zeigen, dass MTs die globale Aktin-Dynamik mittels Drebrin und EB3 regulieren und diese Direktive für die neuronale Polarisierung kritisch ist.

3. Introduction

3.1 Neuronal polarity

“Neurons exhibit a fundamental polarity, independent of physiological considerations concerning information flow, and suggest that this organization may be largely governed by an endogenous program of development.” Quote from (Craig and Banker, 1994)

Neurons display highly polarized properties, morphologically and functionally, which lies in the differentiation between the axon and dendrite. With the differentiation of these two cellular compartments, neurons are capable of wiring and forming a sophisticated network, which is fundamental for the brain function (da Silva and Dotti, 2002; Namba, Funahashi et al., 2015). The differentiation of axon and dendrite is also referred to as neuronal polarization, the process of breaking symmetry in the postmitotic cell to establish the inherent asymmetry characterized by the specification of the axonal and somatodendritic compartments (Dotti, Sullivan et al., 1988).

3.1.1 Axon and dendrite differentiation *in vivo*

So far several neuron types have been investigated in the *in vivo* context. They share some common properties (Barnes and Polleux, 2009): 1) Right after cell division, cells undergo migration; 2) Cells acquire polarity during migration; 3) Cells are in a bipolar shape when polarization occurs. However, distinction also exists, mainly residing in whether cells undergo a multipolar (MP) phase or whether postmitotic neurons inherit the apical-basal polarity from the neuroepithelia, which leads to the classification of two modes: “inheritance of polarity” and “establishment of polarity” (Namba, Funahashi et al., 2015). Retinal bipolar cell and ganglion cell are good examples of ‘inheritance of polarity’ while cerebellar granular cell and cortical pyramidal cell exemplify the mode of ‘establishment of polarity’ (Namba, Funahashi et al., 2015).

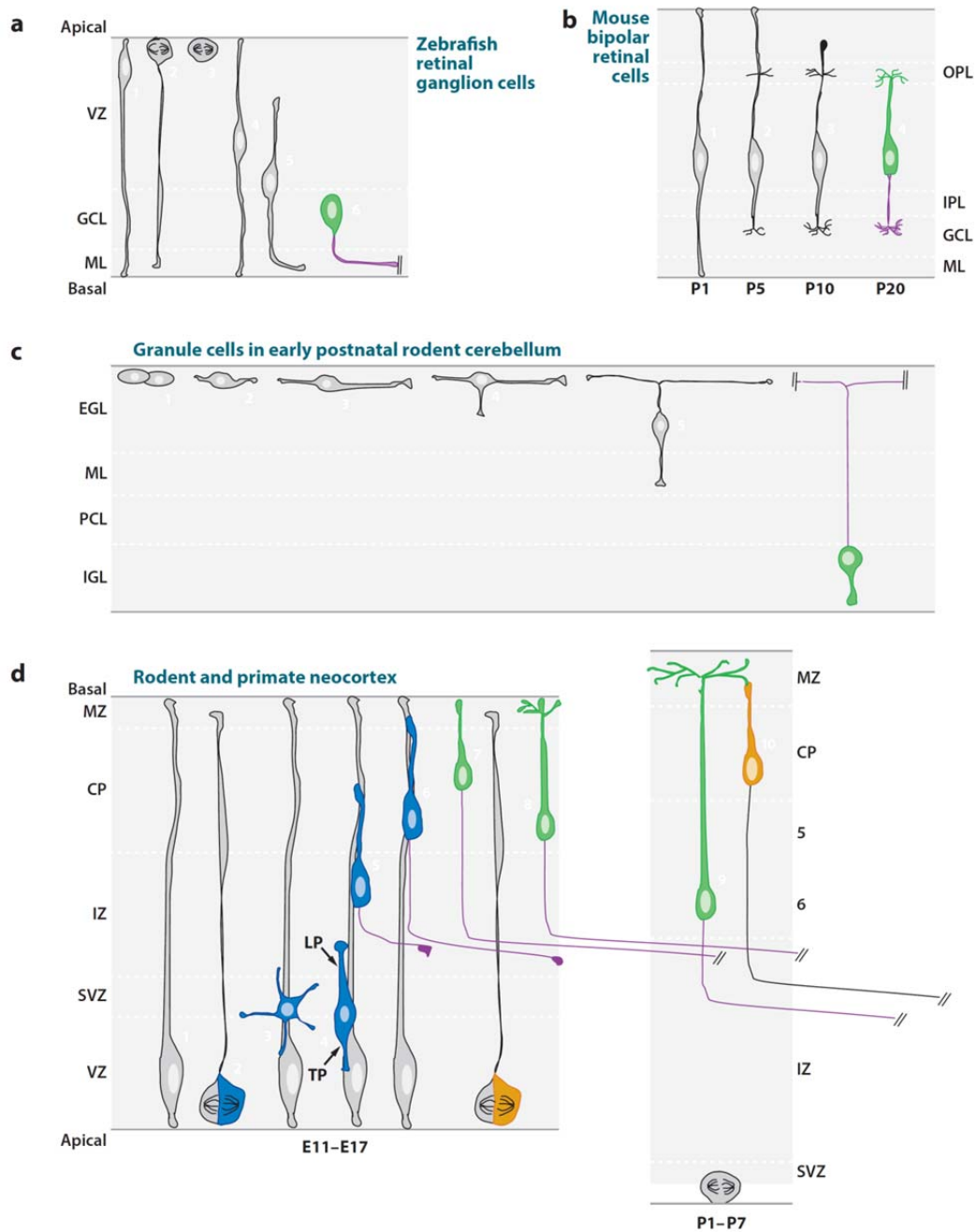


Fig. 3.1 the schematic polarizing models *in vivo*. Nascent axons are depicted in purple and dendritsoma in green. **a)** RGC precursor translocates its soma along the process which initially spans from OLM to ILM. The upper process then retracts and the lower process elongates first towards and afterwards along the basal membrane turning into the axon. **b)** RBC undergoes somal translocation towards OLM along the process which contacts both OLM and IPL. After losing apical and basal attachment, the apical process starts to develop dendritic arbor in OPL and basal process form axonal arbor in IPL. **c)**

CGC undergoes two phases of migration. First the cell migrates tangentially in the EGL and approach the ML. At the interface of EGL and ML, the cell starts to migrate orthogonally and a basal process forms. The apical process eventually develops into the axon with two end branches. **d)** During migration cortical PC extends a leading process and a trailing process which turn into the apical dendrite and axon respectively. Some RGCs (in yellow) translocate to the cortical plate and initiates basal processes which turns into axons in the end. (Barnes and Polleux, 2009) with slight modifications.

3.1.1.1 Retinal bipolar cells and ganglion cells

In developing mouse retina, rod and ON cone bipolar cells extend apical (leading) process up to outer limiting membrane (OLM) and basal (trailing) process down to either inner plexiform layer (IPL) or inner limiting membrane (ILM) during migration (Fig 3.1b). Eventually the apical processes develop into the dendrites and basal processes into the axons (Morgan, Dhingra et al., 2006).

Shortly after the last division, Retinal ganglion cells translocate their somas along basal processes towards the inner limiting membrane and meanwhile undergo the apical retraction (Fig 3.1a). The process that emerges from the basal pole of RGC becomes the axon (Zolessi, Poggi et al., 2006).

3.1.1.2 Cerebellar granule cell

Cerebellar granule cells undergo a two-phase migration, during which polarity is achieved (Fig 3.1c). In the first phase, granule cell progenitors initiate two horizontal processes in the deeper plane parallel to pia surface in the external granular layer (EGL) and migrate tangentially, simultaneously descending towards the molecular layer (ML). Upon arriving at the EGL-ML border, cells reorient their somas vertically towards ML and start to migrate radially along the radial fiber of Bergmann glia (Komuro, Yacubova et al., 2001; Komuro and Yacubova, 2003). The two horizontal processes become the parallel fibers, which are the two end branches of the axon. From the opposite pole descends a migratory process. The axon

Introduction

elongates during radial migration. Finally the cell arrives in the internal granular layer (IGL) and extends several dendrites (Gao and Hatten, 1993).

3.1.1.3 Cortical pyramidal cell

After the last cell division, the daughter neuron starts to migrate from the ventricular zone (VZ) towards the cortical plate (CP) along the radial fiber of the radial glial cell (RGC). After a standby in the intermediate zone (IZ), where the neuron displays a multipolar morphology, it reverses the migration direction and locomotes until contacting the VZ. During this retrograde period, the cell initiates a process pointing to the ventricle, which elongates as the trailing process during recommenced migration towards CP, while from the opposite extends the leading process (Noctor, Martinez-Cerdeno et al., 2004) (Fig 3.1d). The trailing process then develops into the future axon and the leading process into the apical dendrite (Shoukimas and Hinds, 1978).

3.1.2 Neuronal polarization *in vitro*

Dissociated embryonic neuron culture possesses advantages like easy accessibility, well control of the growth environment and excellent visibility of cells in live state et al, making it the choice for many studies of neuronal polarity (Craig and Banker, 1994). In mammal neuronal culture, rat/mouse hippocampal and cortical neurons are the most frequently-used. Besides, a certain amount of studies are also reported in cerebellar granule cells.

3.1.2.1 Hippocampal neuron culture

Hippocampi from E18 (embryonic day) rat embryos are dissociated into single cells. The developing time from being plated to full maturity has been divided into five stages, each of which is characterized by a distinct neuronal morphology. After attaching to the surface of the culture ware, neurons display a round shape surrounded by lamellipodia and filopodia, which characterizes the first stage. At the second stage, the cell extends several neurites, one of which exceeds other peer neurites and elongates as future axon at the third stage. At the

fourth stage, the rest of neurites develop into dendrites and set out to branching. At the fifth stage follows the further dendritic and axonal branching as well as dendritic spinogenesis (Fig. 3.2) (Dotti, Sullivan et al., 1988).

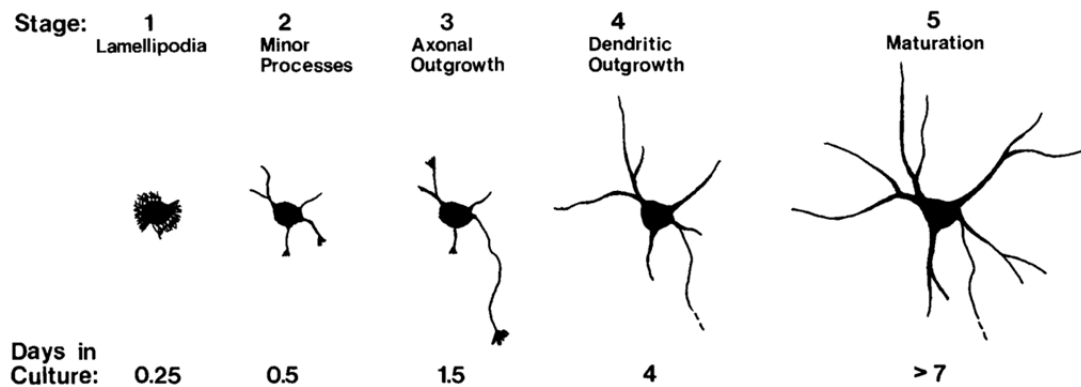


Fig. 3.2 Stages of development of hippocampal neurons in culture. At stage 1, after attaching to the substratum the neuron soma appears round and displays active protrusion of lamellipodia and filopodia. At stage 2, neurons extend several neurites exhibiting a multipolar (MP) morphology. One of the neurites elongates more rapidly than the other and eventually becomes the axon at stage 3. Stage 4 is the period when the rest of neurites acquire the dendritic identity. At stage 5 the neuron develops further and matures, which is characterized with dendritic spine formation and synaptic connection with other neurons. Scheme is from (Dotti, Sullivan et al., 1988)

3.1.2.2 Cerebellar granule neuron *in vitro*

Granule cells prepared from P6 (postnatal day) mouse cerebellum highly resemble the developmental process *in situ*. A five-staged *in vitro* developmental model is also proposed. A lamellipodium-like structure is exhibited around the soma after the cell attached to the substratum. At stage II, a process sprouts from the cell body, characterizing a unipolar shape. The following is that from the opposite pole the cell extends another process, entering the bipolar stage. One of the processes then forms a “Y” branch and develops into the axon. At stage V, the MP stage, several short neurites sprout from the cell body, which turn into future dendrites (Fig 3.3) (Powell, Rivas et al., 1997).

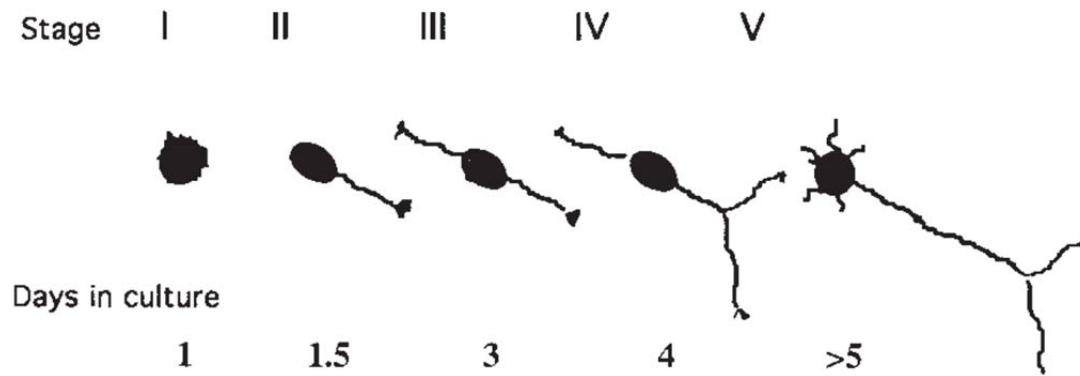


Fig. 3.3 Summary of granule cell morphogenesis *in vitro*. Stage I, the apolar stage, neuron displays a morphology similar to that of stage 1 hippocampal neuron. Stage II, the unipolar stage, one process arises. Stage III, the bipolar stage, symmetrically another process sprouts from the opposite pole. Stage IV, one of the neurites acquires a branch, which makes the prototype of T-shaped axon. Stage V, several neurites form around the soma, designating the MP stage (Powell, Rivas et al., 1997).

3.2 Growth cone structure and function

The growth cone is the pioneering domain of the extending axon, which plays a fundamental role in axon elongation and pathfinding to reach its appropriate target (Cammarata, Bearce et al., 2016).

3.2.1 Structure

Based on the cytoskeletal organization, the whole region of growth cone can be divided into three parts: the central (C) domain, the transitional (T) zone and the peripheral (P) domain (Dent and Gertler, 2003) (Fig. 3.4). The central domain comprises the bundled MT arrays flooding from the axon shaft into the distal area, along with various organelles (such as mitochondria, Golgi and so on), vesicles as well as actin bundles. Following the C domain is the T zone, serving as the bridge between C domain and P domain, which is enriched in actomyosin contractile structures (termed as actin arcs) (Schaefer, Kabir et al., 2002) and myosin II (Medeiros, Burnette et al., 2006). The P domain is the most front region of growth

cone, where are aligned with outward-radial actin filament bundles. Between each two F-actin bundles weaved are branched mesh-like F-actin networks. MT arrays intruded from C domain also enter this area, which are normally along with F-actin bundles and highly dynamic (Schaefer, Kabir et al., 2002).

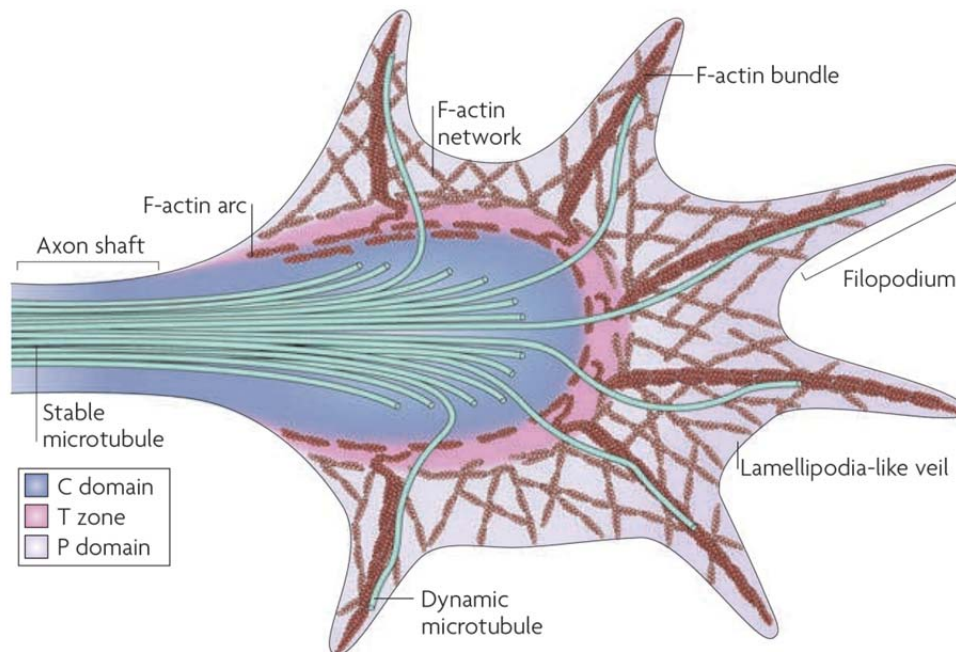


Fig. 3.4 Structural composition of growth cone (Lowery and Vactor, 2009). Three areas are contained: the C domain, the T zone and the P domain. The C domain is the extension of the axon shaft full of MT bundle. The P domain is enriched in F-actin, in the form of either bundle or network, and the two forms are adjacent to each other.

Growth cone advances on the substrate to achieve the axon elongation. Three stages are involved: protrusion, engorgement and consolidation (Dent and Gertler, 2003). Protrusion stage is the time of filopodia and lamellipodia extension, which are rapid and primarily composed of bundled and mesh-like F-actin networks. During engorgement stage, MTs invade the actin-enriched protrusions and simultaneously transport membranous vesicles and organelles (mitochondria, endoplasmic reticulum) (Goldberg and Burmeister, 1986). Consolidation refers to the new axon shaft formation right behind the growth cone. This is achieved through the membrane shrinkage around the MT bundles after the majority of local

F-actin depolymerizes in the neck of the growth cone. This process cycles, enabling the axon elongation.

3.2.2 Function

In the *in vivo* context, neurons extend axons to reach certain destinations for appropriate circuit formation. The growth cone leads the axon extension. The highly dynamic state and fast responsiveness to the spatial factors allow the growth cone to find its target with impressive accuracy (Lowery and Vactor, 2009). Particularly, various environmental factors either assist growth cone movement or navigate it to follow the right path. Adhesive molecules such as transmembrane cell adhesion molecules (CAMs) (Maness and Schachner, 2007) which are present on the neighboring cell surface or assembled into a dense extracellular matrix (ECM; for example, laminin and fibronectin (Evans, Euteneuer et al., 2007)) enable growth cone to attach to the substratum which is the fundamental step before movement and these molecules are also able to activate the intracellular pathways which in turn promote the cytoskeletal machinery. On the other hand, to confine the movement of growth cone, another type of molecules, anti-adhesive, surface-bound molecules, are also needed. For example slits and ephrins are reported to be able to prohibit the advance of the growth cone (Dickson, 2002) and thus assist to define movement boundaries. Further, to reach the final destination, diffusible chemotropic cues serve as the “tour guide” to steer the orientation of the advancing growth cone. To this end, various factors are involved including factors that were initially identified explicitly in axon guidance assays (Chilton, 2006), as well as morphogens (Zou and Lyuksyutova, 2007), secreted transcription factors (Butler and Tear, 2007), neurotrophic factors (Sanford, Gatlin et al., 2008) and neurotransmitters (Mattson, Dou et al., 1988).

3.3 Role of cytoskeleton in neuronal polarization

3.3.1 Basics of the two cytoskeletal components

3.3.1.1 Dynamics of actin

By mass actin is the most abundant protein in most types of eukaryote (Pollard and Borisy, 2003), reflecting its fundamental importance for the cellular activities. Filamentous actin (F-actin) possesses a double-helical structure composed by globular actin (G-actin) monomer. F-actin is also polar polymer with a fast-growing “barbed end” and a shortening end ‘pointed end’. Its life cycle can be approximately divided into three stages (Fig. 3.5) (Pollard and Borisy, 2003; Blanchoin, Boujemaa-Paterski et al., 2014; Coles and Bradke, 2015):

1. **Nucleation:** actin polymerization is normally initiated near the membrane. After external signal activation, WASp/Scar (Wiskott-Aldrich syndrome protein) proteins recruit Arp2/3 complex and actin monomers to the side of preexisting actin filaments before recommencing to form a branch. Formin is another essential actin nucleator, based on which another model was proposed very recently (Breitsprecher, Jaiswal et al., 2012). APC (adenomatous polyposis coli) protein, mDia (one type of formin) and actin monomers form a tripartite nucleation complex which can give rise to actin assembly.
2. **Elongation:** the nucleating complex of WASp/Scar and Arp2/3 insert the ATP-G-actin at the barbed end extending the length of the branch filament. Whereas in the case of APC and mDia complex, APC stays stable, mDia tracks with the barbed end, recruiting profilin-bound G-actin and preventing from capping protein binding.
3. **Disassembly:** as the actin filaments age after releasing the phosphate from ATP, ADP bound actin can be recognized by actin-severing protein such as cofilin. The filament is thereafter dissociated. The liberated ADP-G-actin will then be captured and turned into ATP-G-actin by profilin, which goes to the next treadmilling cycle.

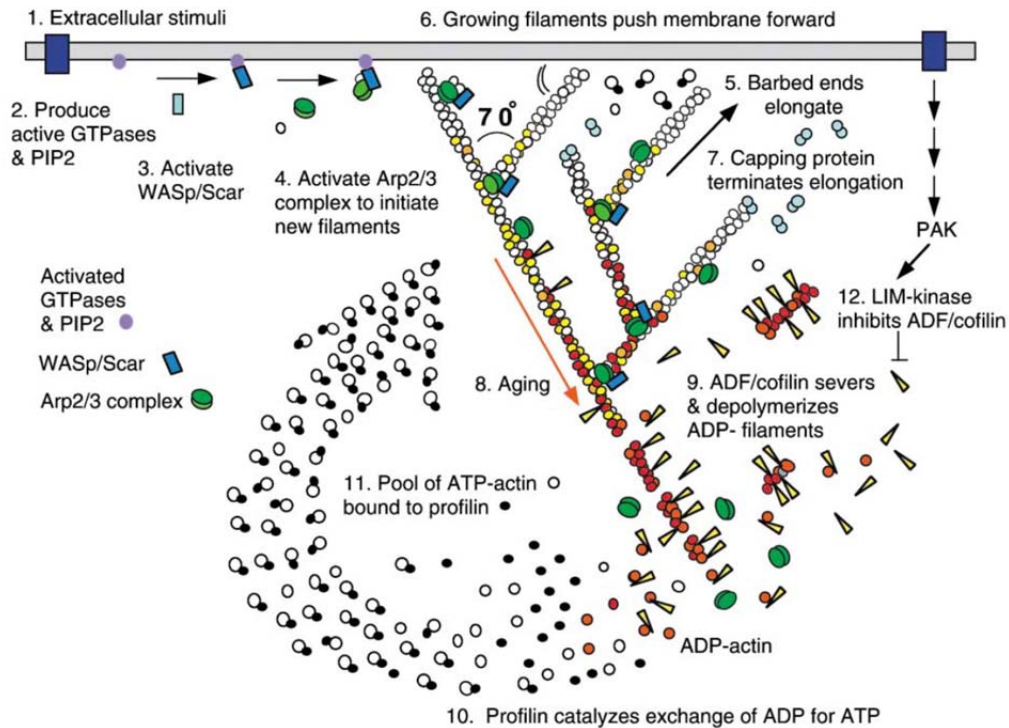


Fig. 3.5 Life cycle of actin in cell. From (Pollard and Borisy, 2003)

3.3.1.2 Dynamics of microtubule

As one of the most important cytoskeletal components, MT plays a central role in many cellular activities such as cell division, migration, differentiation, intracellular trafficking and so on (Kapitein and Hoogenraad, 2015). Structurally MT is a hollow cylindrical tube which typically consists of 13 protofilaments assembled from α - and β - tubulin heterodimers. α - and β - tubulin bind in a head to tail manner endowing the MT a polarized property, which is characterized by a “plus end” and a “minus end” (Fig. 3.6) (Kollman, Merdes et al., 2011).

MT is dynamically unstable, constantly switching between phases of growth (rescue) and shrinkage (catastrophe) (Fig. 3.6), which is driven by the $\alpha\beta$ -tubulin-dimer-triggered cycle of GTP and GDP (Mitchison and Kirschner, 1984). Polymerization and depolymerization of $\alpha\beta$ -tubulin dimers preferentially take place at the outward-splayed plus end. The plus end is capped by β -tubulin, on the surface of which an E-site resides. The E-site also exists on the free GDP-bounded $\alpha\beta$ -tubulin, where a pocket is provided to exchange for GTP. This

exchange enables $\alpha\beta$ -tubulin competent for polymerization. Once the α -tubulin of the incoming dimer binds to the exposed β -tubulin of the plus end at E-site, hydrolysis of the E-site GTP occurs, which enables the extension (Alushin, Lander et al., 2014). Generally the lattice of GTP tubulin favors MT growth while GDP tubulin lattice is more prone to depolymerization (Alushin, Lander et al., 2014).

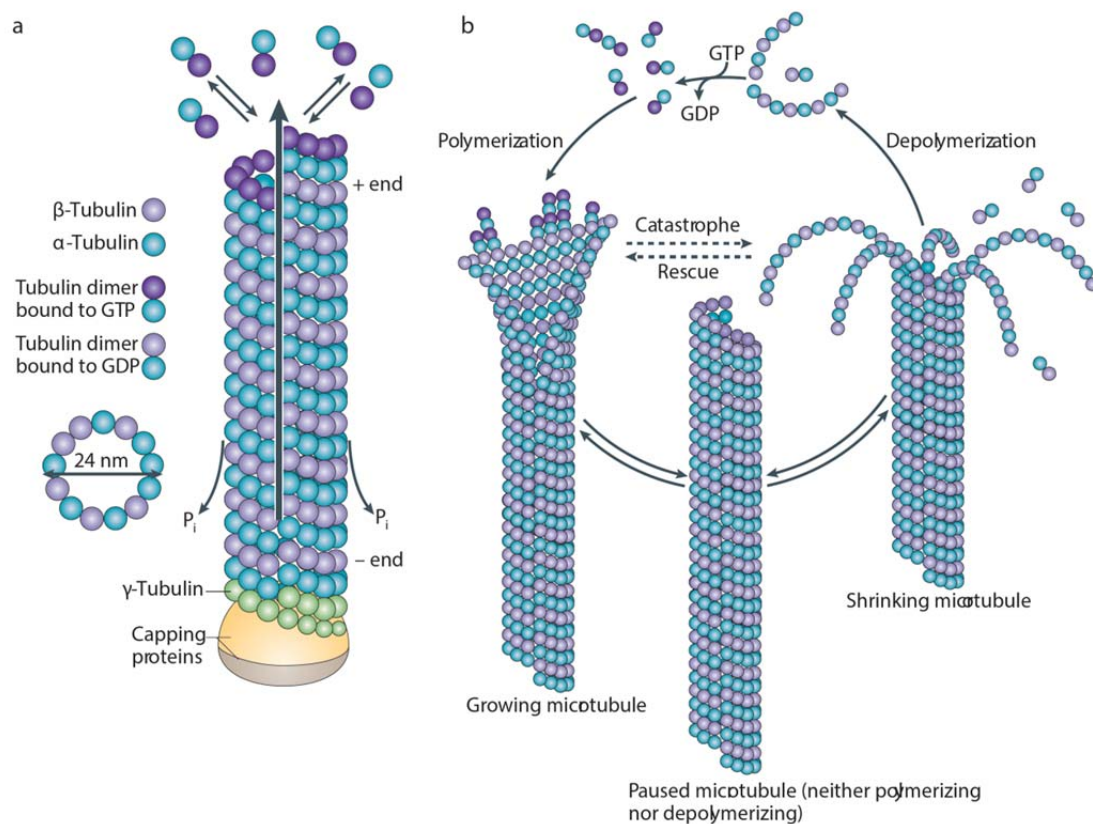


Fig. 3.6 Assembly and disassembly of MT (Conde and Caceres, 2009). **a)** $\alpha\beta$ -tubulin dimers are added to the plus end of microtubule forming a hollow cylindrical structure with a diameter of 24 nm. **b)** MT undergoes polymerization and depolymerization generated by the cycle of GTP- and GDP- bounded tubulin, switching among growth (rescue), shrinkage (catastrophe) and pause.

MT dynamics can be influenced by various proteins (Conde and Caceres, 2009), e.g. MAP2 is known to bind to MT and induce stabilization while katanin and spastin have been shown

Introduction

to sever MT. What is more, a large number of plus-end tracking protein (+TIPs) transiently associate with microtubule plus ends, variously stabilizing or destabilizing filament dynamics (Akhmanova and Steinmetz, 2010). The disordered tails of $\alpha\beta$ -tubulin also provide a major site for further modifying the MT stability and instability, known as PTM (post-translational modification), e.g. polyamination stabilizes MT while tyrosination of released tubulins prevent them back into the polymerization cycle, favoring depolymerization (Song and Brady, 2015).

MTs are also sensitive to a number of chemical compounds; therefore it is often taken as the drug target of diseases, e.g. cancer (Dumontet and Jordan, 2010). Via competing for the binding sites on MT, these compounds can either stabilize or depolymerize MT, e.g. nocodazole has been frequently used as a MT depolymerizer while taxol as a MT stabilizer (Jordan and Wilson, 2004).

3.3.2 MT and actin in axon fate decision

3.3.2.1 The role of actin

As the leading edge of the extending axon, the growth cone exhibits a very dynamic state driven by the retrograde flow of F-actin. Shown that the actin dynamics in the future axon growth-cone outpaces that of the rest of neurites, which is evidenced by the formation of multiple axons after actin destabilizer cytochalasin D treatment (Bradke and Dotti, 1999), the high extent of actin instability has been therefore regarded as the hallmark of the future axon growth-cone.

RhoA small GTPase proteins are most known for their effects on actin cytoskeleton (BurrIDGE and Wennerberg, 2004). In neurons when RhoA activity is inhibited, the neurite outgrowth is consequentially impeded (Bito, Furuyashiki et al., 2000; Schwamborn and Puschel, 2004). RhoA activates and binds its effector kinase ROCK, subsequently recruiting profilin IIa to form a complex, which plays a role in modulating actin stability. When profilin IIa is inhibited, the neuritogenesis is affected, which is the initiating step of axon formation (Da

Silva, Medina et al., 2003). Cdc42 (Cell division cycle 42), another member of the Rho-family, has been reported to be involved in axon specification together with its upstream partners Par3-Par6-aPKC complex (Schwamborn and Puschel, 2004). In Cdc42-deficient mice, the formation of axon tracts is absent and *in vitro* culture knock-out neurons showed a defect in axon formation as well which is shown due to the suppressed actin instability induced by enriched inactive cofilin (Garvalov, Flynn et al., 2007).

Ena/VASP proteins are associated with barbed end of F-actin preventing its being capped from capping proteins therefore facilitate the F-actin dynamics (Krause, Dent et al., 2003). Ena/VASP-null neurons, either *in vitro* culture or *in vivo*, fail to form proper neurites, especially, in the knock-out mice, cortical axonal tracts formation is lost (Kwiatkowski, Rubinson et al.; Dent, Kwiatkowski et al., 2007). Arp2/3 is known as an actin nucleator for F-actin branching. It is found that Arp2/3 is not enriched in the peripheral zone but in the central zone of the neuronal growth cone. Interestingly Arp2/3 inhibition leads not to the actin organization change in the growth cone, the axon elongation is however enhanced (Strasser, Rahim et al., 2004).

3.3.2.2 The role of MT

MTs are polarized tube-like structure. How they are aligned in the dendritic and axonal domains has already drawn attention in last 80s. It has been shown that axonal MT directionality is more uniform and putatively the growing end is distal to the soma (Burton and Paige, 1981; Heidemann, Landers et al., 1981). Not long after, this piece of knowledge was updated by Bass and colleges demonstrating that MT orientation in axon is uniform and directed towards the peripheral growth cone while those in dendrites are mixed and around half are plus-ended towards periphery (Baas, Deitch et al., 1988). Further they found that the aligning orientation changes during the development of the cultured hippocampal neuron, namely MTs in all the processes of stage 2 neurons are plus-end-distally oriented, which is retained in the axon during the whole period of development. However when the rest of

Introduction

processes start to grow and acquire the dendritic identity the MT polarity become mixed (Baas, Black et al., 1989). In *in vivo* context, MT polarity alignment is somehow distinct from that *in vitro*, an organotypic slice culture system demonstrated that the orientation of microtubules in MP cell neurites is uniformly plus-end-distal, whereas in the trailing process (nascent axon) of migrating neuron it is mixed (Sakakibara, Sato et al., 2013).

MTs dynamically polymerize and depolymerize. As early as last 80s, Kirschner and Mitchison have hypothesized that selective stabilization of a subset of MTs could induce asymmetrization of MT cytoskeleton and eventually overall morphological polarization (Kirschner and Mitchison, 1986). Spatial cues are presented in the periphery of the cell, which could relay the signal to the cell cortex and then transduce it to the vicinal MT growing end. By capping the extending end, the MT lattice could be stabilized. The continuity of the MTs would be accordingly reorganized based on this rigid subset; the asymmetry of MT network therefore is achieved. Recently a study in neurons has demonstrated that one of the neurites of stage 2 neuron preferentially display more stabilized MT lattice, reflected by the ratio between acetylated and tyrosinated tubulin, which is then further retained in the developing axon (Witte, Neukirchen et al., 2008). What is more, in the same study, photocaging of low-dosed Taxol (a MT stabilizer) to one of the equal processes of stage 2 neuron, this specific neurite developed into axon. This particular report highlights the role of MT stabilization in axon specification. To date we have known that MT can be stabilized in many ways, e.g. MAPs (MT associated protein) binding, post-translational modulation and Modulating +TIP (plus end binding protein) etc..

Tau and MAP2 are well-known markers for axon and dendrites respectively. In vitro Tau can increase the polymerization rate, inhibit transit from growth phase to shrinkage phase and decrease the rate of depolymerization (Drechsel, Hyman et al., 1992), demonstrating a strong stabilizing effect on MTs. Whereas in cells, illustrated by live imaging, over-expression of tau and MAP2 in non-neuronal cells showed a strong effect on cell morphology, inducing the formation of process-like structure around the cell body (Edson, Weisshaar et al., 1993;

Kaeche, Ludin et al., 1996). Par3 (partition defective 3), a polarity protein has been shown to be enriched in axonal growth cone and critical for axon formation (Shi, Jan et al., 2003). Recently it is reported that Par3 directly binds to and bundles MTs to induce MT stabilization. When this regulatory activity is disrupted, neuronal axonal formation is impaired (Chen, Chen et al., 2013). Illustrated by Cryo-EM method, Dcx (Doublecortin), a risk factor of human X-linked lissencephaly and double cortex syndrome (Gleeson, Allen et al., 1998), is found to be able to bind to the tubulin tetra-polymer and facilitate MT nucleation and stabilization (Moores, Perderiset et al., 2004; Fourniol, Sindelar et al., 2010) and has been reported that it regulates neuronal migration and MP-to-BP transition in developing cerebral cortex (Bai, Ramos et al., 2003; Sapir, Shmueli et al., 2008), implying its role in dendrite and axon development *in vivo*. DOCK7, as a Rac GTPase activator, shows an asymmetric distribution in neuron and preferentially location in axon. Knock down of it leads to retardation of axonal formation while overexpression induces multiple axons. The mechanism behind this is DOCK activation give rise to inactivation of the microtubule destabilizing protein stathmin in the nascent axon (Watabe-Uchida, John et al., 2006). Therefore uncontrolled stabilizing MT can affect axonal development as well. CRMP-2 (Collapsin response mediator protein-2) is shown to be able to bind tubulin-heterodimer and promote MT assembly. In neuron overexpression of CRMP-2 facilitates axonal formation and branching while knockdown of it inhibited the axonal developmental activities (Fukata, Itoh et al., 2002).

PTM (post-translational modification) is also known to modulate MT dynamics (Song and Brady, 2015), which contains many types, such as tyrosination, acetylation, polyamination, phosphorylation, palmitoylation and so on. In neuron, some of them have been studied. Tyrosination takes place normally on the C-termimi of α -tubulin conducted by tubulin tyrosine ligase (TTL) (Raybin and Flavin, 1977), therefore numerous studies on tyrosination focus on TTL activity. In TTL knock-out mice cortical neuron migration is disrupted and cells display a round shape without proper axon formation while in *in vitro* culture axonal growth was much faster than that in WT and knock-out neuron showed multiple axon (Erck, Peris et al., 2005). On the contrary, overexpression of TTL hampers axonal outgrowth (Prota, Magiera et al.,

Introduction

2013). Another recent study showed that the axons of $TLL^{-/-}$ mice exhibit supernumerary branches, enlarged growth cones and an emission of mis-oriented filopodia. Besides, axon number grown from the collagen matrix is significantly less compared to that of WT (Marcos, Moreau et al., 2009). Kinesin-1 preferentially enters into axon, but with an elevated level of dephosphorylation via TTL knock down, it accumulates in all neurites (Konishi and Setou, 2009), implying tyrosination plays a role in axonal trafficking. Acetylation canonically occurs at the site of α -tubulin lys40, which locates on the MT luminal surface (Song and Brady, 2015). In the mouse central nervous system acetylation is catalyzed by MEC17/ α TAT (Kalebic, Sorrentino et al., 2013) and deacetylation by histone deacetylase 6 (HDAC6) (Hubbert, Guardiola et al., 2002). By increasing tubulin acetylation via trichostatin A treatment or HDAC6 knockdown axon elongation was retarded whereas HDAC6 overexpression does not affect axon formation (Tapia, Wandosell et al., 2010).

Plus-end tracking proteins (+TIPs) such as MT end binding protein (EB), APC (adenomatous polyposis coli) protein etc. are a group of cellular factors specially localize at the extending end of MT, which are evolutionarily conserved (Akhmanova and Steinmetz, 2008). APC protein has been shown to initially localize in all the tips of process of MP stage 2 neuron but only enrich in the future axon of stage 3 neuron (Shi, Cheng et al., 2004; Votin, Nelson et al., 2005), suggesting APC is involved in axon specification. The key factor behind it could be that APC forms a complex with mPar3 and KIF (kinesin superfamily) 3A and these three colocalize at the nascent axon tip. Expression of dominant-negative C terminus deletion mutants of APC or ectopic expression of APC induces dislocalization of mPar3 and defects in axon specification (Shi, Cheng et al., 2004). However in extracellular NGF (nerve growth factor)-cued axon generation, APC facilitates axon growth via being activated by the inactivated GSK-3 β (glycogen synthase kinase 3 β) and PI3K (phosphatidylinositol 3-kinase) complex, which NGF can directly activate (Zhou, Zhou et al., 2004). EB1, another +TIP protein, has been reported to accumulate in growing axon (Morrison, Moncur et al., 2002) and facilitate axonal elongation in $MAP1B^{-/-}$ cells (Jiménez-Mateos, Paglini et al., 2005). Recently EB3 has also been demonstrated to be enriched in growth cone filopodia and

involved in neuritogenesis through interacting with actin-binding protein drebrin (Geraldo, Khanzada et al., 2008). LIS1, a noncatalytic subunit of platelet-activating factor acetylhydrolase 1b, together with dynein and dynactin were enriched in axonal growth cones in stage 3 hippocampal neurons. Knockdown of LIS1 leads to both growth cone organization and axon elongation defect (Grabham, Seale et al., 2007).

3.4 Centrosome in neuronal polarization

3.4.1 Centrosome as MT organizing center

MTOC are locations where MT minus ends anchor and MTs spread out radially. A large number of microtubules converge into a zone occupied by amorphous, electron-dense material and organelles (such as centrioles, smooth ER and Golgi) (Brinkley, 1985). The most well-known MTOC is the centrosome, which are present in most eukaryotes and composed of two centrioles and a cloud of pericentriolar matrix (Doxsey, 2001) (Fig. 3.6). Between these two orthogonally-arranged centrioles, one is maternal while the other is daughter. The centriole is a cylinder characterized by a 9-fold radial symmetry, seen as a cartwheel shape from the top view. At the pinheads of nine spokes attached are nine microtubule triplets composed of polyglutamylated α -tubulin and β -tubulin subunits (Azimzadeh and Marshall, 2010; Kitagawa, Vakonakis et al., 2011). However, it is also pointed out that this “cartwheel” only exists in procentrioles but not adult centrioles (Alvey, 1986). Surrounding the centrioles is the pericentriolar matrix (PCM), which is an amorphous, electron-dense complex abundant in coiled-coil-domain-contained proteins (Woodruff, Wueseke et al., 2014), implying this specific region could involve numerous protein-protein interactions since coiled-coil domain is well known to function in protein interaction (Lupas, Van Dyke et al., 1991). PCM contains factors which play roles in spindle formation, centriole duplication, cell cycle, MT nucleator binding etc. (Woodruff, Wueseke et al., 2014).

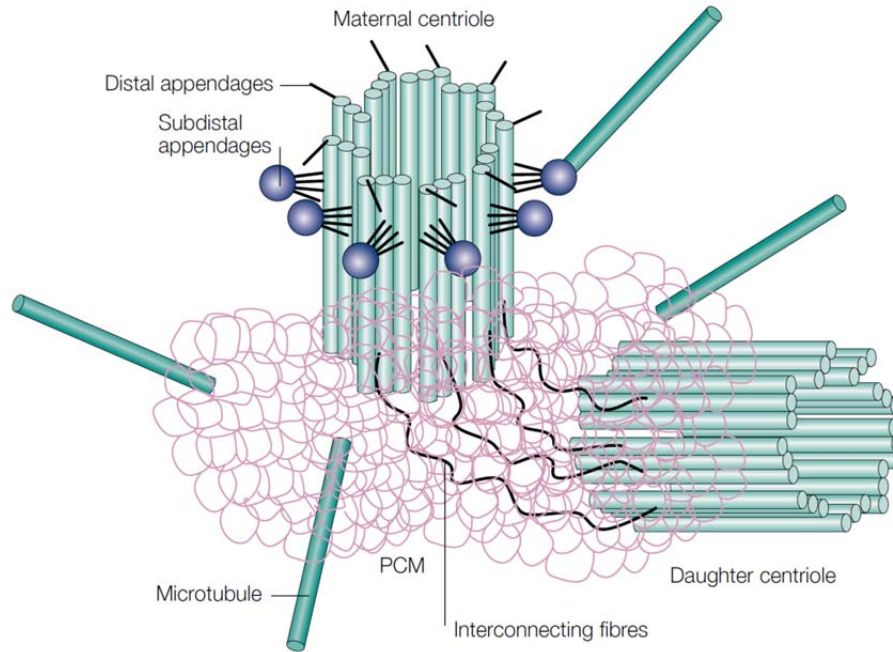


Fig. 3.7 A schematic model of centrosome (Doxsey, 2001). Two centrioles connected by interconnecting fibers reside in the PCM complex, from which MTs radiate out. Green tubes represent MTs, pink cloud for PCM, dark blue balls for subdistal appendage proteins and black curved lines for interconnecting fibers.

MT nucleation relies mainly on γ -tubulin ring complex (γ TuRC). In term of centrosome, γ TuRC anchor in the PCM through numerous proteins (Doxsey, 2001). Component analysis for samples from either *Drosophila melanogaster* embryos or *Xenopus laevis* eggs demonstrates that this complex is around 22MDa, containing γ -tubulin complex protein 2 (GCP2), GCP3, GCP4, GCP5, GCP6, NEDD1 and γ -tubulin itself. This complex formed a ring-like structure as shown by the EM graph (Zheng, Wong et al., 1995; Kollman, Merdes et al., 2011). γ TuRC can be further split into the γ -tubulin small complex (γ TuSC), which is the conserved, essential core of the microtubule nucleating machinery and found in nearly all eukaryotes (Kollman, Merdes et al., 2011). Resolved by EM, it has been described that γ TuRC possesses a “lock washer” shape (Oegema, Wiese et al., 1999), which resembles the aligning pattern of $\alpha\beta$ -tubulin dimer in MT. This shape serves as a template for the growing MT (Fig. 3.7).

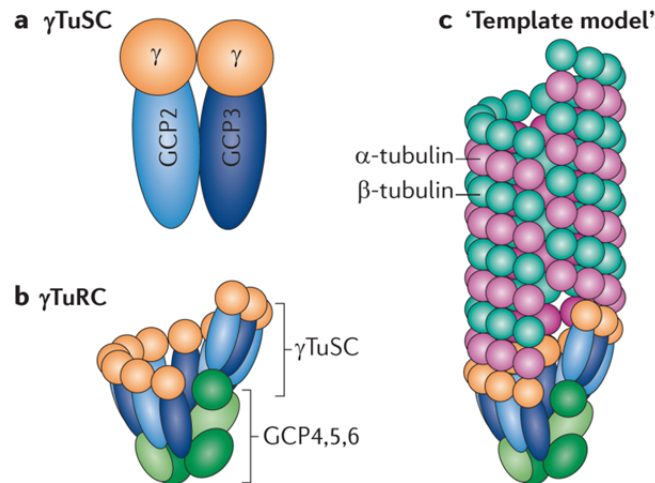


Fig. 3.8 γ -tubulin ring complex and how it serves as a template (Kollman, Merdes et al., 2011) a) the essential core structure of γ TuRC, γ -tubulin small complex (γ TuSC) b) the organizing pattern of γ TuRC c) tubulin dimer addition to the template and MT elongation

Traditionally centrosome serves as the MT organizing center. However more and more attention has been drawn to its role in actin dynamics and vice versa. Very recently it has been reported that centrosome can also act as an F-actin organization center evidenced by that actin monomers assemble radiantly centering the cellular-isolated centrosome (Farina, Gaillard et al., 2016). In another report, centrosome is shown to modulate actin nucleation via Arp2/3, which exerts an effect on the lymphocyte polarization (Obino, Farina et al., 2016). Further during mitosis, to form the spindle, centrosome is positioned at the two poles of the cell. This positioning has been attributed to the subcortical actin cloud with the mediation of Myosin 10 and MT (Kwon, Bagonis et al., 2015). Similarly, centrosome positioning towards the immune synapse in the T cell has been shown to be dependent on formin, which is a key actin nucleating factor (Gomez, Kumar et al., 2007).

3.4.2 Centrosome & axon specification

Numerous factors have been implicated to neuronal polarity, either intracellular or extracellular (Namba, Funahashi et al., 2015). A cluster of these factors are cellular

Introduction

organelles, which are non-randomly positioned in the cellular lumen, shaping the asymmetrical organization of intracellular content (Bornens, 2008). It has been reported that the positioning of a number of organelles have been involved in neuronal polarization, such as golgi apparatus (Zmuda and Rivas, 1998; de Anda, Pollarolo et al., 2005), cytoskeleton (aforementioned review about cytoskeleton), mitochondria, endosome, ribosome (Bradke and Dotti, 1997) as well as centrosome (Zmuda and Rivas, 1998; de Anda, Pollarolo et al., 2005).

Centrosome as the MTOC has been shown to play a role in determining axonal outgrowth site. Zmuda and Rivas showed that in cerebellar granule cells the location of centrosome together with Golgi indicated the site of initial process (future axon) and subsequently moved to the opposite where the second process sprouted (Zmuda and Rivas, 1998). What is more, in another study, cytokinesis-arrested *Drosophila* neuroblasts with double centrosomes form an axon from the vicinity of each centrosome. After disruption the centrosome function with CALI (chromophores -assisted light inactivation), the axon growth is either absent or retarded (de Anda, Pollarolo et al., 2005). Some time later this concept is updated by that the axon extends either from the location of centrosome or from the opposite pole, both *in vivo* and *in vitro* (Calderon de Anda, Gärtner et al., 2008). Further in an *in situ* study using cortical organotypic slice, centrosome inactivation leads to retraction of nascent axon and knockdown of centrosome protein such as Pericentriolar material 1 protein (PCM1), Centrosomal protein of 120kDa (Cep120), both neuronal migration and callosal axon formation are undermined (de Anda, Meletis et al., 2010). Another study provides *in vivo* evidence in zebra fish that ablation of centrosome of Rohon-Beard (RB) sensory neurons inhibits the peripheral axon formation (Andersen and Halloran, 2012), further underscoring the role of centrosome in axon fate decision.

On the other hand, evidence unfavorable of the role of centrosome in axon specification is also present, drawing this issue under debate. *Drosophila* having lost centrosomes developed into morphologically normal adults, with only cilia or flagella formation affected

(Basto, Lau et al., 2006). An *in vivo* study using zebrafish has shown that axonogenesis occurs independent of centrosome proximity (Distel, Hocking et al., 2010). Further Stuess et al showed that centrosome loses its capacity of MT organization during rodent hippocampal neuron development and axon can elongate in absence of centrosome (Stuess, Maghelli et al., 2010). Recently another report claimed that in embryonic mouse brain slice, centrosome reoriented towards the dominant process and the same occurs during nascent axon extension (Sakakibara, Sato et al., 2013) supporting that centrosome location is a result of apical dendrite or axon formation, which is dependent on MT organization. Therefore in the presence of controversy, further studies are needed to elucidate the role of centrosome in this event.

3.5 MT-actin interaction

The interaction of actin and MTs is critical for a range of dynamic cellular activities, including migration, adhesion, cytokinesis, morphogenesis, intracellular traffic and signaling, and structural flexibility, and has been demonstrated both in various cell types and across species (Rodriguez, Schaefer et al., 2003; Coles and Bradke, 2015). However, directly mixing of purified MTs and F-actin *in vitro* seems not to show any sign of crosstalk indicated by that mixture of these two possessed low viscosities close to that of the single constituent (Griffith and Pollard, 1982), implying that a linker protein or complex is involved to bridge these two cytoskeletal components. Indeed, accumulating evidence has supported this idea and depicted the picture of this crosstalk in a detailed way. Based on the crosslinker(s) involved, the interaction could be categorized into the following types.

3.5.1 Direct protein crosslinker

This type of mediators can directly bind to MT and F-actin without other adaptors. Microtubule-associated proteins have long been known as regulators of MT dynamics (Maccioni and Cambiasso, 1995). In one early study, it has been linked to potentially mediation of MT and F-actin interaction based on the finding that mixture of MT and F-actin

Introduction

containing the MAPs is much “stickier” than that without MAPs (Griffith and Pollard, 1982). MAP2c, one isoform of MAP2, highly expressed during early neuronal development (Garner, Brugg et al., 1988), has been shown to induce the formation of actin-rich lamellae and MT-bearing process and be present in the actin-enriched region in melanoma cells, plus *in vitro* capable of organizing actin filaments (Cunningham, Leclerc et al., 1997). Further, it is found that MAP2c colocalization with F-actin is phosphorylation-dependent (Ozer and Halpain, 2000). Whereas in primary hippocampal neurons, MAP2c facilitates neurite formation via stabilizing MT as well as altering F-actin organization, and its MT binding domain and activation of PKC are essential for this event (Dehmelt, Smart et al., 2003).

Coronin also known as Pod1 is a very conserved family of protein and is found to be an actin-binding protein (de Hostos, 1999). *In vitro* coronin promotes actin polymerization and bundling. Meanwhile it can bind to MTs, which could be further enhanced by the presence of F-actin (Goode, Wong et al., 1999). In drosophila, Pod1 is shown to be crucial for axon growth guidance through coordinating MT and actin at the tip of growing axon (Rothenberg, Rogers et al., 2003), suggesting its functional role in cellular activity.

3.5.2 +TIP-associated interaction

Plus-end tracking proteins (+TIPs) are a group of cellular factors specially localizing at the extending end of MT, which are evolutionarily conserved (Akhmanova and Steinmetz, 2008). A study employing an engineered plus-end tracking protein Tipact, which is derived from microtubule–actin cross-linking factor (MACF), found that actin bundles could capture and guide growing MT while growing MT could define the global actin organization (López, Huber et al., 2014), providing a physical basis to understand MT-actin crosstalk. Whereas in the biological context, various +TIP proteins have been reported.

Spectraplakins are a family of giant cytoskeletal crosslinking proteins that have been highly conserved throughout animal evolution (Jefferson, Leung et al., 2004). Through live imaging to track the Shot activity dynamically drosophila spectraplakins Shot has been shown to

mediate the interaction with two different strategies in the periphery and interior respectively (Applewhite, Grode et al., 2010). Further mouse ACF and Shot are reported to modulate filopodia formation (Sanchez-Soriano, Travis et al., 2009). What is more, Shot is also shown to be required for axonogenesis as the crosslinker of MT and actin, which is also Ca^{2+} -binding-dependent (Lee and Kolodziej, 2002). In epidermis cells, ACF7 (one type spectraplaklin) deficiency leads to mistargeting of MT and F-actin to focal adhesions (FA), stabilization of FA-actin and migration defect, which depends on the actin-regulated ATPase domain of ACF7, indicating a role of MT-actin interaction in the FA-involved cell migration (Wu, Kodama et al., 2008). Very recently ACF7 has also been shown to mediate CAMSAP3, the minus-end of non-centrosomal MT stabilizing protein, anchoring to actin filaments and consequently play a role in adhesion size control and cell migration (Ning, Yu et al., 2016).

APC protein is the product of a tumor suppressor gene mutated in colorectal cancer (Groden, Thliveris et al., 1991), which contains MT binding domain, EB1 binding domain, coiled coil domain as well as Armadillo repeats, among which Armadillo repeats is essential for APC in cortical cluster formation (Barth, Siemers et al., 2002). It has been discovered that APC can move at the tip of elongating MT and drop off as soon as MT starts to shorten (Mimori-Kiyosue, Shiina et al., 2000), suggesting its role in MT growth. On the other hand it is also found to be associated with plasma membrane in a actin-dependent manner (Rosin-Arbesfeld, Ihrke et al., 2001). APC is also implicated with the migration of epithelial Madin–Darby canine kidney cells and cell adhesion via forming a complex with Asef, a Rac-specific guanine nucleotide exchange factor, to modulate actin cytoskeleton and other actin-involved activities (Kawasaki, Senda et al., 2000; Kawasaki, Sato et al., 2003). Also in drosophila, it has been reported that APC protein localizes to actin-rich adherent junctions and binds to MTs (Barth and Nelson, 2002). What is more, Drosophila APC2 together with Armadillo has been shown to localize with interphase microtubules and attach to cortical actin (McCartney, McEwen et al., 2001), supporting its role as a linker between cortical attachment site and spindle.

Introduction

CLIP170, initially identified as a nucleotide-sensitive MT binding protein (Rickard and Kreis, 1990), has the activity of accumulating at the plus ends of growing MTs (Perez, Diamantopoulos et al., 1999). CLIP170 has been associated with IQGAP1, known to bind to F-actin and modulate its dynamics (Bashour, Fullerton et al., 1997), in turn activating Rac1 and Cdc42 and playing a role in leading edge formation (Fukata, Watanabe et al., 2002). Also it is shown that in rat hippocampal neuron, CLIP170 cooperates with IQGAP1 regulating neurite formation via PI3K-mTOR pathway (Swiech, Blazejczyk et al., 2011). CLIP-associated proteins (CLASPs) serve as MT-actin crosslinkers via facilitating recognition of actin filaments by the plus ends of growing microtubules at the initial stages of actin-microtubule interaction (Tsvetkov, Samsonov et al., 2007). End binding proteins are another family of +TIP containing very conserved N- and C- terminal domains (Lansbergen and Akhmanova, 2006). Very recently it has been reported that in *in vitro* assay CLIP170 binds to the actin nucleator mDia1 (a subtype of formin) recruited to the MT plus end via EB1 and consequently accelerates F-actin polymerization (Henty-Ridilla, Rankova et al., 2016), highlighting the direct role of plus end protein on the F-actin dynamics. In neuron EB3 is reported to bind to drebrin, an actin binding protein, exerting an effect on neuritogenesis (Geraldo, Khanzada et al., 2008).

3.5.3 Interaction mediated by motor proteins

Motor proteins are responsible for the intracellular transport of cargos directionally along a cytoskeletal track: myosins along actin while kinesins and dyneins along microtubules (Brown, 1999; Vale, 2003). Interestingly work from different labs have unveiled some of motor proteins have been involved in MT-actin interaction. Cortical dynein is associated with cortical actin and has been shown to be able to capture MT plus ends and in turn inhibit its growth inducing MT catastrophe in *in vitro* reconstitution assay (Laan, Pavin et al., 2012). Neuronal dynein has been reported to form a complex with LIS1 and dynactin, which locates at the growth cone, to facilitate MT advance during axon growth (Grabham, Seale et al., 2007). In the budding yeast *Saccharomyces cerevisiae*, during spindle orientation, type V

myosin protein Myo2 interacts with MT plus end binding protein Bim1 and Kar9, associating MT and actin to facilitate spindle positioning (Hwang, Kusch et al., 2003). In drosophila, a class VI unconventional myosin 95F myosin has been implicated with D-CLIP-190, a homolog of MT +TIP protein CLIP170, both of which localize in the posterior pole of the embryo and this colocalization is actin-dependent, highlighting that motor protein could serve as the linker between MT and actin (Lantz and Miller, 1998). Myosin VA, an actin-based vesicle-transport motor has been found to interact directly with a microtubule-based transport motor, KhcU, thus coordinating cargo-trafficking upon the need to switch between different cytoskeletal tracks (Huang, Brady et al., 1999). Similarly, a direct GABA_AR α 1 subunit binding protein muskelin, is reported to associate with both actin-based motor myosin VI and MT-based motor dynein, directing GABA_AR cargo to its destination after endocytosis (Heisler, Loebrich et al., 2011).

3.6 Drebrin-mediated MT and F-actin interaction

3.6.1 Drebrin

Drebrin was first identified from developing chick optic tectum (Shirao and Obata, 1985). It comprises two isoforms: drebrin E, which functions mainly at embryonic stage throughout all tissue type while drebrin A is mainly found in adult brain (Shirao, Kojima et al., 1989). Structurally, drebrin contains 649 amino acids, which can be divided into several domains: an N-terminal actin-depolymerizing factor homology (ADFH) domain, a coiled-coil (CC) domain, a helical (Hel) domain, a proline-rich region (PP), and, at the C terminus, a large domain with no identified homology (blue box, BB) (Fig. 3.9) (Worth, Daly et al., 2013).



Fig. 3.9 Scheme of drebrin structure (Worth, Daly et al., 2013) ADFH: actin-depolymerizing factor homology domain; CC: coiled-coil domain; Hel: helical domain; PP: proline-rich domain; BB: blue box.

Introduction

Drebrin is found to be an actin-binding protein and bind to F-actin at a stoichiometry of 1:5 (Ishikawa, Hayashi et al., 1994). It has turn out that drebrin is actively involved in competing with various other actin-binding proteins, so far as identified as topomyosin, α -actinin (Ishikawa, Hayashi et al., 1994), fascin (Sasaki, Hayashi et al., 1996), myosin V (Ishikawa, Katoh et al., 2007) and cofilin (Grintsevich and Reisler, 2014). Further it is also reported to directly bind to profilin (Mammoto, Sasaki et al., 1998) and connexin-43 (Butkevich, Hülsmann et al., 2004). Additionally, drebrin can induce actin stabilization (Mikati, Grintsevich et al., 2013), which has been hinted in an earlier study that transfection of drebrin cDNA into fibroblastes induced thick, curving bundles of actin (Shirao, Hayashi et al., 1994). This effect has been again studied and is attributed to the bundling function of drebrin on actin filaments via conformation change induced by Cdk5 activation (Worth, Daly et al., 2013).

Drebrin was first found in brain and therefore has been intensively investigated in neuronal cell and tissues. It has been reported to be enriched in spines *in vitro* as well as *in vivo* (Hayashi, Ishikawa et al., 1996; Aoki, Sekino et al., 2005) and modulate spine plasticity (Sekino, Tanaka et al., 2006; Mizui, Sekino et al., 2014). Interestingly, a recently-published study has claimed that drebrin-deficient mouse does not show any basal synaptic transmission and long-term and homeostatic synaptic plasticity change, implying loss of drebrin is not sufficient for synapse dysfunction (Willmes, Mack et al., 2017). It has also been shown that overexpression of drebrin promotes axon growth in primary hippocampal neuron (Mizui, Kojima et al., 2009) and the formation of axonal filopodia and collateral branches *in vivo* and *in vitro* (Ketschek, Spillane et al., 2016). Further, drebrin is also involved in neuronal diseases such as Alzheimer's disease, Down syndrome (Harigaya, Shoji et al., 1996; Shim and Lubec, 2002). Whereas in non-neuronal cells, it has been demonstrated to play a role in cell-substratum adhesion (Ikeda, Shirao et al., 1995) and connexin 43-containing gap junctions at the plasma membrane (Butkevich, Hülsmann et al., 2004). Drebrin has also been implicated with interneuron migration in the olfactory bulb (Sonogo, Oberoi et al., 2015) as well as cerebellar granule cell nucleokinesis during migration (Trivedi, Stabley et al., 2017). Very recently, drebrin is reported to be involved in mediating ectosome release form filia tip

together with myosin 6 (Nager, Goldstein et al., 2017), suggesting drebrin has been involved in diverse cellular activities.

3.6.2 EB3

As a member of EB1 family EB3 is initially discovered via screening the APCL-interacting partners and found to be preferentially expressed in central nervous system and associated with cytoplasmic MTs (Nakagawa, Koyama et al., 2000). Later EB3 is reported to bind to MT plus ends as a plus end tracking protein (+TIP) (Stepanova, Slemmer et al., 2003) and has been frequently used thereafter. EB3 is also shown to directly bind to CLIP and facilitate its association with the MT plus ends (Komarova, Lansbergen et al., 2005). In neuron, EB3 has been implicated with the maintenance of axon initial segment (AIS) via interacting with Ankyrin G (Leterrier, Vacher et al., 2011) and spine morphology modulation and synaptic plasticity via entering spine and interacting with p140Cap/SNIP, a regulator of Src tyrosine kinase (Jaworski, Kapitein et al., 2009). It has also been reported that during muscle differentiation myoblast elongation and fusion into myotubes are dependent on EB3-mediated MT organization (Straube and Merdes, 2007).

3.6.3 Drebrin and EB3 link MT and F-actin

Work from Geraldo et al. has demonstrated that the actin-binding protein drebrin can interact with EB3, thus link MT and F-actin together (Geraldo, Khanzada et al., 2008). Later this interaction is also reported to be involved in actin bundling via drebrin conformation change via being phosphorylated by Cdk5 (Worth, Daly et al., 2013) (Fig. 3.10).

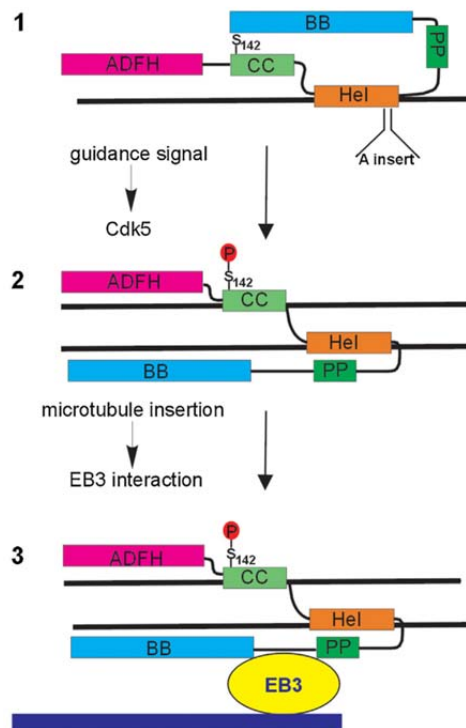


Fig. 3.10 Drebrin and EB3 mediated MT-actin interaction (Gordon-Weeks, 2016).

Initially one drebrin molecule binds to one actin filament due to the closed conformation generated by BB domain attaching to CC domain. With S142 phosphorylated by Cdk5, the released CC domain of opened drebrin binds to another actin filament. Meanwhile EB3 obtains the access to the C-terminal and the interaction is consequently achieved.

Since both drebrin and EB3 have been shown involved in axon development, it would be thus interesting to study how these two coordinate with each other during neuronal polarization.

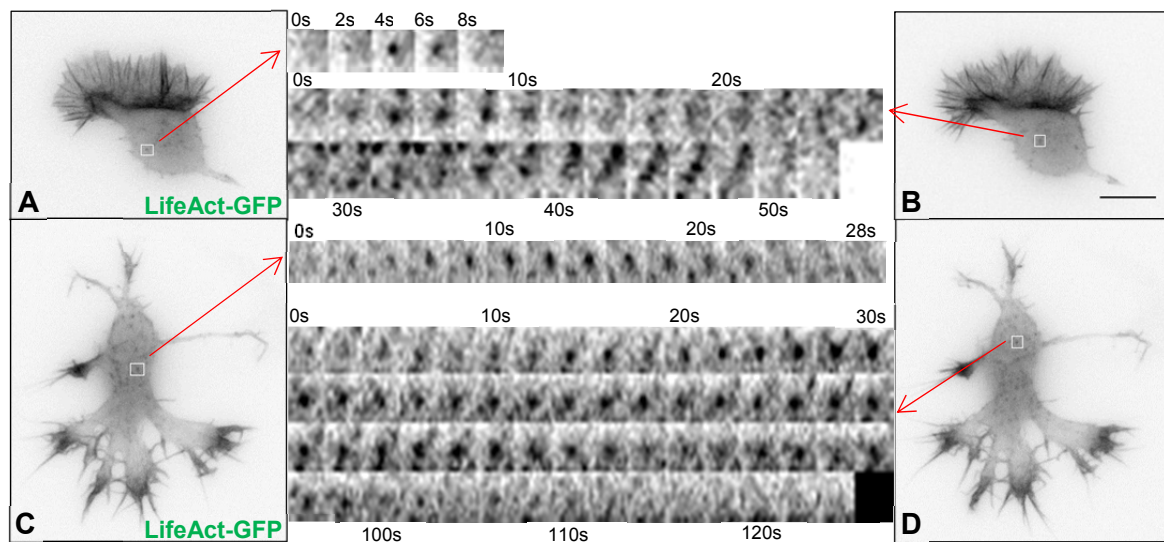
4. Aim of the work

How axon is formed is a fundamental question in neuroscience. Microtubule (MT) and actin cytoskeleton have been shown to play an important role in axon formation. However, how MT and actin interact during axon growth and whether this interplay plays a role in axon development remains elusive. Therefore the aim of this study is to characterize the interaction of MT and actin during axon growth and test whether this interplay is fundamental for axonogenesis.

5. Results

5.1. LifeAct labeling unveils F-actin dynamic puncta structure in neuronal soma

LifeAct is a widely-used marker for F-actin (Riedl, Crevenna et al., 2008), which allows me to track the F-actin behavior in live cells. LifeAct-GFP was transfected into hippocampi neurons at embryonic age of 18d and time lapses from stage 1 to stage 3 neurons were acquired. In the somas of all neurons, dot-like structures can be observed, appearing and disappearing with irregular lifetimes (Fig. 5.1A-D). By presenting all dot durations into kymographs, the lifetime of each somatic dot is measured. Pooling values from 26 cells together allows us to see a general distribution of the F-actin dot lifetime (Fig. 5.1E). The most prominent population is those with lifetime shorter than 15s, nearly 90%, suggesting that most dots are very dynamic. Then comes the population with lifetime of 31-60s, around 4.54%.



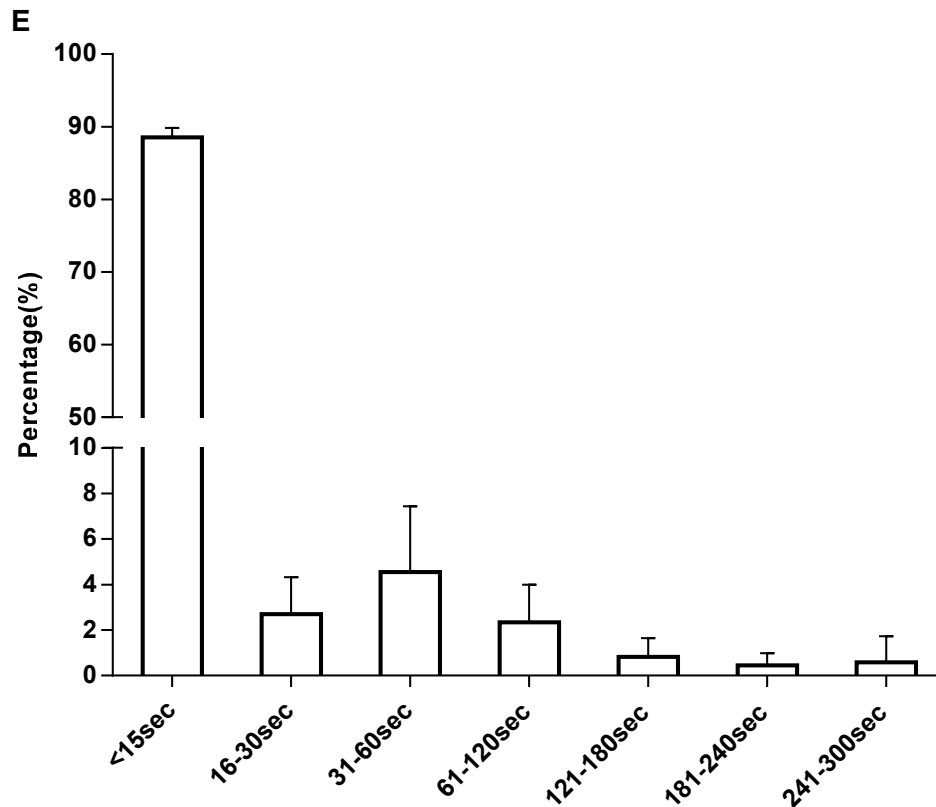


Fig. 5.1 Somatic F-actin dots behavior montage and life time distribution. (A-D) F-actin dot examples from either stage 1 or Stage 2 neurons transfected with LifeAct-GFP. Red arrows denote montage series of each actin dot example. Scale bar, 10 μ m **(E)** Lifetime distribution of somatic F-actin dots. 6 categories are present: <15sec, 16-30sec, 31-60sec, 61-120sec, 121-180sec, 181-240sec and 241-300sec. Dot percentage of each category is plotted. (Mean \pm S.E.M.).

Lifetime distribution through the early three stages is also examined. In order to capture any subtle change of the dot lifetime during early neuronal development, lifetime values were classified into 3 categories: dot population less than 15s, named by “fast-blinking”, dot population between 15s and 240s, by “intermediate blinking”, and dots with lifetime of 240 to 300s, by “long-lasting”. Under these three categories, dot percentages of stage 1 to late stage 3 were plotted (Fig. 5.2A). As shown in the graph, through the early developmental time, number of fast-blinking dots decreases but that of intermediate-blinking and long-lasting dots increases, especially number of fast-blinking dots at stage 1 compare to that at late stage 3, significantly higher (Fig. 5.2A, mean of fast-blinking dots in %, Stage 1: 91.48 \pm

2.587 to Late stage 3: 83.23 ± 2.50 , $p=0.023$ two-way ANOVA, *post hoc* Bonferroni test ($*p<0.05$). Additionally, dot densities of different stages were also determined and Stage 1 cells show a significantly higher value compared to cells of other three phases (Fig. 5.2B, mean of dots density in dots/ μm^2 , Stage 1: 11.43 to Stage 2: 6.160, Early stage 3: 5.634 and Late stage 3: 5.324, $p=0.0012$, one-way ANOVA, *post hoc* Bonferroni test $**p<0.01$).

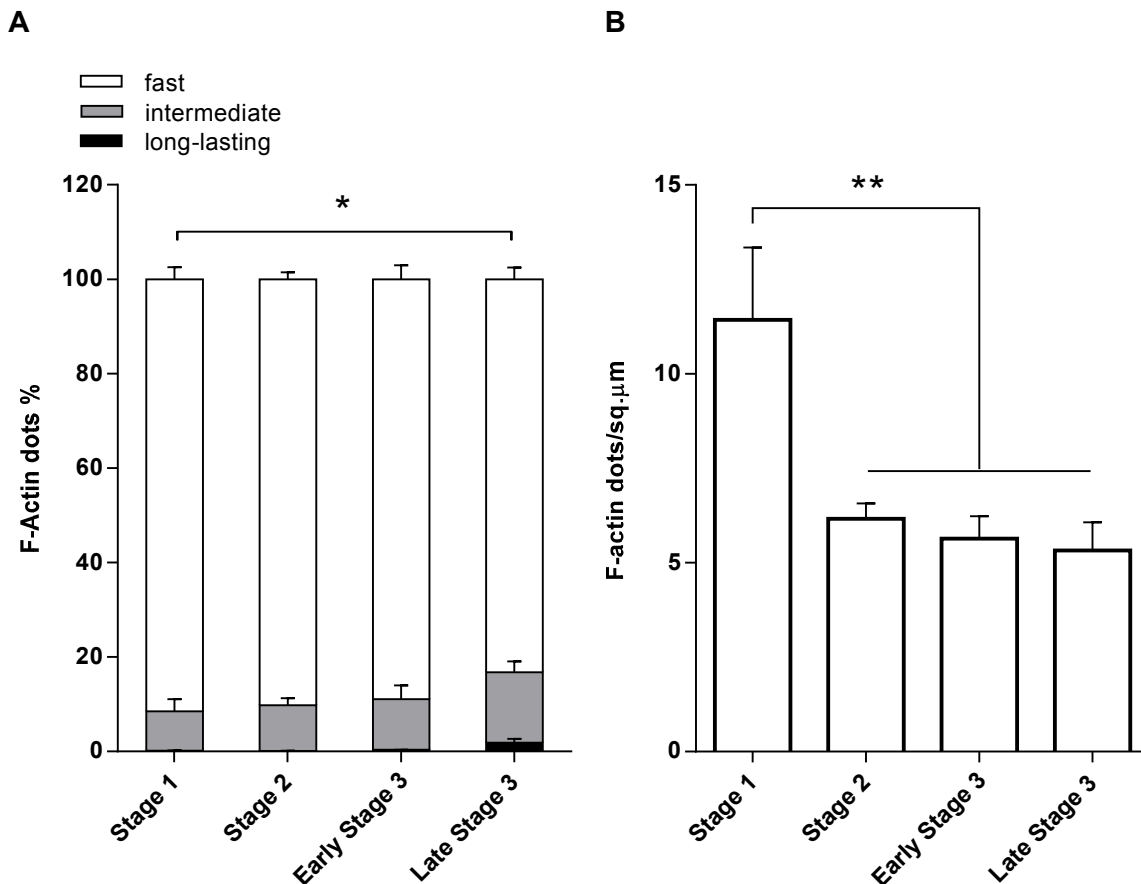
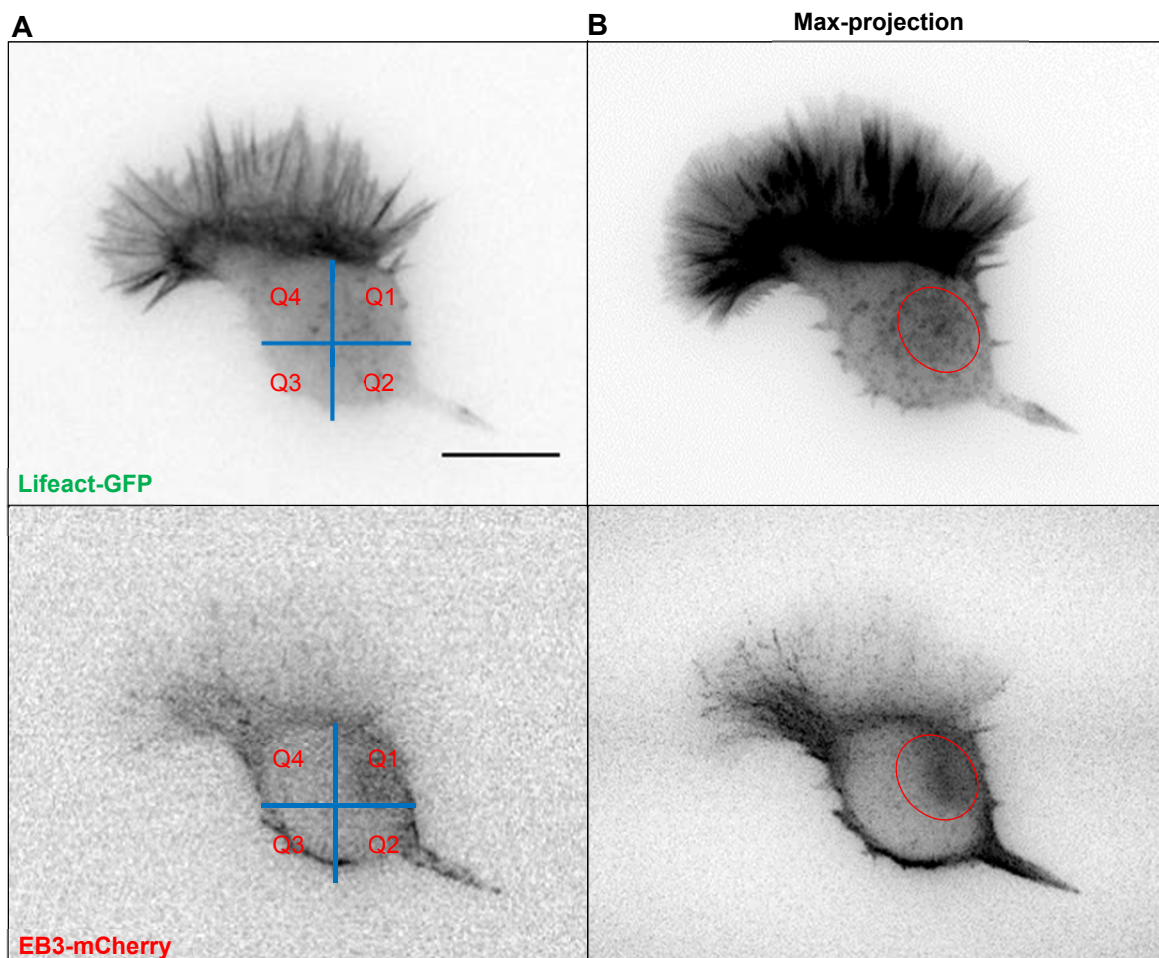


Fig. 5.2 F-actin dot lifetime and density change through the first 3 neuronal developmental stages. (A) F-actin dot percentage of three categories: “Fast-blinking” (<15s), “intermediate-blinking” (15-240s) and “long-lasting” (240-300s) (Mean \pm S.E.M., Two-way ANOVA, $*p<0.05$) **(B)** F-actin dot density in neuronal soma (dots per μm^2). (Mean \pm S.E.M., One-way ANOVA, $**p<0.01$). (Quantification partially by Dr. Meka, ZMNH, Hamburg)

5.2. Actin dots preferentially behave over centrosome

Somatic F-actin dots scatter through the whole cell body; interestingly their preferential appearance close to centrosome can be observed (Fig. 5.3B). To characterize this distributing property, neuronal somas of the first three stages are divided into 4 quadrants, and the quadrant where centrosome (MTOC) locates is assigned as 'Q1', clockwise, following Q2, Q3 and Q4 (Fig. 5.3A). Dots of each quadrant through the whole time lapse were counted. As shown in Fig. 5.3 C, in all three stages, dots appearing in Q1 are significantly more than that in other three quadrants (percentage of dot appearance in %, Stage1: Q1 31.34 ± 1.175 to Q2 22.68 ± 0.8992 Q3 20.77 ± 0.8277 and Q4 25.22 ± 0.5164 , $P < 0.0001$; Stage 2: 32.09 ± 1.011 to Q2 23.54 ± 0.9301 , Q3 19.56 ± 0.7233 and Q4 24.80 ± 0.9967 , $P < 0.0001$; Stage 3: Q1 30.68 ± 1.068 to Q2 24.32 ± 1.016 , Q3 21.01 ± 1.131 and Q4 23.99 ± 0.7794 , $P < 0.0001$. One-way ANOVA).



C

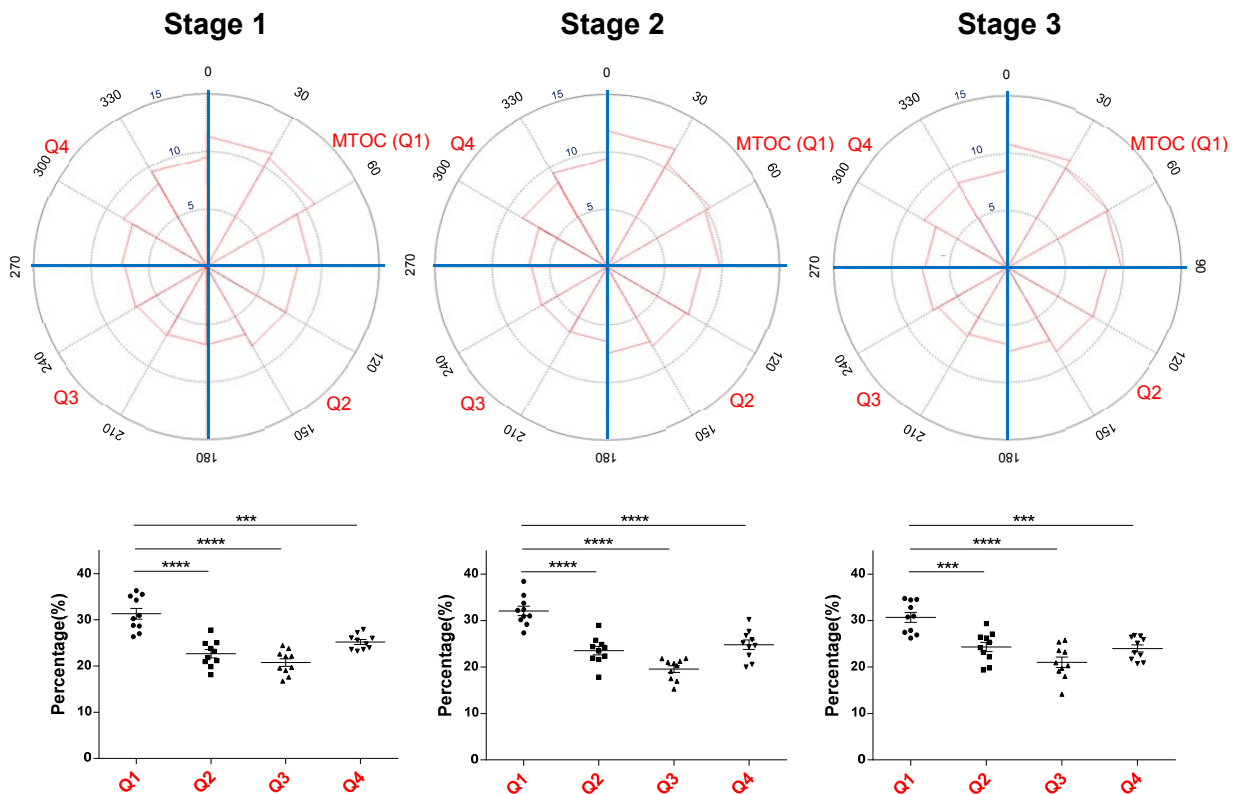


Fig. 5.3 F-actin dots blinking preferentially over centrosome. (A) The cell body of neurons transfected with LifeAct-GFP and EB3-mCherry were divided into four quadrants, Q1 with centrosome (MTOC) located. Scale bar, 10 μ m (B) Max-projection indicates over MTOC area (circled area) higher dot density can be observed. (C) Dots percentage of each quadrant (%) (Mean \pm S.E.M., One-way ANOVA, *** p <0.001, **** p <0.0001).

5.3. Super resolution microscopy exposes fine actin puncta structure surrounding centrosome

To gain insights into the F-actin dots organization around centrosome, super resolution microscopy technique STED was employed. Somatic region of Stage 1 to Early stage 3 neurons were examined. From the max-projection overview of cell body, preferential distribution of F-actin dots around centrosome can again be seen, supporting the aforementioned findings (Fig. 5.4 A2, B2, C2). In zoom-ins (Fig. 5.4 A3,4, B3,4, C3,4), fine dot-like structures of F-actin surround centrosome, in the manner of attaching or floating in

Results

the proximity. Notably, in Early stage 3, over centrosome F-actin structure becomes more condensed (Fig. 5.4 C3,4).

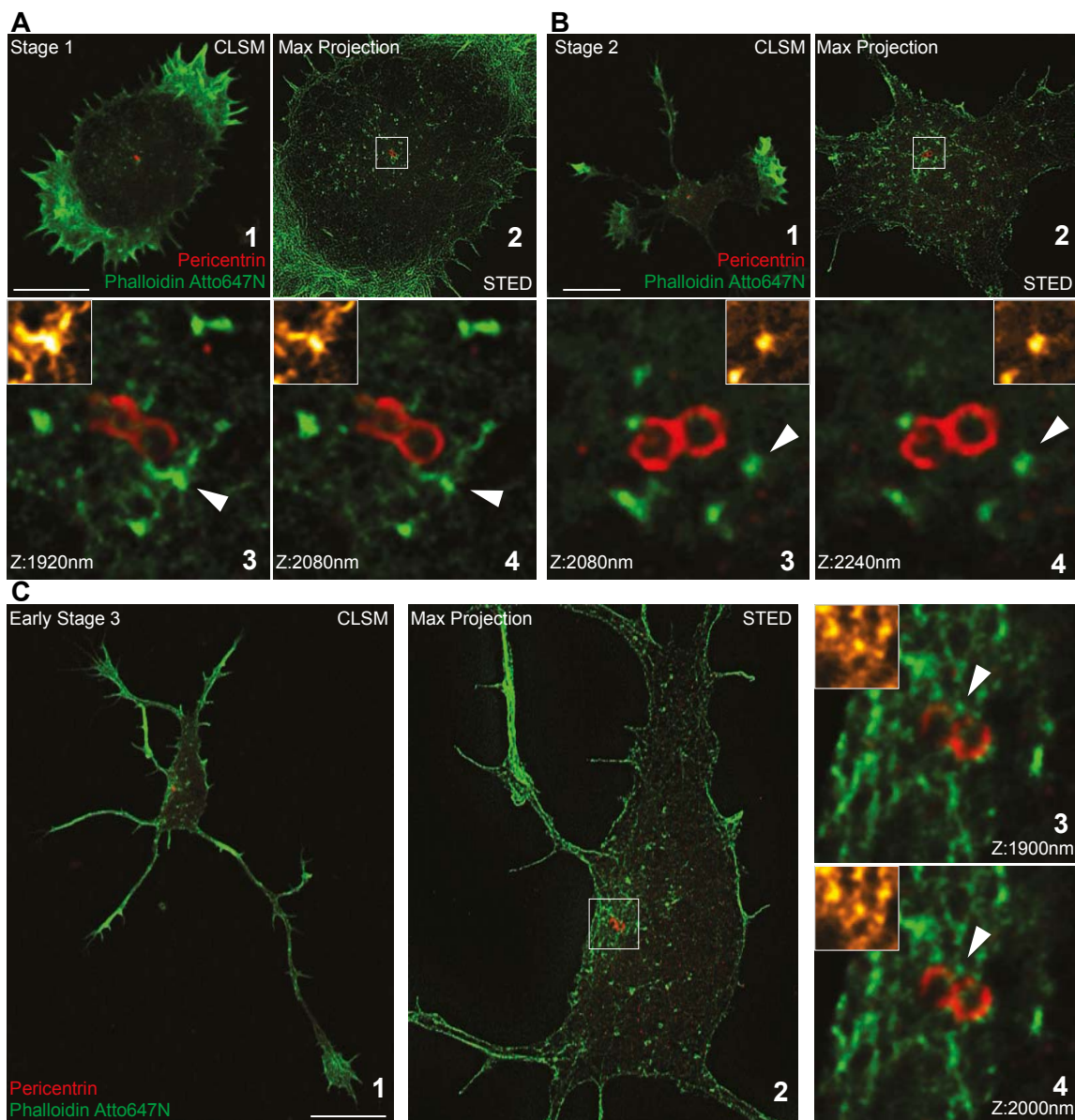
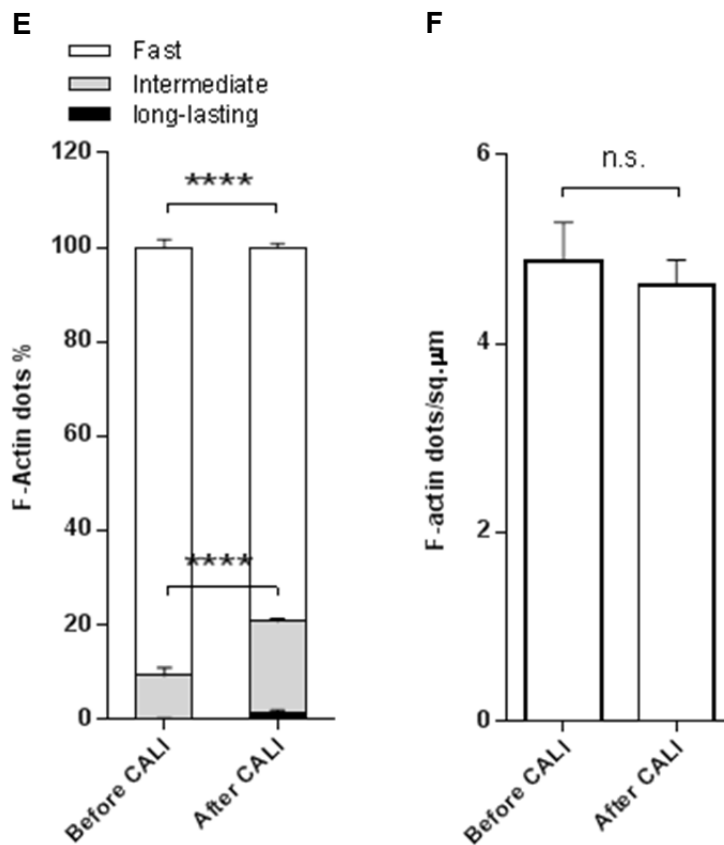
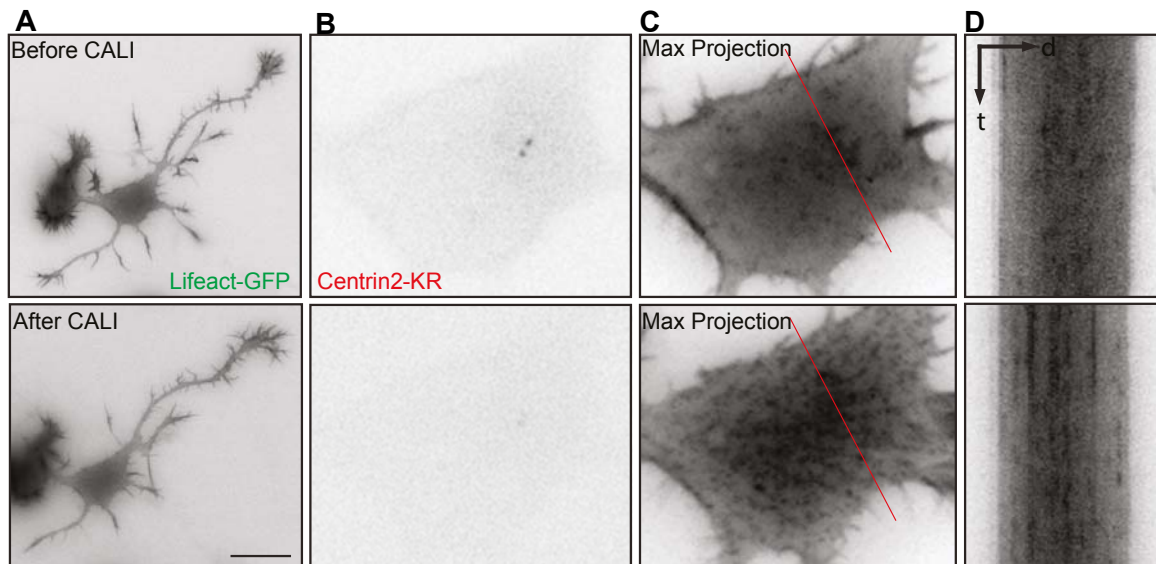


Fig. 5.4 F-actin dots organization around centrosome resolved by STED microscopy. (A1, B1, C1) Confocal images of stage 1 to early stage 3 neurons labeled by anti-pericentrin and phalloidin Atto647N. (A2, B2, C2) Max-projections of z-stacks of image acquired by STED. (A3,4, B3,4 and C3,4) F-actin dots present in a certain depth. Scale bar, 5 μm (A); 10 μm (B, C) (Imaging by Oliver Kobler, CNI, Magdeburg)

5.4. Centrosome inactivation leads to puncta distribution alteration and overall actin dynamic change

Fascinated by this special distribution of F-actin dots, I next got down to finding out the role of centrosome in it. To this end, chromophore-assisted light inactivation(CALI) was employed, centrosomal protein centrin-2 was conjugated to KillerRed, which can be activated via green light (wavelength 520-553 nm), producing reactive oxygen species and in turn inactivate the protein of interest (Bulina, Chudakov et al., 2006).



Results

Fig. 5.5 Centrosome disruption by CALI. (A, B) neurons were transfected with LifeAct-GFP and centrosome were labeled by Centrin-2-KillerRed. Scale bar, 10 μm (C) Max-projection of somatic F-actin dots before and after CALI. (D) Dot profile of a random line region (red line in C) across the neuronal soma before and after CALI. (E) F-actin dot percentage of three categories: “Fast-blinking” (<15s), “intermediate-blinking” (15-240s) and “long-lasting” (240-300s) (Mean \pm S.E.M., Two-way ANOVA, **** $p < 0.0001$). (F) F-actin dot density in neuronal soma (dots per μm^2). (Mean \pm S.E.M., t test). (Quantification done by Dr. Meka, ZMNH, Hamburg)

After disrupting the activity of centrosome, instead of concentrating over centrosome, more evenly-distributing F-actin dots can be seen, forming fiber-like tracks as shown by max-projection (Fig. 5.5C). Interestingly, F-actin dot dynamics is also affected, illustrated by the quantifications of Fig. 5.5E, cells subjected to CALI show a higher percentage of intermediate-blinking dots but lower of fast-blinking dots (mean of F-actin dots in %, intermediate-blinking: before CALI 9.049 ± 1.710 , after CALI 19.296 ± 0.705 ; fast-blinking: before CALI 90.786 ± 1.728 , after CALI 79.309 ± 0.879 ; $p < 0.0001$ by repeated measures two-way ANOVA, *post hoc* Bonferroni test **** $p < 0.0001$). However, dot density before and after CALI has no significant change (Fig. 5.5F). Surprisingly, F-actin dynamics in peripheral growth-cone is also influenced, significantly decreased (Fig. 5.6C, retrograde flow speed of F-actin in $\mu\text{m}/\text{min}$, before CALI: 3.623 ± 0.1735 ; after CALI = 2.721 ± 0.1205 ; **** $p < 0.0001$ by t test).

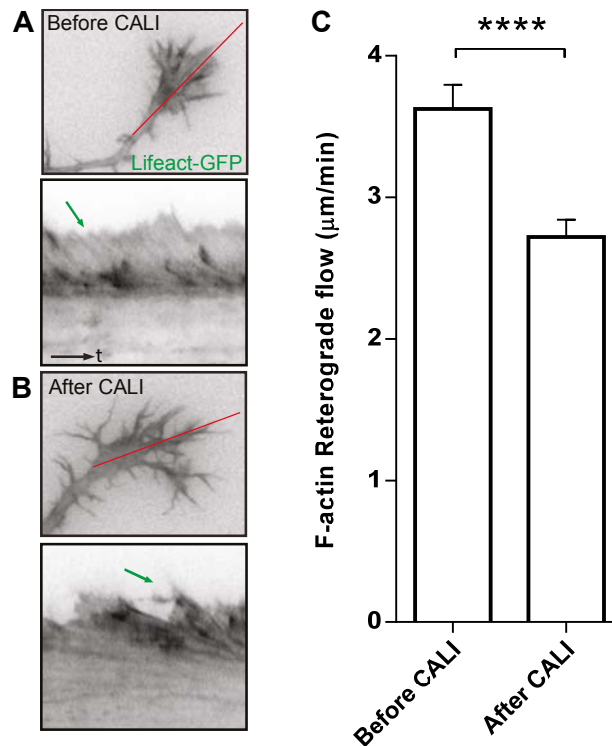


Fig. 5.6 F-actin retrograde flow speed in peripheral tips of neurites. (A,B) Growth-cone of the neuron shown in Fig. 5 A before and after CALI, and accordingly example kymographs demonstrating the speed of retrograde flow. (C) F-actin retrograde flow speed before and after CALI (Mean \pm S.E.M., **** indicates $p < 0.0001$, by t test). (Quantification by Dr. Meka, ZMNH, Hamburg)

5.5. Acute centrosome inactivation alters MT organization

Considering the crucial role of centrosome in MT dynamics (Luders and Stearns, 2007), and also further looking into the mechanism of this centrosome-dependent dot distribution, I also did CALI in term of MT dynamics. MT was labeled by EB3-GFP, a MT plus-end binding protein, allowing me to track the MT behavior in real time (Stepanova, Slemmer et al., 2003). After affecting centrosome activity by green light irradiating, with max-projection, I can see that significantly less and shorter EB3 trajectories present (Fig. 5.7A, B) in the cell body (Fig. 5.7C, D, EB3 trajectories per μm^2 : before CALI 0.1895 ± 0.0095 ; after CALI 0.1427 ± 0.0129 , ** $p = 0.0083$ by t test; EB3 trajectory length in μm : before CALI 4.427 ± 0.1531 ; after CALI 3.134 ± 0.1170 , **** $p < 0.0001$ by t test), suggesting that MT amount and extension is affected,

Results

hence implying under the same context (centrosome inactivation) MT should be involved in this centrosome-dependent dot distribution and possibly in F-actin dynamics.

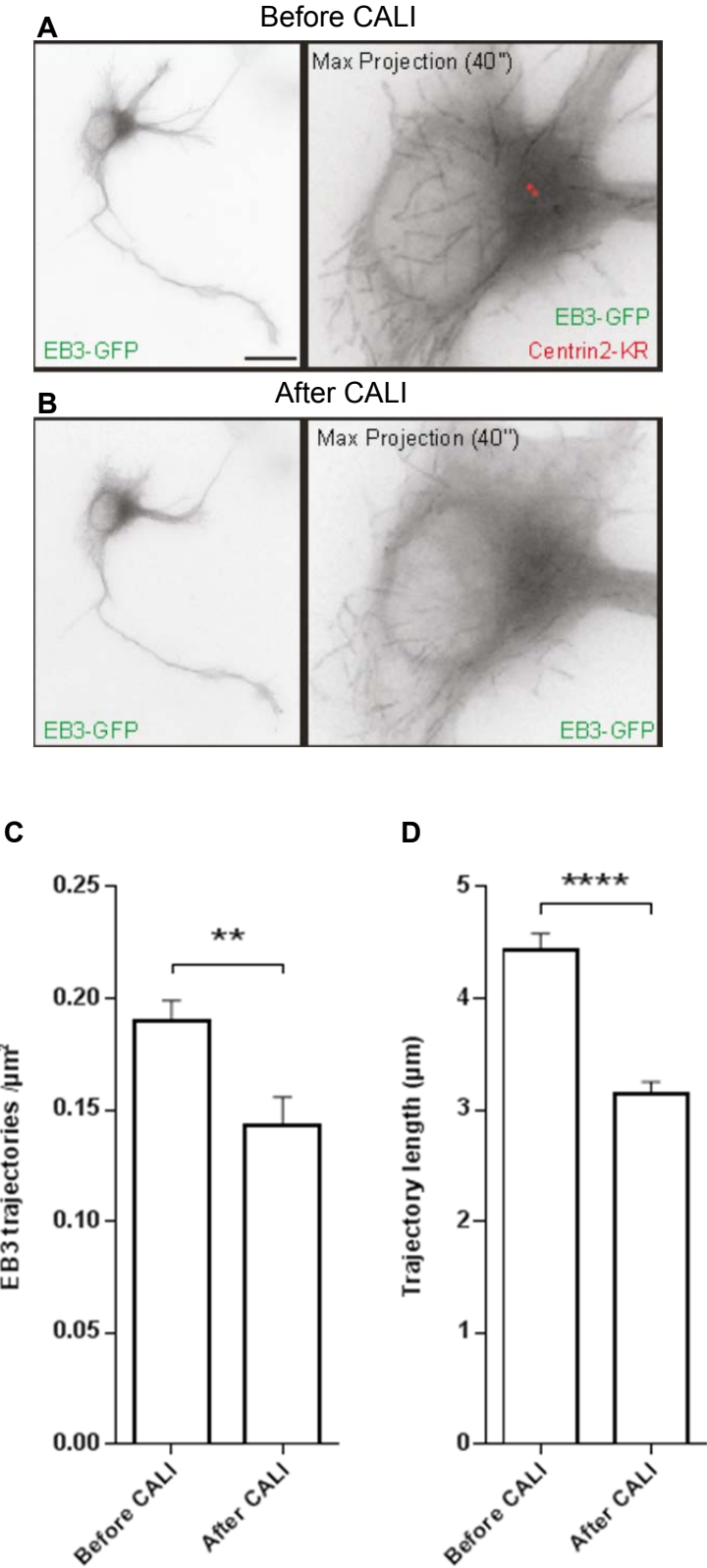


Fig. 5.7 EB3 comet trajectories before and after CALI. (A, B) A neuron transfected with EB3-GFP before and after CALI. Max-projections demonstrate EB3 comet trajectories. Insets are centrosome signal before and after CALI, labeled by Centrin-2-KillerRed. Scale bar: 10 μm (C) EB3 comet trajectory number per μm^2 . $p=0.0083$ $**p<0.01$, by t test). (D) EB3 trajectory length in μm (**** indicates $p<0.0001$, by t test).

5.6. Global MT disruption severely undermine actin dynamics

To further examine how MT could influence F-actin behavior, a strategy to disrupt the overall MT assembly was employed. To this end, Nocodazole was applied to the cultured neurons, which is known to inhibit MT polymerization. Strikingly, after MT breakdown, overall F-actin dynamics is severely undermined, in some extreme case, as shown in Fig. 5.8C, D, somatic F-actin dots cannot be observed anymore, and instead static fiber-like structure is present. In general this change is also reflected by the statistics (Fig. 5.8E, mean of somatic F-actin dots in %: fast-blinking in untreated cells 88.396 ± 2.731 , in Nocodazole-treated cells 32.873 ± 13.829 ; long-lasting dots including fibre-like structures in untreated cells 0.254 ± 0.071 , Nocodazole-treated cells 34.276 ± 12.018 ; $p<0.0001$ by two-way ANOVA, *post hoc* Bonferroni test $**p<0.01$, $***p<0.001$). The dot density is also decreased severely (Fig. 5.8F, mean of dots density in dots/ μm^2 , untreated 7.259 ± 0.3415 , Nocodazole-treated 1.690 ± 0.5506 , by t test $****p<0.0001$). Further, with the drug treatment, much lowered growth-cone activity is also observed (Figure 5.8A, B, G, retrograde flow speed of F-actin in $\mu\text{m}/\text{min}$, untreated 4.7258 ± 0.1918 , Nocodazole-treated 1.6522 ± 0.1183 , by t test $****p<0.0001$).

Results

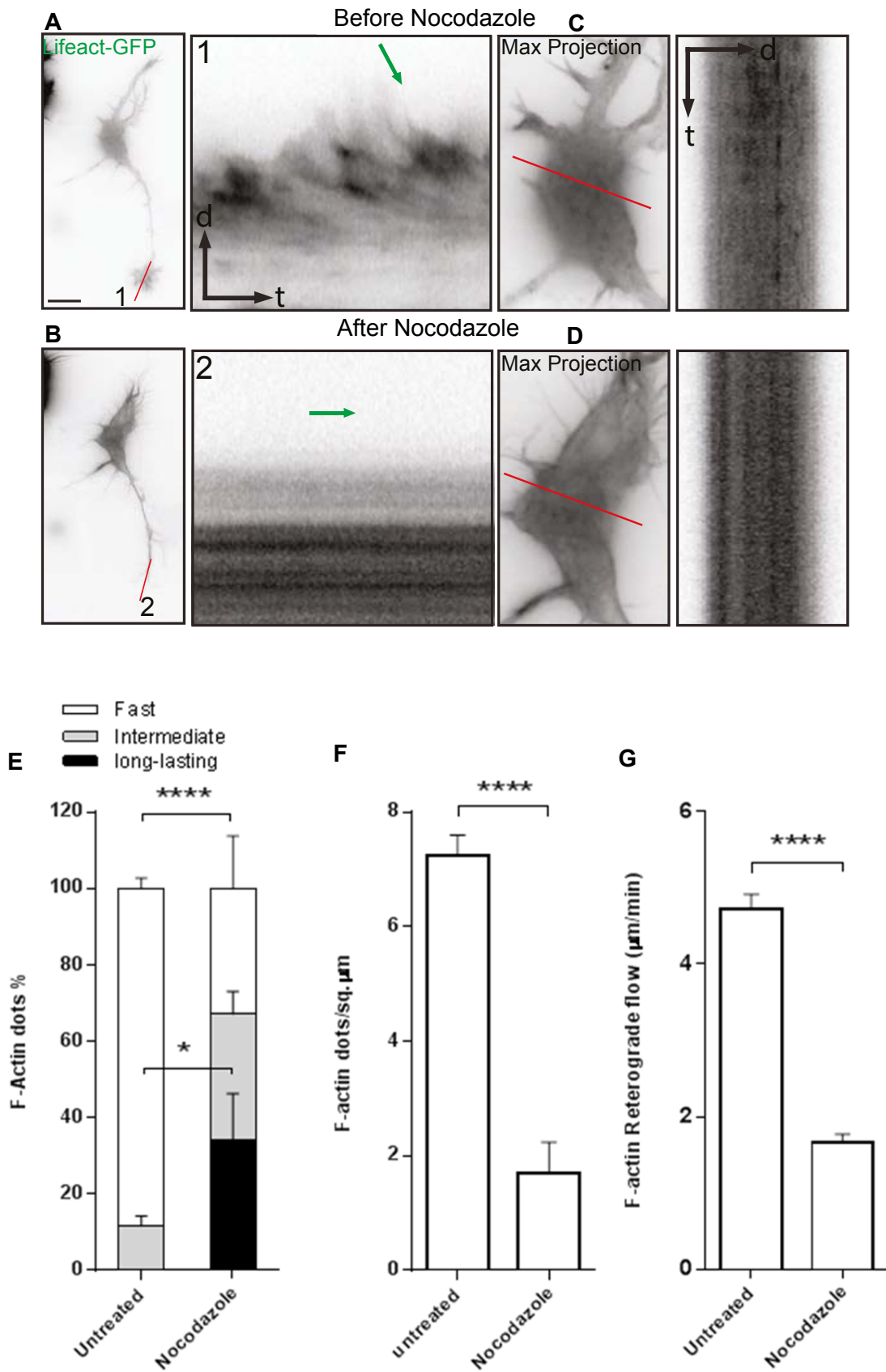


Fig. 5.8 MT destruction generates F-actin stabilization. (A, B) The F-actin activity of a growth-cone before and after treatment, characterized by kymograph. Scale bar: 10 μm

(C, D) Max projection of somatic F-actin dots before and after treatment, illustrated by the reslicing profile of a random line region (red line). (E) F-actin dot percentage of three categories: “Fast-blinking” (<15s), “intermediate-blinking” (15-240s) and “long-lasting” (240-300s) (Mean \pm S.E.M., Two-way ANOVA, * p <0.05, **** p <0.0001). (F) F-actin dot density in neuronal soma (dots per μm^2). (Mean \pm S.E.M., **** indicates p <0.0001, by t test). (G) F-actin retrograde flow speed before and after treatment (Mean \pm S.E.M., **** indicates p <0.0001, by t test).

5.7. MT stabilization favors F-actin dynamics

MT breakdown induces stabilization of F-actin, implying a negative correlation between MT and F-actin dynamics. Therefore we hypothesized that stabilization of MT would increase F-actin dynamics. To test this, I made use of Taxol, which is known to stabilize microtubule and protect it from disassembly. A very low dose (10nM) Taxol was applied to cultured neurons in order to only increase MT stability slightly (Fig. 5.9C, EB3 comet speed in $\mu\text{m}/\text{min}$: untreated 18.85 ± 0.5427 ; Taxol-treated $13.95 \pm 0.4807 \mu\text{m}/\text{min}$, **** p <0.0001 by t test). Interestingly, after drug treatment, somatic F-actin dots show an increased dynamic tendency, with significantly higher percentage of Fast-blinking dots and lower percentage of intermediate-blinking dots (Fig. 5.9B, D; mean of F-actin dots in %, fast-blinking: untreated 88.396 ± 2.731 , Taxol-treated 98.177 ± 0.385 ; intermediate-blinking: untreated 11.35 ± 2.681 , Taxol-treated 1.790 ± 0.384 ; p <0.0001 by two-way ANOVA, *post hoc* Bonferroni test *** p <0.001.). Meanwhile dot density is also elevated (Fig. 5.9E, mean of dots density in dots/ μm^2 , untreated 7.259 ± 0.3415 , Taxol-treated 11.30 ± 0.8245 , by t test ** p <0.01). Expectedly, peripheral F-actin dynamics is enhanced as well (Fig. 5.9A, F, retrograde flow speed of F-actin in $\mu\text{m}/\text{min}$, untreated 4.7258 ± 0.1918 , Taxol-treated 5.7273 ± 0.2150 , $p=0.0006$, by t test *** p <0.001).

Results

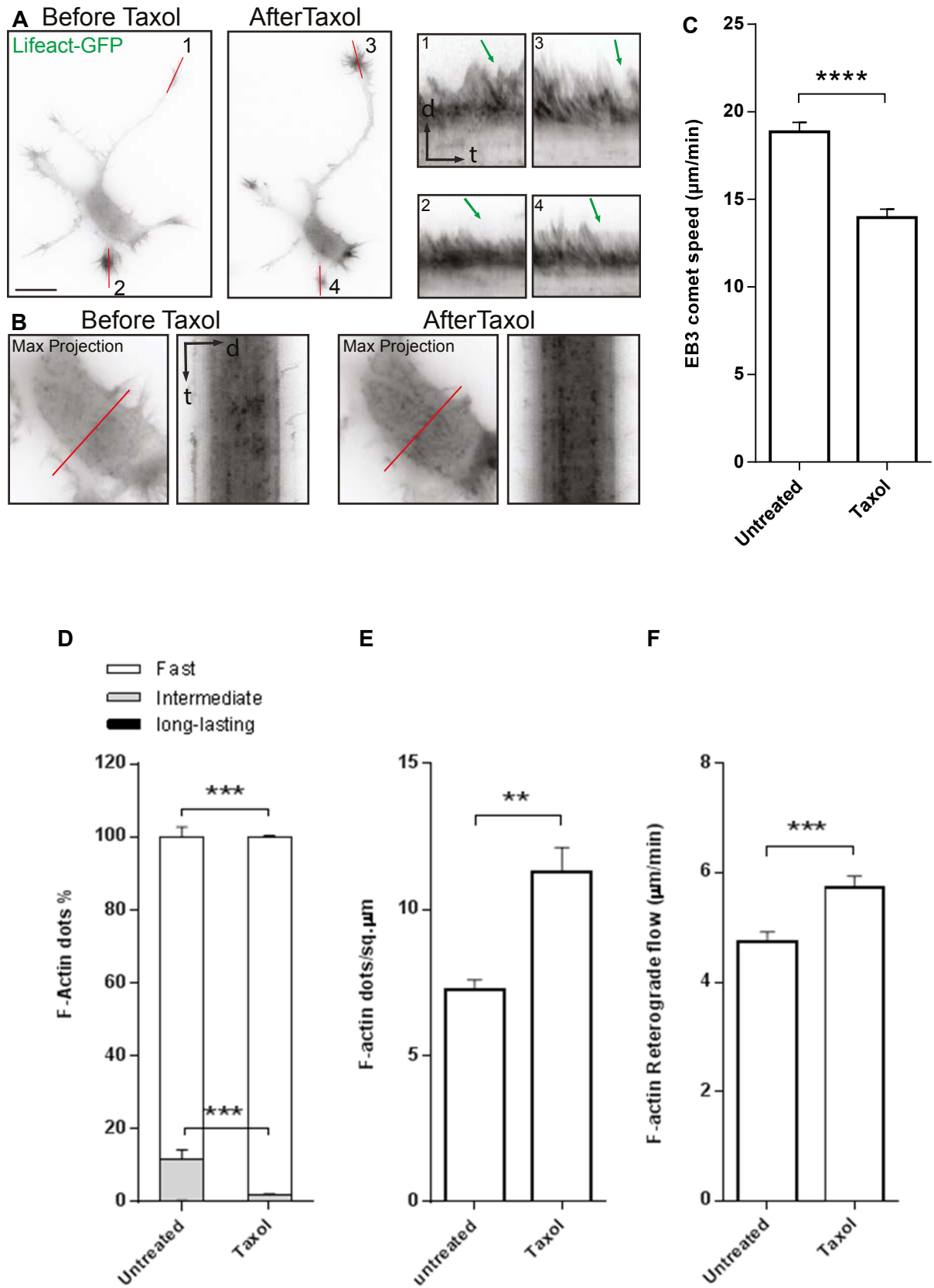


Fig. 5.9 Taxol treatment elevates F-actin dynamics. (A) The F-actin dynamics of growth-cones before and after treatment, demonstrated by kymographs. Scale bar: 10 µm

(B) Max projection of somatic F-actin dots before and after treatment, illustrated by the reslicing profile of a random line region (red line). (C) EB3 comet speed before and after treatment. (Mean \pm S.E.M., **** indicates $p < 0.0001$, by t test). (D) F-actin dot percentage of three categories: “Fast-blinking” (<15s), “intermediate-blinking” (15-240s) and “long-lasting” (240-300s) (Mean \pm S.E.M., Two-way ANOVA, *** indicates $p < 0.001$). (E) F-actin dot density in neuronal soma (dots per μm^2). (Mean \pm S.E.M., ** indicates $p < 0.01$, by t test). (F) F-actin retrograde flow speed before and after treatment (Mean \pm S.E.M., *** indicates $p < 0.001$, by t test).

5.8. The MT and F-actin linker drebrin E is actively involved in overall actin dynamics

Drebrin E, which binds directly to F-actin (Ishikawa, Hayashi et al., 1994), has been shown to interact with MT via binding to EB3, a plus-end protein of microtubule (Geraldo, Khanzada et al., 2008). Knowing of this, I next investigated how drebrin E is involved in the interaction in term of MT and F-actin dynamics. Firstly the endogenous drebrin was checked by immunofluorescence staining, together with F-actin labeling by phalloidin. As shown in Fig. 5.11, I found that drebrin colocalizes with somatic F-actin dots and in peripheral neurites, drebrin also overlaps with F-actin signal. Next I also examined whether drebrin is involved in F-actin dynamics. To do this, neurons which have been recorded by time lapse were fixed and stained with anti-drebrin antibody. With this method, I managed to correlate drebrin intensity to F-actin dynamics and found that where more drebrin distributes is also with faster F-actin dynamics (Fig. 5.12C, retrograde flow speed of F-actin in $\mu\text{m}/\text{min}$, <60% drebrin intensity 2.8868 ± 0.287 , 60-80% drebrin intensity 3.222 ± 0.3432 , 80-100% drebrin intensity 4.0902 ± 0.3153 , $p = 0.0189$ by one-way ANOVA, *post hoc* Dunnett test * $p < 0.05$).

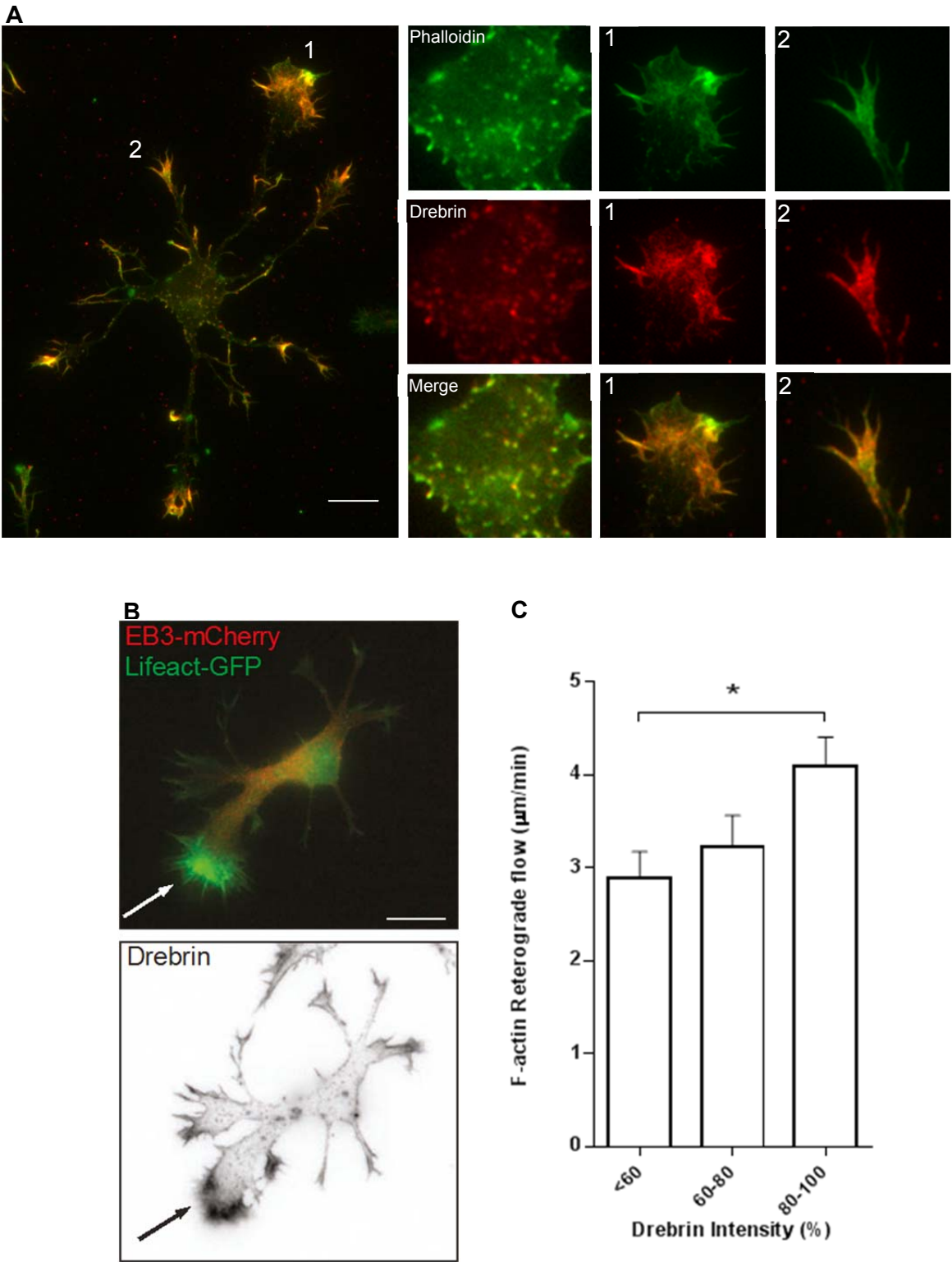


Fig. 5.10 Endogenous Drebrin correlates with F-actin dynamics. (A) Endogenous drebrin (red) colocalizes with F-actin (Green, labeled by phalloidin) both in neuronal soma and in peripheral growth cones and neurite tips. Scale bar, 10µm (B) Neuron transfected with LifeAct-GFP and EB3-mCherry (for live imaging) and labeled by anti-drebrin (after

fixiation). Scale bar, 10 μm . (C) Correlation between drebrin intensity and F-actin dynamical rate. (Mean \pm S.E.M., One-way ANOVA, * indicates $p < 0.05$).

To track drebrin in a dynamical state, drebrin-YFP was transfected into E18 hippocampal neurons and time lapses were taken. Interestingly, the colocalization of drebrin and somatic F-actin dots can be observed (Fig. 5.12D), also confirmed by kymograph analysis (Fig. 5.12E), suggesting drebrin is involved in the F-actin dots. In the periphery, the neurite tip with highest drebrin intensity, excessively protruding beyond F-actin, shows the fastest dynamics, while in neurite with less drebrin there is also lower F-actin motility, suggesting again the correlation between drebrin intensity and F-actin dynamics (Fig. 5.12G, retrograde flow speed of F-actin in $\mu\text{m}/\text{min}$, <60% drebrin intensity 0.8008 ± 0.0891 , 60-80% drebrin intensity 1.3621 ± 0.3494 , 80-100% drebrin intensity 3.1499 ± 0.2479 , $p < 0.0001$ by one-way ANOVA, *post hoc* Dunnett test *** $p < 0.001$).

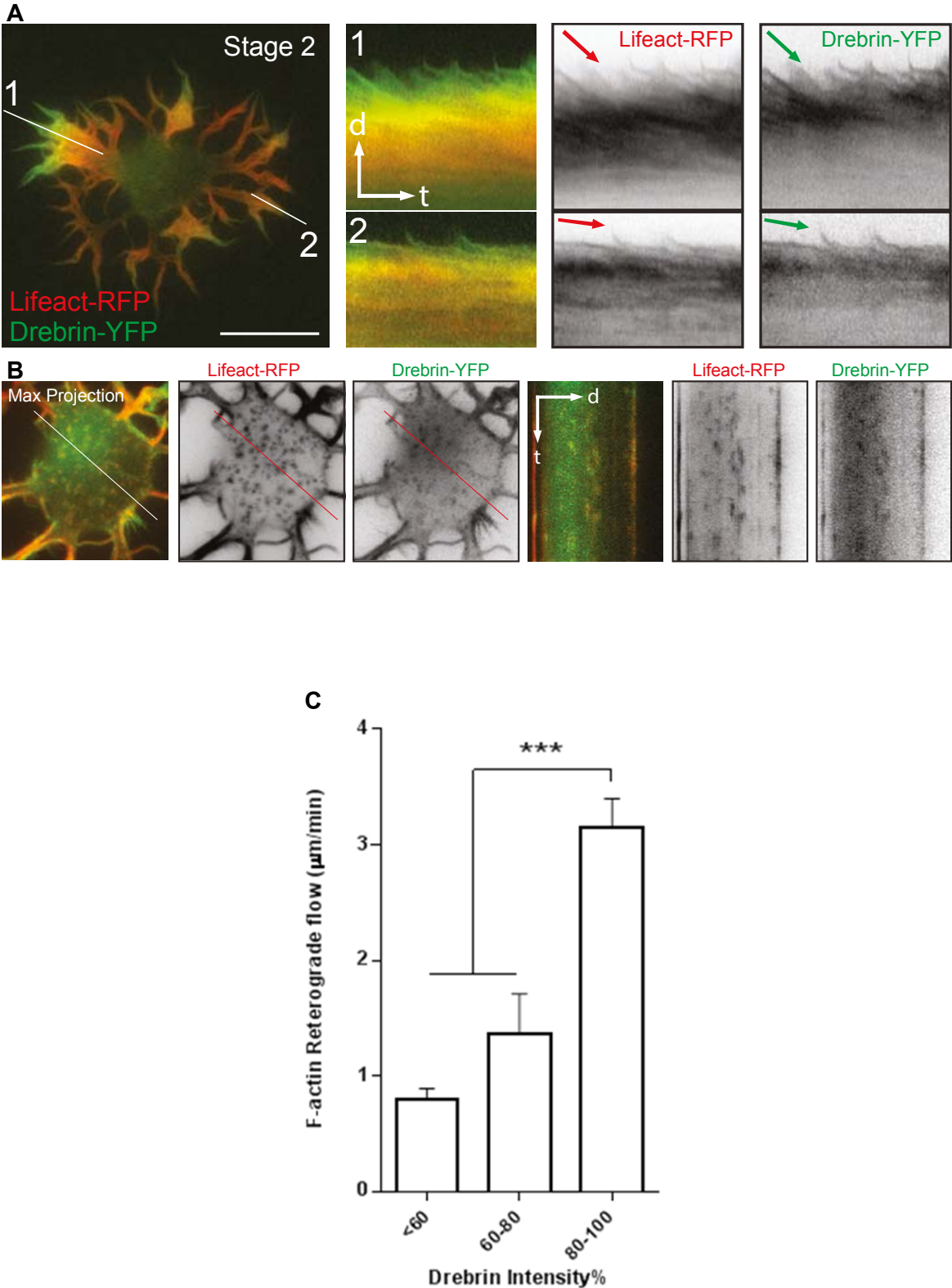


Fig. 5.11 Over-expressed Drebrin is associated with F-actin dynamics. (A) Neuron transfected with LifeAct-RFP and Drebrin-YFP (for live imaging). Scale bar, 10 μm **(B)** Colocalization of LifeAct and Drebrin signal in neuronal soma **(C)** Correlation between

drebrin intensity and F-actin dynamical rate. (Mean \pm S.E.M., One-way ANOVA, *** indicates $p < 0.001$). (Quantification by Dr. Meka, ZMNH, Hamburg)

5.9. Enriched drebrin leads the path of axon extension

To examine how drebrin behaves in a long period, more specifically, during axon elongation, neurons labeled with LifeAct-RFP and Drebrin-YFP were recorded overnight by time lapses (10min interval, 8h long). Interestingly, the neurite tip with enriched drebrin, which is also more motile, extends preferentially and turns into the axon, which is validated by the staining of axonal marker tau-1 (Fig. 5.12 B). During the axon extension, higher intensity of drebrin is always present at the tip (Fig. 5.12 A). However, what should also be noticed is that enriched drebrin does not constantly stay in the same neurite tip but shifts among several tips at the same side of the neuron, which indicates that drebrin itself is also very dynamical.

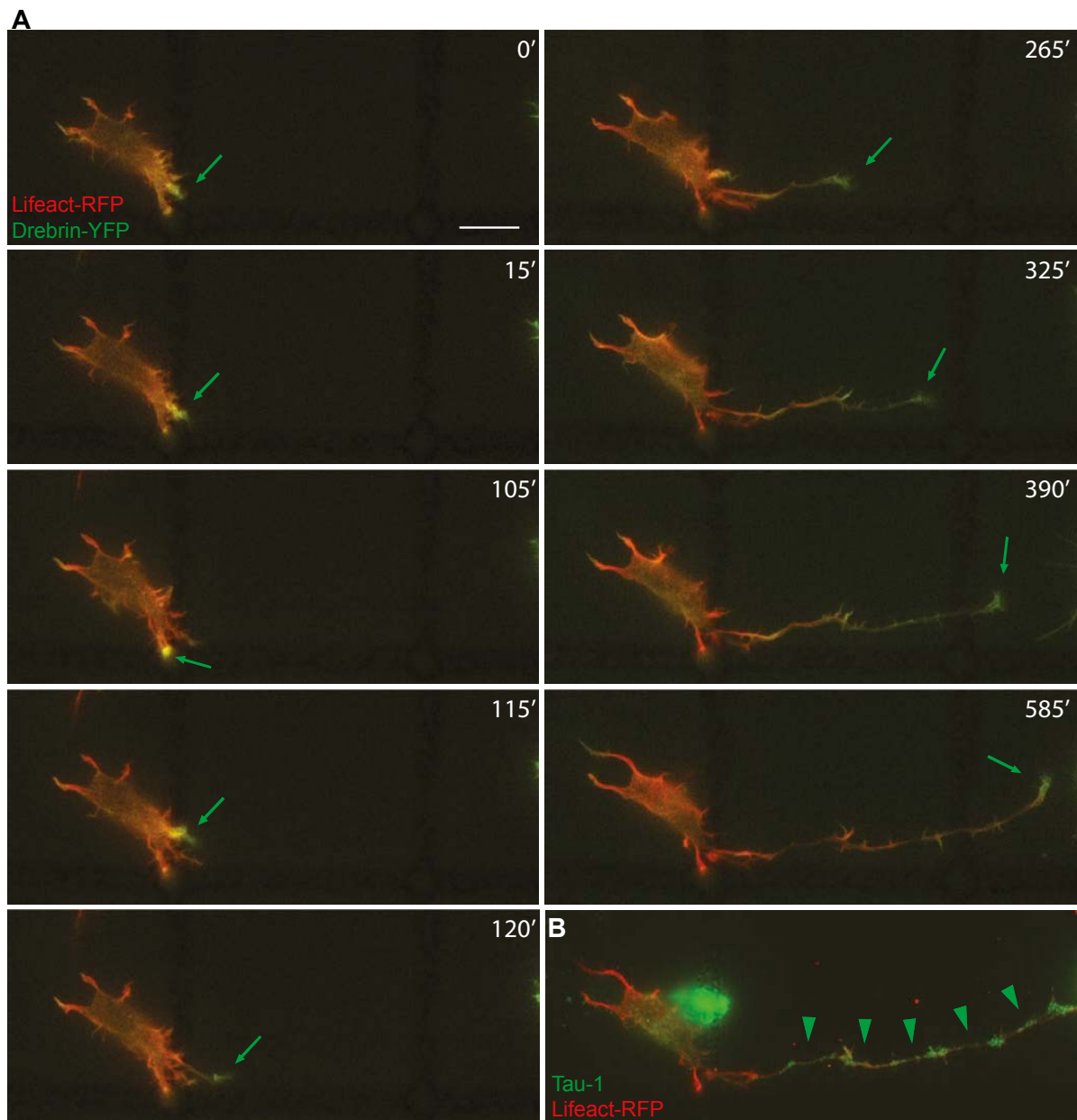
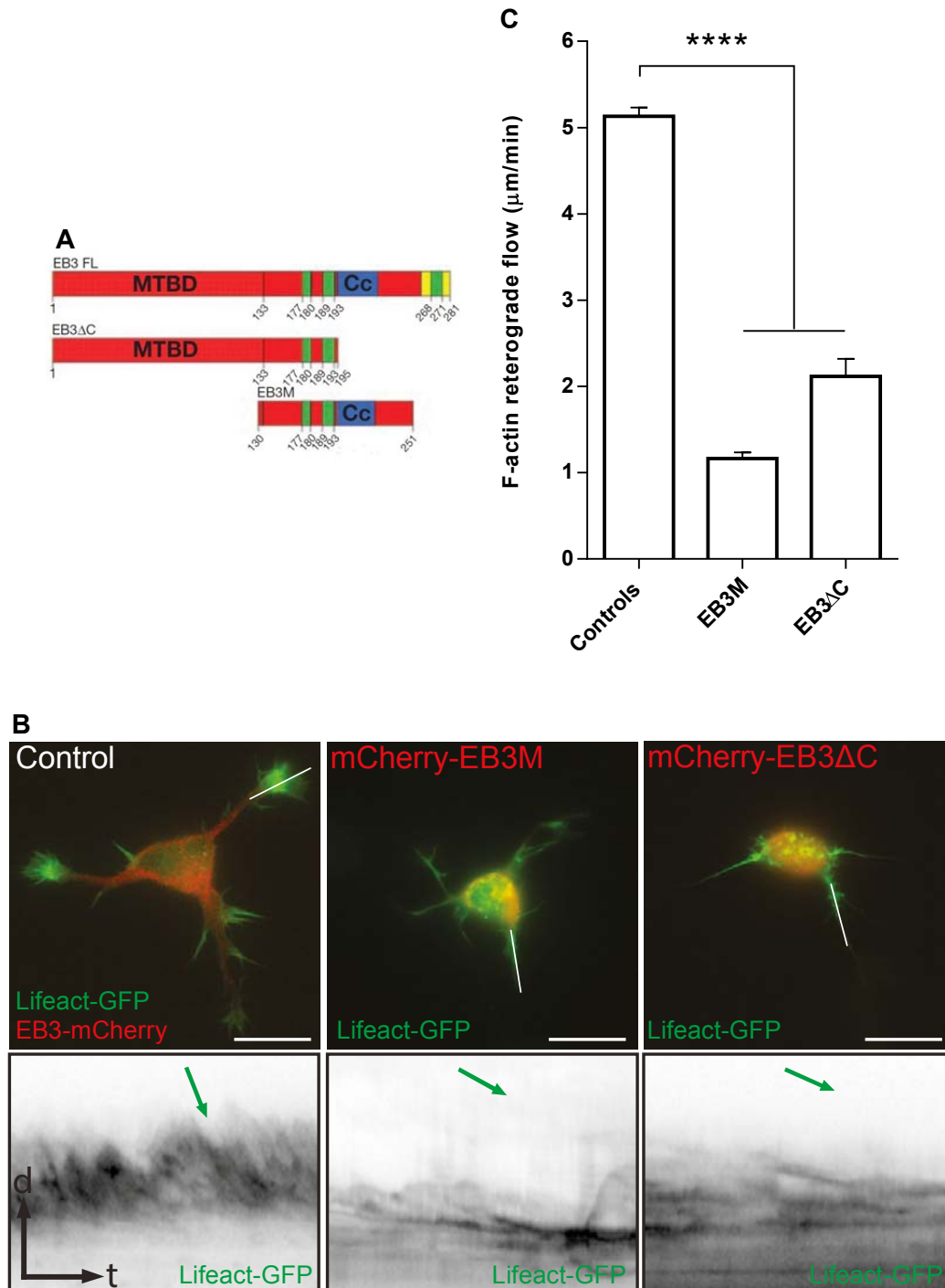


Fig. 5.12 Drebrin is enriched at the neurite tip during axon elongation. (A) Montages from the overnight-recorded neuron transfected with LifeAct-RFP and Drebrin-YFP. Scale bar, 10 μ m **(B)** Immunocytochemistry staining of tau-1 (green), the axonal marker.

5.10. Disruption of MT-actin interaction impairs actin dynamics

Previous studies have described the mechanism of how MT interacts with F-actin via EB3 and drebrin (Worth, Daly et al., 2013). In light of this idea, I decided to find out the

consequence of specifically disconnecting this pathway. To achieve this goal, two types of truncated EB3 (EB3M and EB3ΔC, Fig. 5.13A, (Geraldo, Khanzada et al., 2008)) and one drebrin mutation with an abolition of key phosphorylation at Serine 142 (Drebrin S142A) were employed. All these three constructs were transfected into E18 neurons respectively along with LifeAct and time lapses were acquired.



Results

Fig. 5.13 Truncated EB3s undermine peripheral F-actin dynamics. (A) Scheme of EB3 FL, EB3M and EB3 Δ C (B) Neurons transfected with LifeAct-GFP and either FL EB3-mCherry, or mCherry-EB3M or mCherry-EB3 Δ C, and according kymographs demonstrating the retrograde flow. Scale bar, 10 μ m (C) F-actin retrograde flow speed (Mean \pm S.E.M., One-way ANOVA, **** indicates $p < 0.0001$). (Quantification by Dr. Meka, ZMNH, Hamburg)

As shown in Fig. 5.13B, cells transfected by truncated EB3 show sick morphology with no proper growth cones. The impaired F-actin dynamics in the peripheral neurites could be demonstrated quantitatively (Fig. 5.13C, retrograde flow speed of F-actin in μ m/min, control 5.130 ± 0.1017 , EB3M 1.1623 ± 0.0737 , EB3 Δ C 2.1153 ± 0.2027 , $p < 0.0001$ by one-way ANOVA, *post hoc* Dunnett test **** $p < 0.0001$). Somatic F-actin dots have formed larger and more stabilized clusters (Fig. 5.14A), with significantly decreasing Fast-blinking dots but increasing intermediate-blinking and/ or Long-lasting dots (Fig. 5.14B, mean of F-actin dots in %, fast-blinking: control 90.201 ± 1.489 , EB3M 72.528 ± 2.349 , EB3 Δ C cells 78.636 ± 1.874 ; intermediate-blinking: control 9.681 ± 1.458 , EB3M 20.721 ± 2.426 ; long-lasting: control cells 0.1171 ± 0.045 , EB3M 6.752 ± 0.865 , EB3 Δ C 9.180 ± 3.041 ; $p < 0.0001$ by two-way ANOVA, *post hoc* Dunnett test * $p < 0.05$, ** $p < 0.01$, *** $p < 0.001$ and **** $p < 0.0001$). Also dot intensity decreased accordingly (Fig. 5.14C, mean of dot density in dots/ μ m², control 6.160 ± 0.4068 , EB3M 4.249 ± 0.4423 , EB3 Δ C 3.10 ± 0.7043 ; $p = 0.0028$ by one-way ANOVA, *post hoc* Dunnett test * $p < 0.05$, ** $p < 0.01$).

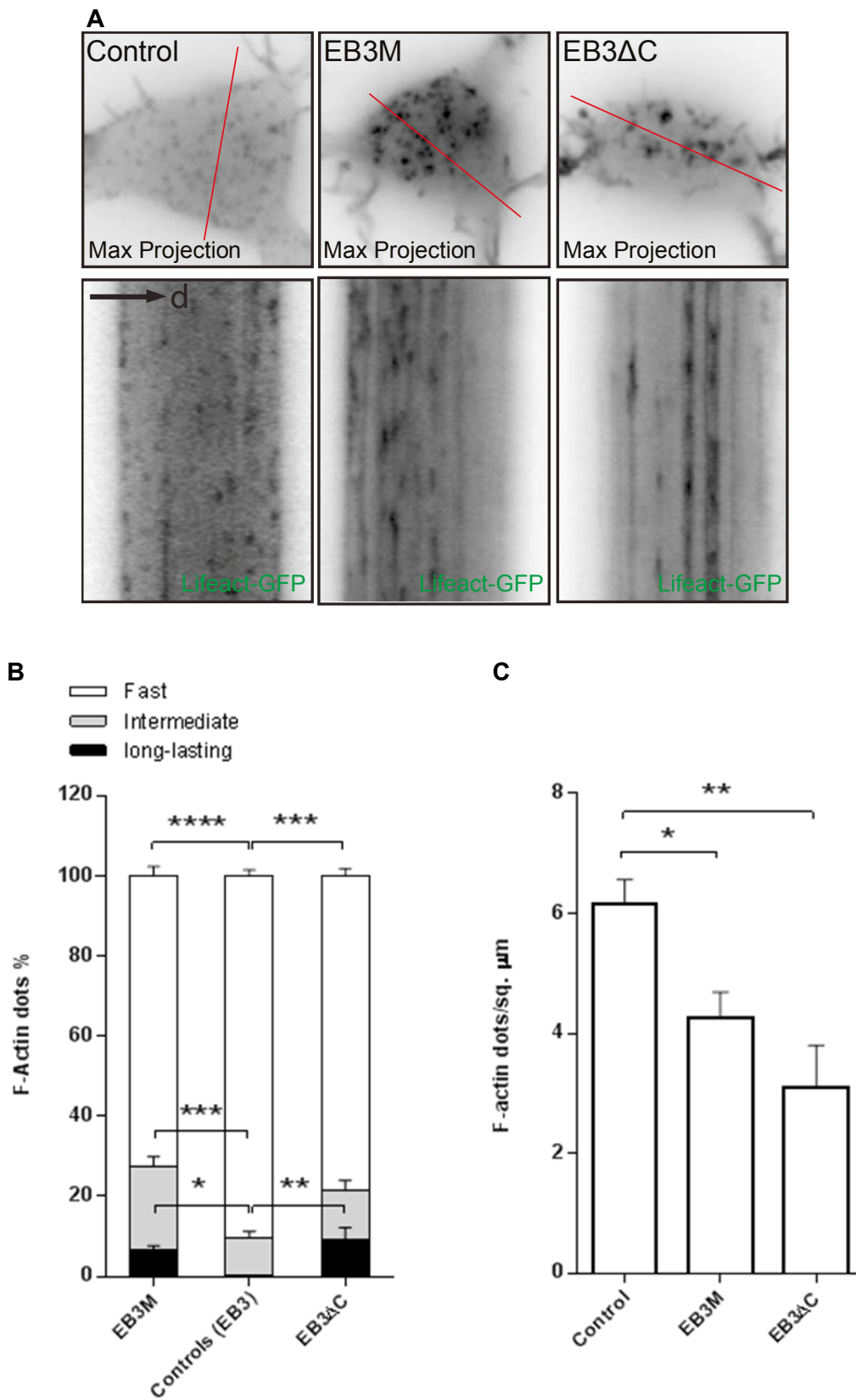


Fig. 5.14 Somatic F-actin dots affected by Truncated EB3s. (A) Neurons transfected with LifeAct-GFP and either FL EB3-mCherry, or mCherry-EB3M or mCherry-EB3ΔC,

Results

and according kymographs illustrating dot profile. **(B)** F-actin dot percentage of three categories: “Fast-blinking” (<15s), “intermediate-blinking” (15-240s) and “long-lasting” (240-300s) (Mean \pm S.E.M., Two-way ANOVA, * p <0.05, ** p <0.01, *** p <0.001, **** p <0.0001). **(C)** F-actin dot density in neuronal soma (dots per μm^2). (Mean \pm S.E.M., One-way ANOVA, * p <0.05, ** p <0.01). (Quantification by Dr. Meka, ZMNH, Hamburg)

Next, drebrin S142A-over-expressed cells were also examined. From the phospho-dead drebrin transfected cells, less F-actin dots appear in the cell body (Fig. 5.14B, F, mean of dot density in dots/ μm^2 , drebrin WT 5.142 ± 0.3395 , Drebrin S142A 2.456 ± 0.3457 , *** p =0.0001 by t test,) and neurite tips tend to be more static (Fig. 5.15A, E, retrograde flow speed of F-actin in $\mu\text{m}/\text{min}$, drebrin WT 1.579 ± 0.1030 $\mu\text{m}/\text{min}$, drebrin S142A 1.090 ± 0.0659 , *** p =0.0001 by t test). By analyzing the lifetimes of F-actin dots, the whole population shows an increasing stability as less Fast-blinking but more intermediate-blinking dots are appearing (Fig. 5.15C, mean of F-actin dots in %, fast-blinking: drebrin WT 91.430 ± 1.614 , drebrin S142A 83.197 ± 2.10 ; intermediate-blinking: drebrin WT 8.189 ± 1.574 , drebrin S142A cells 14.551 ± 2.159 , p =0.0001 by two-way ANOVA, *post hoc* Bonferroni test * p <0.05, ** p <0.01).

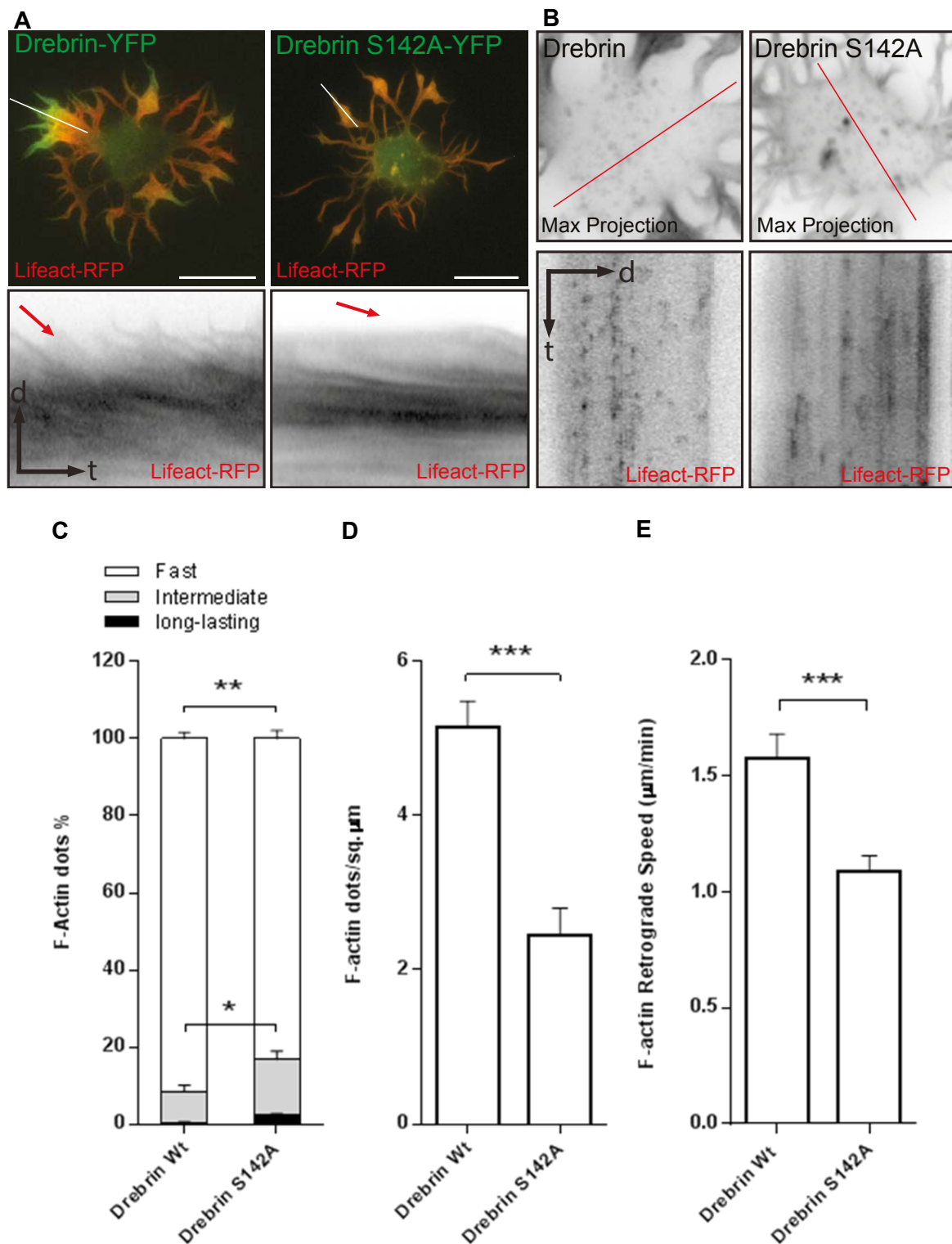


Fig. 5.15 Drebrin S142A (phosphor-dead) decreases overall F-actin dynamics. (A) Neurons transfected with LifeAct-RFP and either WT Drebrin-YFP or Drebrin S142A, according kymographs illustrating retrograde flow. Scale bar, 10 μm (B) Somatic F-actin dots and their profile illustrated by kymograph. (C) F-actin dot percentage of three

Results

categories: “Fast-blinking” (<15s), “intermediate-blinking” (15-240s) and “long-lasting” (240-300s) (Mean \pm S.E.M., Two-way ANOVA, * p <0.05, ** p <0.01). (D) F-actin dot density in neuronal soma (dots per μm^2). (Mean \pm S.E.M., *** indicates p <0.001, by t test). (F) F-actin retrograde flow speed in WT and mutated drebrin transfected neurons (Mean \pm S.E.M., *** indicates p <0.001, by t test). (Quantification by Dr. Meka, ZMNH, Hamburg)

5.11. Breaking of MT-actin interaction stalls growth cone formation

Further I checked the growth cone formation either in control or mutation-transfected cells finding that in all mutated cells the growth cone number has significantly decreased (Fig. 5.16, EB3 1.862 ± 0.1968 VS EB3M 0.2143 ± 0.0802 or EB3 Δ C 0.2162 ± 0.07880 , EB3 $n=29$, EB3M $n=42$, EB3 Δ C $n=37$ cells from at least three different cultures, p <0.0001 by one-way ANOVA, Dunnett's multiple comparisons test, **** p <0.0001; drebrin WT 3.122 ± 0.1812 VS drebrin S142A 2.216 ± 0.2424 , drebrin WT $n=49$, drebrin S142A $n=37$ cells from at least three different cultures, ** p =0.0030), suggesting the effect of EB3 and phosphorylated-drebrin mediated MT-actin interaction on growth cone formation. Additionally neuritogenesis is also impaired in EB3M- or EB3 Δ C- transfected cells (Fig 5.16, total neurite number EB3 5.414 ± 0.3274 VS EB3M 3.810 ± 0.3128 or EB3 Δ C 2.081 ± 0.2986 , EB3 $n=29$, EB3M $n=42$, EB3 Δ C $n=37$ cells from at least three different cultures, p <0.0001 by one-way ANOVA, Turkey's multiple comparisons test, ** p <0.01, **** p <0.0001). However in drebrin S142A transfected cells, the total neurite number shows no significant change (drebrin WT 6.531 ± 0.2125 VS drebrin S142A 7.595 ± 0.5334 , drebrin WT $n=49$, drebrin S142A $n=37$, p <0.0001 by one-way ANOVA, Turkey's multiple comparisons test, non-significant), suggesting phosphorylation does not affect neuritogenesis.

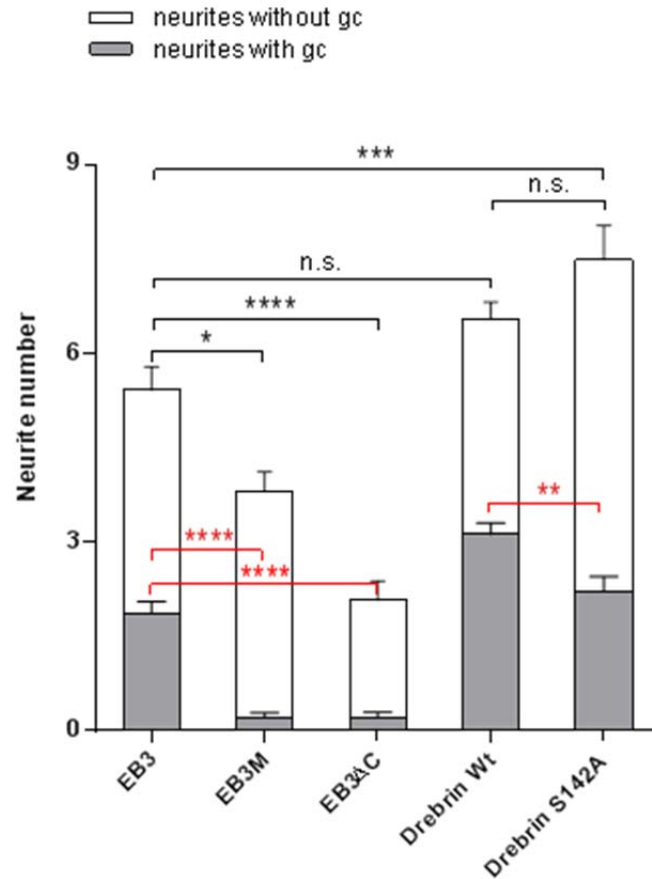


Fig. 5.16 Growth cone formation in control and mutation-transfected cells. The number of neurite with or without growth cone were counted and then subjected to statistical analysis, red markers indicated statistic comparison for growth cone number (Mean \pm S.E.M., One-way ANOVA was conducted for the dataset of EB3, EB3M and EB3 Δ C and for drebrin WT and drebrin S142A student's t test respectively, ** $p < 0.01$, **** $p < 0.0001$). Total neurite number = number of growth cone + number of neurite without growth cone, indicated in black (Mean \pm S.E.M., one-way ANOVA, * $p < 0.05$, *** $p < 0.001$, **** $p < 0.0001$, n.s. =nonsignificant).

6. Discussion

Neuronal polarization occurs at the expense of the coordination of MT and F-actin dynamics, therefore looking into the interaction of MT and actin during neuronal polarization could provide insights into understanding the mechanism of axon formation. In the present study, I have first characterized the neuronal soma actin organization which appears as dot-like structure. Preferential location over centrosome of these dots implies a potential correlation of centrosome with these dots. Inactivation of centrosome leads to the loose distribution of somatic actin dots and the shift to a more stabilized profile and the peripheral actin retrograde flow in growth cone is also surprisingly downregulated, suggesting centrosome is involved in the global actin dynamics in young neurons. Disordered MT organization after centrosome inactivation implies that MTs could play a role in this event. Manipulation of MT stability via pharmacological treatment demonstrates the dominate role of MT in actin dynamics. Drebrin, the linker between MT and actin together with EB3, is turned out involved in and essential for actin dynamics. Further, I have shown that drebrin-mediated MT-dependent actin dynamics is essential for growth cone formation and axon growth. Breakdown of this interaction via introducing truncated EB3 and phosphor-dead drebrin attenuates actin dynamical rate, both in soma and peripheral growth cone, and impairs growth cone formation and hence axon growth. These data underscore the critical role of drebrin-and-EB3-mediated MT-dependent actin dynamics in neuronal polarization.

6.1 Somatic dots, the presence form of dynamic F-actin in neuronal cell body

F-actin dynamics have long been studied in the periphery of the cell, e.g. lamellipodium or protrusion edge of fibroblasts (Pollard and Borisy, 2003; Blanchoin, Boujemaa-Paterski et al., 2014), or neuronal growth cone (Dent, Gupton et al., 2011). Via phalloidin staining and LifeAct labeling, I have observed a population of F-actin-enriched, puncta-like structure in the neuronal soma, which are named as F-actin dots. In live state, these dots continuously appear and disappear with a spectrum of lifetime (Fig 5.1), behaving as ‘blinking’. Here I introduce the somatic F-actin dots as the F-actin dynamic presence in the neuronal cell body. Unlike in growth cone F-actin dynamics is reflected by actin retrograde flow (Forscher, Lin et al., 1992; Van Goor, Hyland et al., 2012), the lifetime of F-actin dot is more representative to its dynamic property. As shown by the lifetime distribution of F-actin dots (Fig 5.1 B) most dots (nearly 90% of the whole population) have a lifetime of less than 15s, contrast to the 2-6min lifetime of veil actin in growth cone (filopodial actin even much more stable) (Mallavarapu and Mitchison, 1999) suggesting that they are mostly highly dynamic. Categorized into three populations: “fast-blinking” (<15s), “intermediate-blinking” (15-240s) and “long-lasting” (240s-300s), the change profile of these dots through the early developmental stages can be tracked. Overall trend shows that fast-blinking dots lessen while intermediate-blinking and long-lasting dots increase. Interestingly, the density of somatic dots drops significantly after stage 1 but sustains relatively stable since then, implying that these dots might be involved in Stage 1 to 2 transition.

Up to date somatic actin architecture has not been systematically investigated rather most studies have been focused on the protruding cell edge, lamellipodia of migrating cell and neuronal growth cone. Technical advance in optical microscopy such as emerging of super resolution microscopy has enabled the thin and highly-dense actin network visible (Hell, 2007; Huang, Babcock et al., 2010). Based on findings and summaries from published work and reviews, it is possible to deduce the organization of the somatic actin. Globally, beneath the

lipid bilayer eukaryotes are coated by a layer of actin network which possesses distinct organizing properties through different area of the cell (Blanchoin, Boujemaa-Paterski et al., 2014). Ventral actin appear as a dense network sheet, embedded by adhesion plaques with actin bundles projected towards other adhesion sites or to the cell edge in epithelial and fibroblast cells (Xu, Babcock et al., 2012). A very detailed depiction about the focal adhesion 'architecture' has been made (Kanchanawong, Shtengel et al., 2010), which could shed light on the longitudinal constitution of ventral layer: residing on the extracellular matrix, integrin signaling layer crosses the cell membrane and connects to force transduction layer where the adhesion marker molecules sit. Then the actin regulatory layer follows and sticks directly to the actin stress fiber. Even though these descriptions cannot directly apply to neurons, they shed light on the neuronal ventral actin structure, favoring to get structural insights about neuronal actin dots

Podosomes are actin-dependent dynamic protrusions of the plasma membrane of metazoan cells into the extracellular matrix (ECM) via protease degradation, which play a role in cell protrusion, motility, migration and so on (Murphy and Courtneidge, 2011). One of criteria to define podosome is the extracellular matrix degradation. The other is the F-actin presence. The colocalization of these two factors identifies the podosome (Murphy and Courtneidge, 2011). After phalloidin staining podosomes also appear morphologically as puncta. This raises the suspicion that podosomes could be the same as the F-actin dots I am characterizing. However, spatially there are differences. Podosomes locate in the ventral cell membrane and intrude into the ECM after maturation (Beaty and Condeelis, 2014). Whereas these somatic F-actin dots distribute through the soma space illustrated by the ultrastructural examination (Fig. 5.4), from the cell bottom to the upper cortex. Even though the non-identical spatial distribution cannot clarify that they are distinct populations, considering the larger scale of actin dot dispersion it could at least manifest that F-actin dots are more than podosomes and might be involved in other cellular activities as well. In other words, podosomes might be only one of the structures that these dots are involved. Since

understanding about these dots is still scant, further studies are needed to elucidate their detailed structure and function.

6.2 F-actin dots are distributed preferentially around centrosome

By quantifying the appearance frequency of dots in the time lapses, I have found that the dots preferentially behave over the centrosome area (Fig. 5.3). Concurrently via super resolution microscopy technology I am capable of observing a small population of dots in the immediate vicinity of centrosome (Fig. 5.4). These evidences have strongly demonstrated that centrosome may exert an effect on the organization of actin dots. This is indeed conceivable since more and more attention has been drawn to the function of centrosome in actin-involved events. For example work from Farina et al. has shown that *in vitro* centrosome could act as an F-actin organization center evidenced by that actin monomers assemble radiantly centering the cellular-isolated centrosome complex (Farina, Gaillard et al., 2016). Centrosome is also shown to modulate actin nucleation in a Arp2/3-dependent way during lymphocyte polarization (Obino, Farina et al., 2016). Interestingly after the centrosome activity is disrupted by CALI, the preferential location of these dots is also lost (Fig. 5.5 C). Therefore this special distribution can be attributed to the centrosome. However the detailed mechanism about how this distribution is achieved remains unknown, further investigation is therefore needed.

6.3 Centrosomal MT is involved in neuronal F-actin dynamics

Early studies on the role of MTs in the cell migration or protrusion have elegantly illustrated that intact MT arrays are essential for cellular motility in various cell types such as fibroblasts (Goldman, 1971), endothelial cells (Gotlieb, Subrahmanyam et al., 1983), monocytes (Zakhireh and Malech, 1980) as well as neuronal growth cones (Bamburg, Bray et al., 1986).

Since the leading lamellar of cell migration or protrusion is actin-enriched and actin-

treadmilling-dependent (Mitchison and Cramer, 1996), it is totally conceivable that MTs exert effects on cellular motility via modulating actin dynamics. In neuron, the growth cone, a highly motile protrusion site, has long been the center for investigating cytoskeletal dynamics. Actin-related processes such as retrograde flow and actin treadmilling have been shown essential for growth cone motility while MTs is known to interact with actin and are more crucial for growth cone advance (Mitchison and Kirschner, 1988; Dent and Gertler, 2003; Lowery and Vactor, 2009). In line with this, results from my thesis have demonstrated that MTs affect actin dynamics in peripheral growth cones, evidenced by that when disturbing the MT organization via either CALI or pharmacological manipulation actin retrograde flow rate is altered.

Of more interest, somatic actin dynamics, illustrated by the various durations of actin dots, has also been affected, which shows a larger population of stabilized dots after centrosomal activity disruption and MT breakdown. Since most previous studies have been focused on growth cone and these dots have not been well characterized yet, these results could be the first time to include the somatic actin dynamics into the description of neuronal actin dynamics. As an analogue, it is noteworthy that the podosomes, which also appear as puncta, have been shown to be MT-dependent (Linder, Hufner et al., 2000; Beaty and Condeelis, 2014).

6.4 Centrosomal MT instructs global F-actin dynamics

6.4.1 Role of centrosomal MT on peripheral actin dynamics

Centrosome inactivation leads to the overall decreased F-actin dynamics. In the peripheral growth cone, lower F-actin retrograde flow rate is induced (Fig. 5.6 A, B, C). Disruption of centrosome activity also gives rise to shorter MT trajectory and lower MT number (Fig. 5.7 C, D), suggesting that MT organization is undermined, which could account for the affected F-actin dynamics. Indeed, with nocodazole treatment to directly abolish the MT polymerization, actin retrograde flow rate has been severely decreased (Fig. 5.8 G). On the other hand,

Discussion

stabilization of MT with low dose of Taxol increases significantly retrograde flow rate (Fig. 5.9 F). This is surprisingly in line with a previous study showing that destabilizing microtubules via nocodazole leads to little lamellipodia protrusion while wash out of nocodazole or switch to taxol treatment activates the cell edge protrusion (Waterman-Storer, Worthylake et al., 1999), which is driven by actin machinery (Pollard and Borisy, 2003). Further, a growth cone guidance study has shown that local application of taxol by uncaging technique attracted growth cone to advance, more noteworthy is that subsequent enhanced lamellipodia protrusion could be observed after taxol application (Buck and Zheng, 2002). These evidences together suggest that a negative correlation exist between MT and F-actin dynamics, namely, when MT instability is elevated, actin is then stabilized and vice versa. This implies that presence of MT polymers is essential for F-actin depolymerization. Additionally the aforementioned study has also emphasized on the role of MT polymerization, highlighting the importance of not only the MT itself but also MT dynamics. This is consistent with a former study that through a gradient treatment assay of nocodazole they uncovered that even 60% of the migration speed of fibroblasts was abolished by nocodazole treatment, the MT level was however not altered very prominently, indicating that MT level does not fully account for the cell locomotion rather another factor is involved, which turned out to be the MT dynamics, confirmed by the taxol treatment assay (Liao, Nagasaki et al., 1995). This is also the case in neuronal growth cone, suggested by e.g. a previous study showed that when abolishing the MT polymerization via nocodazole treatment, the growth cone structure was lost and advance was stalled (Goslin, Birgbauer et al., 1989; Rochlin, Wickline et al., 1996). Very interestingly, on the other hand when the actin polymerization was broken down by cytochalasin B while MT dynamics was intact, the neurite growth still proceeded despite the loss of growth cone (Marsh and Letourneau, 1984). These evidence together further support the active role of MTs in F-actin dynamics.

6.4.2 Modulation of centrosomal MT on somatic actin dynamics

After disrupting the centrosome activity, the somatic F-actin dynamics is also affected: higher percent intermediate-blinking and long-lasting dots appear (Fig. 5.5 E). The same assay was applied to MTs unveiling impaired MT organization characterized by shorter MT length and lower MT density (Fig. 5.7 C, D). This drew my attention to the function of MT. Further pharmacological treatment has directly demonstrated the importance of MT in somatic dots dynamics. With nocodazole treatment actin dots were dramatically slowed down (Fig. 5.8 E) whereas stabilization of MT with low dose of taxol generates significantly more fast-blinking dots (Fig. 5.9 D). These evidences also reflect that MT and actin dynamics are reversely correlated, again implying that MT is essential for actin depolymerization. Notably a very recent study has shown that microtubule plus ends accelerate actin polymerization via forming a complex containing plus end protein CLIP170 and EB1 together with mDia1 (Henty-Ridilla, Rankova et al., 2016) highlighting the modulating role of MT plus ends in F-actin dynamics. Based on this idea I could speculate that disrupting centrosome activity or abolishing MT dynamics would induce much less or even no available plus end proteins, while stabilizing provides more for assisting actin treadmilling. To borrow insights from other ventral actin-containing structures, it has been shown that MTs could induce focal adhesion disassembly via modulating F-actin assembly (Kaverina, Krylyshkina et al., 1999; Ezratty, Partridge et al., 2005), reflecting the reverse correlation between MT and actin.

Pharmacological treatment reveals that MT arrays and its dynamics have correlated with somatic actin dot formation as well. Breakdown of MT arrays and dynamics leads to significant lower dot density while slight increase MT stability induce higher (Fig. 5.8 F and 5.9 E), suggesting that MT has been involved in actin dot formation. However after centrosome activity disruption actin dot density does not show significant change suggesting that acute affection of MT organization somehow does not influence the dot assembly. It has been known that MT dynamics is essential for normal actin treadmilling (Liao, Nagasaki et al., 1995; Waterman-Storer, Worthylake et al., 1999), therefore the reason for this discrepancy

Discussion

could be after centrosome activity disruption there is still MT nucleation available, only at a lower dynamic level and density (Fig. 5.7 C, D), which is however sufficient for assisting actin dot formation. Besides, non-centrosomal MT nucleation also exists in parallel, compensating for decreased centrosomal MT dynamics. Drug treatment is more like an 'all or nothing' effect. With higher concentration of nocodazole (7 μ m), dynamic MT arrays are broken down completely, therefore no available MT nucleation available for promoting actin polymerization. Lower dose of taxol (10nm) only stabilize MTs in a slight degree, which does not abolish MT dynamics but simultaneously makes MT-associated molecules such as plus end binding proteins, which have been shown involved in interacting with actin (Coles and Bradke, 2015), more accessible, thus enhances its effect on actin assembly. Interestingly, podosomes have also been reported to be MT-dependent, when treated with nocodazole, macrophages formed no podosomes, as indicated by actin staining, no show of that typical puncta structure, indicating MTs affect actin organization (Linder, Hufner et al., 2000; Beaty and Condeelis, 2014).

6.5 Drebrin-dependent MT-actin interaction is essential for normal F-actin dynamics

Since MTs and actin have no direct interaction with each other (Griffith and Pollard, 1982), there should be a linker involved. Drebrin, an actin-binding protein, has shown to mediate interaction between MT and actin together with EB3, a MT plus end binding protein (Geraldo, Khanzada et al., 2008). Endogenous drebrin staining reveals that drebrin is enriched in the growth cone and overlapped with F-actin (Fig. 5.10 A) consistent with the aforementioned work. In soma drebrin signal also colocalize with F-actin dots (Fig. 5.10 A), which is expected since drebrin is F-actin-binding protein. This is also the case in drebrin-overexpressed cells, somatic actin overlaps with drebrin (Fig. 5.11 B). While in the growth cone, an interesting phenomenon can be observed, drebrin somehow is excessively protruding over actin (Fig. 5.11 A). What is more, drebrin intensity displays a positive correlation with actin retrograde flow rate, in both endogenous (Fig. 5.10 C) and overexpressed (Fig. 5.11 C) conditions. This

is particular intricate since early work has shown the stabilizing effect of drebrin on actin (Mikati, Grintsevich et al., 2013), which has also been confirmed by the F-actin retrograde rate difference from endogenous-leveled and overexpressed cells (Fig. 5.10 C VS Fig. 5.11 C). So there is an obvious question, why drebrin still promotes actin dynamics since it is supposed to suppress it. The factor behind this could be MTs, which has been reported to be promoted entry into spines by drebrin (Merriam, Millette et al., 2013), the same effect has been observed by me in growth cone as well (data not shown). These evidences highlight the role of MT in this event, which can promote actin dynamics irrespective of the stabilizing effect of drebrin. This is in line with a very recent report showing that MTs accelerate actin polymerization via forming a complex containing plus end protein CLIP170 and EB1 together with mDia1, the actin nucleator (Henty-Ridilla, Rankova et al., 2016). On the other hand it is also confirmed by the pharmacological manipulations, emphasizing that MTs could be the engine driving the actin dynamics.

When I disrupted the MT-actin interaction via introducing siRNA to knock down drebrin (data not shown), or truncated EB3 into developing neurons, the overall actin dynamics is then significantly decreased (F 5.13 C, and 5.14 B), suggesting that drebrin and EB3 are indispensable for MT modulating actin dynamics. Drebrin has also been shown to link MT plus end (EB3) to F-actin through being phosphorylated at serine 142 by Cdk5 (Worth, Daly et al., 2013) (Fig. 3.10). Therefore I also set out to breaking the MT-actin interaction via manipulating this phosphorylation site. After transfected by phospho-dead (S142A) drebrin, neurons display altered morphology, no more polarized drebrin at one tip (Fig. 5.15 A). Meanwhile the somatic and peripheral actin dynamics are also decreased significantly (Fig. 5.15 A-C, E). This further confirms that drebrin is involved in MT modulating actin, which is also phosphorylation-dependent.

In short the above evidences demonstrate that actin treadmilling requires the involvement of dynamic MTs and the interaction between these two is achieved via EB3 and phosphorylated drebrin.

6.6 Drebrin-mediated MT-dependent actin dynamics is essential for neuronal polarization

Early study has shown that the growth cone with higher actin instability often develops into the axon (Bradke and Dotti, 1999), highlighting the role of dynamic actin in the axon fate decision. Interestingly drebrin is enriched in the dynamic growth cone; higher drebrin intensity correlates with faster actin dynamics (Fig. 5.10 B, C). Overexpressed drebrin signal excessively protrudes at the tip of one neurite (Fig. 5.11 A), which can eventually elongate as the axon (Fig. 5.12 A, B). During the whole process of axon extension, a drebrin-enriched tip pioneers, suggesting elevated drebrin level could be necessary for the axon growth. Previous studies have shown that overexpression of drebrin promotes axon growth in primary hippocampal neuron (Mizui, Kojima et al., 2009) and the formation of axonal filopodia and collateral branches *in vivo* and *in vitro* (Ketschek, Spillane et al., 2016), suggesting that drebrin plays a role in axon formation.

High actin dynamics in growth cone accounts for the axon formation. After transfected into neurons, phospho-dead drebrin (drebrin S142A) significantly decreases actin dynamics (Fig. 5.15 D) and also expectedly disrupts growth cone formation (Fig. 5.15 A, drebrin S142A and 5.16). Moreover knockdown of drebrin via siRNA could impair growth cone formation severely (data not shown), implying that both drebrin itself and its phosphorylation are indispensable for intact actin dynamics and growth cone formation. Enriched drebrin promotes MTs entry into the growth cone (data not shown), whereas disruption of MT polymerization abolishes actin dynamics and growth cone formation (Fig. 5.8 B), further previous work has shown that MTs are essential for growth cone genesis (Goslin, Birgbauer et al., 1989), therefore MT could be the crucial factor that drives actin treadmilling and growth cone formation, and eventually axonogenesis. The necessity of MTs in axonogenesis has long been illustrated (Yamada, Spooner et al., 1970; Witte, Neukirchen et al., 2008) and here I have added drebrin to solve this puzzle and provided further understanding about the mechanism.

Meanwhile, the transfection of truncated EB3 (EB3M and EB3 Δ C), which cuts off the link between MT and actin, also leads to impaired actin dynamics and growth cone formation as well as neuritogenesis. This highlights the importance of intact MT-actin interaction in neuronal development.

6.7 Concluding remarks

Taken together, here I have characterized the somatic actin organization, which appears as dot structure and is highly dynamic. Together with actin retrograde flow in the peripheral growth cones, they comprise the global actin dynamics. Preferential distribution of actin dots over centrosome shed light on the correlation of these dots with centrosome, which is validated by the population composition change of dots reflected by different lifetimes and density alteration after centrosome inactivation. Since centrosome has been long known as MT organizing center, this points to the involvement of MTs in actin dynamics, which is also further implied by the organization alteration of MT after centrosome activity disruption. Manipulations of MT stability highlight the instructive role of MT in overall actin dynamics, which also clearly demonstrates an interaction between these two cytoskeletal components. Drebrin E, a known crosslinker of MT and actin together with EB3, is shown to play an essential role in actin dynamics, suggested by the undermined actin polymerization after introducing mutated drebrin and truncated EB3 into neurons. Drebrin E has also been involved in axon formation since sustaining enrichment at axon growing tip can be tracked by long-time time lapse and mutated drebrin abolishes this polarized drebrin-enriched tip as well as growth cone formation. MTs could eventually account for actin dynamics and axonal extension due to the favorable role of drebrin on MTs. Therefore, the present study has provided a new perspective to understand the axon formation question.

7. Materials and Methods

7.1 Materials

7.1.1 Plasmids

Name	Vector	Description
LifeAct-GFP	pEGFP-N1	A gift from Prof. Bradke
RFP-LifeAct	mTagRFP-Lifeact	A gift from Michael Davidson (Addgene plasmid # 54586)
EB3-mCherry	pmCherry-C1	Tagged by Fluorescence Protein of Cherry, A gift from Prof. Bradke
EB3M-mCherry	pmCherry-C1	Created by Dr. Meka based on the backbone of EB3-mCherry
EB3 Δ C-mCherry	pmCherry-C1	Created by Dr. Meka based on the backbone of EB3-mCherry
EB3-GFP	pEGFP-N1	Tagged by GFP, a gift from Prof. Kneussel
Centrin-2-KillerRed	pKillerRed-N	Created by Dr. Claderon de Anda
Drebrin-YFP	pEYFP-N1	WT drebrin, a gift from Prof. Gordon-Weeks(Addgene plasmid #40359)
S142A Drebrin-YFP	pEYFP-N1	S142A, a phosphor-dead mutation, a gift from Prof. Gordon-Weeks(Addgene plasmid # 58335)

7.1.2 Staining reagents

Name	Host	Supplier	Catalogue number
Anti-pericentrin	rabbit	Convance/dcs diagnostics	PRB-432C

Materials and Methods

Anti-drebrin	mouse	Abcam	ab12350
Anti-tau-1	mouse	Millipore	MAB3420
Anti-mouse Alex 647	donkey	Invitrogen	A31571
Anti-rabbit Atto 594	goat	Sigma-Aldrich	77671-1ML-F
Anti-rabbit Abberior STAR 580	goat	Abberior GmbH	2-0012-005-8
Atto 647N Phalloidin		Sigma-Aldrich	#65906
Acti-stain 488 phalloidin		Cytoskeleton, Inc.	# PHDG1-A
Hoechst (DAPI)		Invitrogen	33258

7.1.3 Culture reagents

Name	Provider	Catalogue number
DMEM+GlutaMAX™-I	gibco	61965-026
Neurobasal® Medium	gibco	21103-049
Horse Serum	Capricorn Scientific	DHS-1A
HBSS 1×	gibco	14170-088
Sodium Pyruvate	gibco	11360-039
HEPES buffer solution	Sigma	83264-100ML-F

7.1.4 Chemicals

Name	Provider	Catalogue number
Nocodazole	Sigma Aldrich	M1404-10MG
Taxol	Sigma Aldrich	T7402-1mg
DNase I	Sigma Aldrich	D4263-5VL

Papain	Sigma Aldrich	P5306-25mg
Glucose D-(+)	Sigma Aldrich	G7021-1kg
Poly-L-lysine	Sigma Aldrich	P2636-25mg
Poly-D-lysine	Sigma Aldrich	P7280-50mg
Nitric Acid	Karl Roth	X943.1
Ethanol	Karl Roth	9065.2
Boric acid	Sigma Aldrich	B6768-500g

7.1.5 MEM-HS formula

DMEM+GlutaMAX™-I	428.75ml
Horse serum (heat-inactivated)	50ml
Sodium Pyruvate (100mM)	5ml
HEPES buffer solution (1M)	12.5ml
20% glucose solution	3.75ml

Total volume is 500ml. Filter through 0.22µm filter. Store at 4°C.

7.1.6 Kit

Amata™ Rat Neuron Nucleofector® Kit (Lonza), Cat. No.: VPG-1003

7.2 Methods

7.2.1 Pre-treatment of coverslips or culture chambers

For coverslips (CSc) (Menzel GmbH)

Materials and Methods

300× 12mm (or 100× 25mm) CSs were placed into 1l Glass beaker. Then around 100ml 65% nitric acid was added and the beaker was sealed tightly with parafilm (1st layer) and Alu-foil (2nd layer). Shake vigorously for 2d in a fume hood. Dispose nitric acid in the container for special chemical hazard. Rinse 3× with ddH₂O to remove the remaining acid. Wash at least 5× 10min in 400ml ddH₂O, with vigorous agitation. Separate each CS with dipping shortly in the pure ethanol and place single CS onto different layers of 3mm Whatman paper in a glass petri dish. Bake them overnight at 200°C.

For Culture chamber (Glass-bottomed μ -Dish, ibidi, Cat. No. 81148 or 4-well tissue culture chamber on cover glass II, SARSTEDT, Ref. 94.6190.402)

The 4-well chamber or ibidi dish was placed in glassware. 400 μ l/well nitric acid was added into 4-well chamber or 1ml into ibidi dish. Wash for at least 4h with vigorous agitation. Dispose nitric acid in the container for special chemical hazard and then rinse 5× with ddH₂O. After being washed at least 3× 10min in ddH₂O with vigorous agitation, 100% ethanol was added into the chamber or dish for quick rinsing. Afterwards the wares were dried in the bench and following was sterilization for 30min under UV light. Note: Do not cover the lid during irradiation and expose the inside of wares thoroughly.

7.2.2 Poly-L-lysine or Poly-D-lysine coating

PLL or PDL was dissolved in 0.1M boric acid (pH8.5) with a concentration of 1mg/ml. PLL normally was applied at the concentration of 1mg/ml and PDL at 250 μ g/ml. Coating was carried out overnight at 37°C in the cell culture incubator.

7.2.3 Primary hippocampi neurons preparation

Rats pregnant for 18d were sacrificed after anaesthetized by gas mixture of CO₂/O₂. The utero was fully exposed and all healthy embryos were taken out. Embryo Heads were then decapitated and collected in petri dishes kept on ice. The skull was peeled starting from the

side in order to keep the brain intact and then brains were dissociated and placed in HBSS. After separating the two hemispheres, meninges were carefully removed. Hippocampus were then exposed and dissociated.

All isolated hippocampus were collected in a 15ml falcon tube with 2ml HBSS. After washing twice by HBSS, 2ml fresh HBSS was added plus 25 μ l Papain and 20 μ l DNase I. After digested for 10min at 37°C, the HBSS was removed and 2ml DMEM containing 10%FCS was added to stop the enzymatic reaction. After washed twice by HBSS, the tissues were triturated in 2ml HBSS. 3ml more was then added before 10min centrifugation at 150g. After centrifugation the cell pellet was then dissolved in 5ml MEM-HS and cell number per ml was then determined.

7.2.4 Hippocampi neuronal transfections

Transfections were performed according to the manufacturer's instruction (http://bio.lonza.com/fileadmin/groups/marketing/Downloads/Protocols/Generated/Optimized_Procedure_101.pdf) via the Amaxa nucleoporation system. Briefly, for each transfection 5×10^6 cells were taken, together with 3 μ g plasmids dissolved in 100 μ l transfection buffer in the cuvette, an instant electric shock was then applied. By being transferred in the fresh and pre-warmed medium, the electroporated cells were allowed to recover for 30min and afterwards plated either on glass coverslips (for immunostaining) or on glass-bottomed dish/ tissue culture chamber (for live imaging) in MEM-HS, kept in incubator at 37°C with 5% CO₂ for 4~48 hours before use.

7.2.5 Pharmacological treatments

The following day after plating, certain cells labeled by LifeAct-GFP and EB3-mCherry were selected and recorded via live imaging. Nocodazole was afterwards applied at a concentration of 7 μ M. After 3h treatment, cells were imaged again. Similarly, taxol was used

Materials and Methods

at a concentration of 10 nM after live imaging acquisition, 4h after, time lapses were acquired again.

7.2.6 Immunocytochemistry

Neurons were fixed in 4% paraformaldehyde (PFA) supplemented with 4% sucrose at 37°C for 10min following 3× washing. To permeabilize cell membrane 0.25% Triton X-100 PBS solution was used for 10min. After 3× washing 5% donkey serum was applied for 1h for blocking unspecific protein binding. Primary antibodies were incubated for 2h at room temperature after dilution in PBS plus 2% donkey serum (anti-drebrin at 1/500; anti-pericentrin at 1/500). After 3× washing, fluorophore-conjugated secondary antibodies (anti-mouse (or rabbit) Alexa fluor -568 or -647, 1/500) were incubated at room temperature for 1h. For nuclei staining, Hoechst dye (1/10000) was used. After 3× washing, cells on coverslips were mounted onto the slides using prolong gold (Invitrogen) and stored light-protected and cells on dish or chamber were kept in PBS and stored at 4°C in dark.

7.2.7 Epi-fluorescence imaging

Epi-fluorescence imaging was performed on an inverted microscope (Nikon, Eclipse, Ti) with a 60× objective (NA 1.4). For picture acquiring, cells mounted on slides were placed in the specific holder and single pictures were taken, with the highest light intensity at 1 for each channel of color. For live imaging, cells plated on glass-bottomed dish (ibidi) or culture chamber (Sarstedt) were kept in an acrylic chamber at 37°C with 5% CO₂. Light intensity of each channel was normally set at 8, with exposure time of 300~800ms. Images were captured by CoolSNAP HQ2 camera (Roper Scientific) using NIS-Elements AR software (version 4.20.01 from Nikon Corporation).

7.2.8 Chromophore-assisted light inactivation of Centrosome

The previously-reported method was followed (de Anda, Meletis et al., 2010). Briefly, E18 rat neurons labeled by centrin-2-KR together with LifeAct-GFP or EB3-GFP were plated on glass-bottomed dish (ibidi) or culture chamber (Sarstedt). 24h after plating stage 2 or early stage 3 cells were selected and imaged via time lapses (5min long, 2sec interval) under 60× objective (Nikon, Plan Apo, oil, NA 1.40). Green light (mercury lamp, 520–553 nm excitation filter, 7 W/cm²) was shed on the centrosomes at intensity of 1 for 5-6min. Afterwards cells were allowed to recover for 2-3h before the 2nd time lapse was acquired.

7.2.9 STED microscopy

The imaging was performed with a gated STED microscope (Leica TCS SP8) equipped with a pulsed 775nm depletion laser (80MHz) and a pulsed white light laser (WLL) for excitation. The microscope was covered by an incubation chamber Black i8 2000 LS (PeCon GmbH, Erbach, Germany) fitted to the Leica microscope stand DMI 6000AFC. This chamber can be temperature controlled with the PeCon Temp Controller 2000-2 and Heating Unit 2000. For acquiring Images the Leica Objective HC APO CS2 100x/1.40 Oil was used.

Neurons stained for actin with Atto 647N-Phalloidin (Stock 10nM, 1:40) and pericentrin with anti-rabbit Atto 594 (1:200; Sigma-Aldrich) or anti-rabbit Abberior Star 580 (Abberior GmbH, 1:200), embedded in Mowiol where excited by the WLL at 650nm and 561nm, respectively. Emission was acquired between 660 -730nm for Atto 647N and 580-620nm for Atto 594. The detector time gates for both channels were set from 0.5-1ns to 6ns. Both Dyes were depleted with 775nm. Respective confocal channels uses the same settings as STED channels, except the excitation power was reduced and the detection time gates were set to 300ps to 6ns for both channels. The Format for all images were set to 1024x1024. With an optical Zoom of 5, the resulting voxel size is 23nm for xy and 100-160nm for z. Images were taken with 600 lines per second and line averaging of 8.

7.2.10 Analysis of somatic F-actin dots distribution

Time lapses of 5 min with 2 sec interval (151 stacks) from the cells transfected with Lifeact-GFP were analyzed. Soma area was selected and radially divided into 12 equal segments. Recognizable dots of each segment through 151 stacks were quantified. To characterize dots distribution in the cell body, dot number of each segment through all stacks was summed up and dot density was determined by divided by the area value of each segment in soma. To better specify the MTOC location and use it as a reference, the 'Quadrant' concept was introduced. The 3 segments covering the central microtubule organization area (judged based on the co-transfected EB3-mCherry signal) was considered as the first quadrant, namely Q1, followed by Q2, Q3, and Q4 clockwise (each quadrant covers 3 segments accordingly). Dot density value of each quadrant was normalized to percentage via being divided by the sum number of 4 quadrants in order to rule out the influence of the large range of density values from different cells. Percentage values of each quadrant from 10 cells were then compared.

7.2.11 Analysis of blinking duration and total number of somatic F-actin dots.

Soma area of Lifeact transfected neurons present in the 5 min time-lapses was marked and Reslice plugin of ImageJ was applied, with an output spacing of 1.0 pixel. The reslicing generated a stack of kymographs for each 1.0 pixel throughout the selection, with y-axis representing time (5 min) and x-axis representing distance. Blinking duration and total number of the F-actin dots present in the soma area were then analyzed by manual clicking in ImageJ ROI manager. The Lifeact labeled structures in the kymographs are inhomogeneous, some of them appeared as distinct spots and others appeared as vertical lines of varying lengths along the y-axis. Since y-axis represent time, Lifeact structures that appeared for a very short time appears as distinct spots and the ones which remained for a period of time in the same position appears as vertical lines. The lengths of the vertical lines

are measured in pixels and each pixel represents one frame, which is nearly 2 seconds (since we have 151 frames for a 5 min time-lapse video). Based on lengths, the Lifeact labeled structures are distinguished as fast blinking dots: distinct Lifeact spots or the vertical lines which are less than 7 pixels in length are the ones that disappear in 15 seconds or less; intermediate blinking: vertical Lifeact lines, 8 to 120 pixels in length are the ones which appear for 16 to 240 seconds duration and long-lasting dots: vertical Lifeact lines that are in the range of 121 to 151 pixels in length appears for a period of 241 to 300 seconds. In some experiments, fibers like structures were formed in the cell bodies. After reslicing, these fiber-like structures appeared as vertical and continuous lines in the kymographs, hence these structures were also considered among the long-lasting dots. The total number of blinking dots per square μm was obtained when the sum of fast-blinking, intermediate-blinking and long-lasting F-actin dots normalized to the area of soma marked for analysis.

7.2.12 Analysis of F-actin retrograde flow in growth cones

After defining a line region (1 pixel wide) along the F-actin retrograde flow either in the growth cone or in the lamellipodia of Lifeact (tagged with GFP or RFP) transfected rat hippocampal or mouse cortical neurons which are present in the 5 min time-lapse videos, kymograph was generated using ImageJ (Menu “Analyze” → Multikymograph → Multikymograph). From the kymographs, individual retrograde trajectories of F-actin were tracked and average slope value of these trajectories was measured and present in $\mu\text{m}/\text{min}$.

7.2.13 EB3 comets quantifications

For measuring the average speed of EB3 comets in the neurites, time-lapses of rat hippocampal neurons (stage 2 and stage 3) co-transfected with EB3mCherry and Lifeact-GFP were used. Lines were drawn along the length of each neurite shaft to generate kymographs (with a line width of 1 pixel). From the kymographs, slope of each recognizable

Materials and Methods

EB3 comet was measured. Data were represented as average speed of EB3 comets ($\mu\text{m}/\text{min}$).

For CALI-treated cells, the soma area was selected and all stacks from the time-lapse were merged with “Max-projection” (ImageJ). I traced EB3 trajectories within this area using “ROI manager” (ImageJ), to count the number of trajectories and measure the length. The density of the traced EB3 trajectories was calculated by dividing the number of EB3 trajectories by soma area (μm^2).

7.2.14 Drebrin fluorescence intensity measurement in the growth cones

Fluorescence intensities of endogenous drebrin (stained by drebrin antibody) and drebrin overexpressing neurons (the 5 min time-lapse videos of cells transfected with Drebrin-YFP plasmid) in all the growth cones of the neurites from stage 2 cells were measured. We obtained xy coordinates of all pixels in the region by delineating the individual growth cone areas for each neurite. In case of endogenous drebrin intensity measurements, we delineated the individual growth cone areas for each neurite by applying Renyi's entropy auto thresholding method (Image J). In case of Drebrin-YFP overexpression time-lapse videos, for delineation, each neurite growth cone area was cropped from the 5 min time-lapse video and by applying mean auto thresholding method (Image J). Using this approach, we were able to define the location of the dynamic neurites more precisely throughout the time-lapse from all the 151 frames of 5 min videos (frame interval, approx. 2 sec). We used the obtained xy coordinates to retrieve the original intensity values from the growth cones. Since there are 151 frames in the time lapses of drebrin overexpressing cells, the procedure was automated with an R-script. Within each cell, the neurite with highest intensity of drebrin was set to 100% and other neurites were normalized accordingly, to obtain drebrin intensity (%). In the graphs, the drebrin intensity (%) values were plotted against the F-actin retrograde flow values from the respective neurites.

7.2.15 Neurite and growth cone number quantifications

The total number of neurites, with and without growth cones, within each cell was manually counted. Growth cones were distinguished by their round or conical shape with thin finger-like filopodia and flat lamellipodia between them. Bar graph depicts the mean of number of neurites obtained from each group.

7.2.16 Image processing

Linear adjustments of brightness and contrast were performed on images using Photoshop CS or ImageJ.

7.2.17 Statistical analysis

Statistical analysis was performed using the GraphPad Prism 6 software. Data shown in the graphs were collected from at least three independent experiments. The Student's t test (two-tailed) was used to compare means of two groups, whereas analysis of variance (ANOVA) test was used when comparing more than two groups. Asterisks *, **, *** and **** represents $p < 0.05$, 0.01, 0.001 and 0.0001 respectively. Error bars in the graphs always represent standard error of mean.

8. References

- Akhmanova, A. and M. O. Steinmetz (2008). Tracking the ends: a dynamic protein network controls the fate of microtubule tips. *Nat Rev Mol Cell Biol* 9(4): 309-322.
- Akhmanova, A. and M. O. Steinmetz (2010). Microtubule +TIPs at a glance. *Journal of Cell Science* 123(20): 3415-3419.
- Alushin, G. M., G. C. Lander, E. H. Kellogg, R. Zhang, D. Baker and E. Nogales (2014). High-Resolution Microtubule Structures Reveal the Structural Transitions in $\alpha\beta$ -Tubulin upon GTP Hydrolysis. *Cell* 157(5): 1117-1129.
- Alvey, P. L. (1986). Do adult centrioles contain cartwheels and lie at right angles to each other? *Cell Biology International Reports* 10(8): 589-598.
- Andersen, E. F. and M. C. Halloran (2012). Centrosome movements in vivo correlate with specific neurite formation downstream of LIM homeodomain transcription factor activity. *Development* 139(19): 3590-3599.
- Aoki, C., Y. Sekino, K. Hanamura, S. Fujisawa, V. Mahadomrongkul, Y. Ren and T. Shirao (2005). Drebrin A is a postsynaptic protein that localizes in vivo to the submembranous surface of dendritic sites forming excitatory synapses. *The Journal of Comparative Neurology* 483(4): 383-402.
- Applewhite, D. A., K. D. Grode, D. Keller, A. Zadeh, K. C. Slep and S. L. Rogers (2010). The Spectraplakins Short Stop Is an Actin–Microtubule Cross-Linker That Contributes to Organization of the Microtubule Network. *Molecular Biology of the Cell* 21(10): 1714-1724.
- Azimzadeh, J. and W. F. Marshall (2010). Building the Centriole. *Current Biology* 20(18): R816-R825.
- Baas, P. W., M. M. Black and G. A. Banker (1989). Changes in microtubule polarity orientation during the development of hippocampal neurons in culture. *The Journal of Cell Biology* 109(6): 3085-3094.
- Baas, P. W., J. S. Deitch, M. M. Black and G. A. Banker (1988). Polarity orientation of microtubules in hippocampal neurons: uniformity in the axon and nonuniformity in the dendrite. *Proceedings of the National Academy of Sciences of the United States of America* 85(21): 8335-8339.
- Bai, J., R. L. Ramos, J. B. Ackman, A. M. Thomas, R. V. Lee and J. J. LoTurco (2003). RNAi reveals doublecortin is required for radial migration in rat neocortex. *Nat Neurosci* 6(12): 1277-1283.

References

- Bamburg, J. R., D. Bray and K. Chapman (1986). Assembly of microtubules at the tip of growing axons. *Nature* 321(6072): 788-790.
- Barnes, A. P. and F. Polleux (2009). Establishment of axon-dendrite polarity in developing neurons. *Annu Rev Neurosci* 32: 347-381.
- Barth, A. I. M. and W. J. Nelson (2002). What can humans learn from flies about adenomatous polyposis coli? *BioEssays* 24(9): 771-774.
- Barth, A. I. M., K. A. Siemers and W. J. Nelson (2002). Dissecting interactions between EB1, microtubules and APC in cortical clusters at the plasma membrane. *Journal of Cell Science* 115(8): 1583-1590.
- Bashour, A.-M., A. T. Fullerton, M. J. Hart and G. S. Bloom (1997). IQGAP1, a Rac- and Cdc42-binding Protein, Directly Binds and Cross-links Microfilaments. *The Journal of Cell Biology* 137(7): 1555-1566.
- Basto, R., J. Lau, T. Vinogradova, A. Gardiol, C. G. Woods, A. Khodjakov and J. W. Raff (2006). Flies without Centrioles. *Cell* 125(7): 1375-1386.
- Beaty, B. T. and J. Condeelis (2014). Digging a little deeper: The stages of invadopodium formation and maturation. *European Journal of Cell Biology* 93(10–12): 438-444.
- Bito, H., T. Furuyashiki, H. Ishihara, Y. Shibasaki, K. Ohashi, K. Mizuno, M. Maekawa, T. Ishizaki and S. Narumiya (2000). A Critical Role for a Rho-Associated Kinase, p160ROCK, in Determining Axon Outgrowth in Mammalian CNS Neurons. *Neuron* 26(2): 431-441.
- Blanchoin, L., R. Boujemaa-Paterski, C. Sykes and J. Plastino (2014). Actin Dynamics, Architecture, and Mechanics in Cell Motility. *Physiological Reviews* 94(1): 235-263.
- Bornens, M. (2008). Organelle positioning and cell polarity. *Nat Rev Mol Cell Biol* 9(11): 874-886.
- Bradke, F. and C. G. Dotti (1997). Neuronal Polarity: Vectorial Cytoplasmic Flow Precedes Axon Formation. *Neuron* 19(6): 1175-1186.
- Bradke, F. and C. G. Dotti (1999). The Role of Local Actin Instability in Axon Formation. *Science* 283(5409): 1931-1934.
- Breitsprecher, D., R. Jaiswal, J. P. Bombardier, C. J. Gould, J. Gelles and B. L. Goode (2012). Rocket Launcher Mechanism of Collaborative Actin Assembly Defined by Single-Molecule Imaging. *Science* 336(6085): 1164-1168.
- Brinkley, B. R. (1985). Microtubule Organizing Centers. *Annual Review of Cell Biology* 1(1): 145-172.

- Brown, S. S. (1999). Cooperation Between Microtubule- and Actin-Based Motor Proteins. *Annual Review of Cell and Developmental Biology* 15(1): 63-80.
- Buck, K. B. and J. Q. Zheng (2002). Growth Cone Turning Induced by Direct Local Modification of Microtubule Dynamics. *The Journal of Neuroscience* 22(21): 9358-9367.
- Bulina, M. E., D. M. Chudakov, O. V. Britanova, Y. G. Yanushevich, D. B. Staroverov, T. V. Chepurnykh, E. M. Merzlyak, M. A. Shkrob, S. Lukyanov and K. A. Lukyanov (2006). A genetically encoded photosensitizer. *Nat Biotech* 24(1): 95-99.
- Burridge, K. and K. Wennerberg (2004). Rho and Rac Take Center Stage. *Cell* 116(2): 167-179.
- Burton, P. R. and J. L. Paige (1981). Polarity of axoplasmic microtubules in the olfactory nerve of the frog. *Proceedings of the National Academy of Sciences of the United States of America* 78(5): 3269-3273.
- Butkevich, E., S. Hülsmann, D. Wenzel, T. Shirao, R. Duden and I. Majoul (2004). Drebrin Is a Novel Connexin-43 Binding Partner that Links Gap Junctions to the Submembrane Cytoskeleton. *Current Biology* 14(8): 650-658.
- Butler, S. J. and G. Tear (2007). Getting axons onto the right path: the role of transcription factors in axon guidance. *Development* 134(3): 439-448.
- Calderon de Anda, F., A. Gärtner, L.-H. Tsai and C. G. Dotti (2008). Pyramidal neuron polarity axis is defined at the bipolar stage. *Journal of Cell Science* 121(2): 178-185.
- Cammarata, G. M., E. A. Bearce and L. A. Lowery (2016). Cytoskeletal social networking in the growth cone: How +TIPs mediate microtubule-actin cross-linking to drive axon outgrowth and guidance. *Cytoskeleton* 73(9): 461-476.
- Chen, S., J. Chen, H. Shi, M. Wei, D. R. Castaneda-Castellanos, R. S. Bultje, X. Pei, A. R. Kriegstein, M. Zhang and S.-H. Shi (2013). Regulation of Microtubule Stability and Organization by Mammalian Par3 in Specifying Neuronal Polarity. *Developmental Cell* 24(1): 26-40.
- Chilton, J. K. (2006). Molecular mechanisms of axon guidance. *Developmental Biology* 292(1): 13-24.
- Coles, C. H. and F. Bradke (2015). Coordinating Neuronal Actin–Microtubule Dynamics. *Current Biology* 25(15): R677-R691.
- Conde, C. and A. Caceres (2009). Microtubule assembly, organization and dynamics in axons and dendrites. *Nat Rev Neurosci* 10(5): 319-332.

References

- Craig, A. M. and G. Banker (1994). Neuronal Polarity. *Annual Review of Neuroscience* 17(1): 267-310.
- Cunningham, C. C., N. Leclerc, L. A. Flanagan, M. Lu, P. A. Janmey and K. S. Kosik (1997). Microtubule-associated Protein 2c Reorganizes Both Microtubules and Microfilaments into Distinct Cytological Structures in an Actin-binding Protein-280-deficient Melanoma Cell Line. *The Journal of Cell Biology* 136(4): 845-857.
- da Silva, J. S. and C. G. Dotti (2002). Breaking the neuronal sphere: regulation of the actin cytoskeleton in neuritogenesis. *Nat Rev Neurosci* 3(9): 694-704.
- Da Silva, J. S., M. Medina, C. Zuliani, A. Di Nardo, W. Witke and C. G. Dotti (2003). RhoA/ROCK regulation of neuritogenesis via profilin Ila-mediated control of actin stability. *The Journal of Cell Biology* 162(7): 1267-1279.
- de Anda, F. C., K. Meletis, X. Ge, D. Rei and L.-H. Tsai (2010). Centrosome Motility Is Essential for Initial Axon Formation in the Neocortex. *The Journal of Neuroscience* 30(31): 10391-10406.
- de Anda, F. C., G. Pollarolo, J. S. Da Silva, P. G. Camoletto, F. Feiguin and C. G. Dotti (2005). Centrosome localization determines neuronal polarity. *Nature* 436(7051): 704-708.
- de Hostos, E. L. (1999). The coronin family of actin-associated proteins. *Trends in Cell Biology* 9(9): 345-350.
- Dehmelt, L., F. M. Smart, R. S. Ozer and S. Halpain (2003). The Role of Microtubule-Associated Protein 2c in the Reorganization of Microtubules and Lamellipodia during Neurite Initiation. *The Journal of Neuroscience* 23(29): 9479-9490.
- Dent, E. W. and F. B. Gertler (2003). Cytoskeletal Dynamics and Transport in Growth Cone Motility and Axon Guidance. *Neuron* 40(2): 209-227.
- Dent, E. W., S. L. Gupton and F. B. Gertler (2011). The Growth Cone Cytoskeleton in Axon Outgrowth and Guidance. *Cold Spring Harbor Perspectives in Biology* 3(3).
- Dent, E. W., A. V. Kwiatkowski, L. M. Mebane, U. Philippar, M. Barzik, D. A. Rubinson, S. Gupton, J. E. Van Veen, C. Furman, J. Zhang, et al. (2007). Filopodia are required for cortical neurite initiation. *Nat Cell Biol* 9(12): 1347-1359.
- Dickson, B. J. (2002). Molecular Mechanisms of Axon Guidance. *Science* 298(5600): 1959-1964.
- Distel, M., J. C. Hocking, K. Volkmann and R. W. Köster (2010). The centrosome neither persistently leads migration nor determines the site of axonogenesis in migrating neurons in vivo. *The Journal of Cell Biology* 191(4): 875-890.

- Dotti, C., C. Sullivan and G. Banker (1988). The establishment of polarity by hippocampal neurons in culture. *The Journal of Neuroscience* 8(4): 1454-1468.
- Doxsey, S. (2001). Re-evaluating centrosome function. *Nat Rev Mol Cell Biol* 2(9): 688-698.
- Drechsel, D. N., A. A. Hyman, M. H. Cobb and M. W. Kirschner (1992). Modulation of the dynamic instability of tubulin assembly by the microtubule-associated protein tau. *Molecular Biology of the Cell* 3(10): 1141-1154.
- Dumontet, C. and M. A. Jordan (2010). Microtubule-binding agents: a dynamic field of cancer therapeutics. *Nat Rev Drug Discov* 9(10): 790-803.
- Edson, K., B. Weisshaar and A. Matus (1993). Actin depolymerisation induces process formation on MAP2-transfected non-neuronal cells. *Development* 117(2): 689-700.
- Erck, C., L. Peris, A. Andrieux, C. Meissirel, A. D. Gruber, M. Vernet, A. Schweitzer, Y. Saoudi, H. Pointu, C. Bosc, et al. (2005). A vital role of tubulin-tyrosine-ligase for neuronal organization. *Proceedings of the National Academy of Sciences* 102(22): 7853-7858.
- Evans, A. R., S. Euteneuer, E. Chavez, L. M. Mullen, E. E. Hui, S. N. Bhatia and A. F. Ryan (2007). Laminin and fibronectin modulate inner ear spiral ganglion neurite outgrowth in an in vitro alternate choice assay. *Developmental Neurobiology* 67(13): 1721-1730.
- Ezratty, E. J., M. A. Partridge and G. G. Gundersen (2005). Microtubule-induced focal adhesion disassembly is mediated by dynamin and focal adhesion kinase. *Nat Cell Biol* 7(6): 581-590.
- Farina, F., J. Gaillard, C. Guerin, Y. Coute, J. Sillibourne, L. Blanchoin and M. Thery (2016). The centrosome is an actin-organizing centre. *Nat Cell Biol* 18(1): 65-75.
- Forscher, P., C. H. Lin and C. Thompson (1992). Novel form of growth cone motility involving site-directed actin filament assembly. *Nature* 357(6378): 515-518.
- Fourniol, F. J., C. V. Sindelar, B. Amigues, D. K. Clare, G. Thomas, M. Perderiset, F. Francis, A. Houdusse and C. A. Moores (2010). Template-free 13-protofilament microtubule-MAP assembly visualized at 8 Å resolution. *The Journal of Cell Biology* 191(3): 463-470.
- Fukata, M., T. Watanabe, J. Noritake, M. Nakagawa, M. Yamaga, S. Kuroda, Y. Matsuura, A. Iwamatsu, F. Perez and K. Kaibuchi (2002). Rac1 and Cdc42 Capture Microtubules through IQGAP1 and CLIP-170. *Cell* 109(7): 873-885.
- Fukata, Y., T. J. Itoh, T. Kimura, C. Menager, T. Nishimura, T. Shiromizu, H. Watanabe, N. Inagaki, A. Iwamatsu, H. Hotani, et al. (2002). CRMP-2 binds to tubulin heterodimers to promote microtubule assembly. *Nat Cell Biol* 4(8): 583-591.

References

- Gao, W. and M. Hatten (1993). Neuronal differentiation rescued by implantation of Weaver granule cell precursors into wild-type cerebellar cortex. *Science* 260(5106): 367-369.
- Garner, C. C., B. Brugg and A. Matus (1988). A 70-Kilodalton Microtubule-Associated Protein (MAP2c), Related to MAP2. *Journal of Neurochemistry* 50(2): 609-615.
- Garvalov, B. K., K. C. Flynn, D. Neukirchen, L. Meyn, N. Teusch, X. Wu, C. Brakebusch, J. R. Bamberg and F. Bradke (2007). Cdc42 Regulates Cofilin during the Establishment of Neuronal Polarity. *The Journal of Neuroscience* 27(48): 13117-13129.
- Geraldo, S., U. K. Khanzada, M. Parsons, J. K. Chilton and P. R. Gordon-Weeks (2008). Targeting of the F-actin-binding protein drebrin by the microtubule plus-tip protein EB3 is required for neuritogenesis. *Nat Cell Biol* 10(10): 1181-1189.
- Gleeson, J. G., K. M. Allen, J. W. Fox, E. D. Lamperti, S. Berkovic, I. Scheffer, E. C. Cooper, W. B. Dobyns, S. R. Minnerath, M. E. Ross, et al. (1998). doublecortin, a Brain-Specific Gene Mutated in Human X-Linked Lissencephaly and Double Cortex Syndrome, Encodes a Putative Signaling Protein. *Cell* 92(1): 63-72.
- Goldberg, D. J. and D. W. Burmeister (1986). Stages in axon formation: observations of growth of Aplysia axons in culture using video-enhanced contrast-differential interference contrast microscopy. *The Journal of Cell Biology* 103(5): 1921-1931.
- Goldman, R. D. (1971). THE ROLE OF THREE CYTOPLASMIC FIBERS IN BHK-21 CELL MOTILITY. *I. Microtubules and the Effects of Colchicine* 51(3): 752-762.
- Gomez, T. S., K. Kumar, R. B. Medeiros, Y. Shimizu, P. J. Leibson and D. D. Billadeau (2007). Formins Regulate the Actin-Related Protein 2/3 Complex-Independent Polarization of the Centrosome to the Immunological Synapse. *Immunity* 26(2): 177-190.
- Goode, B. L., J. J. Wong, A.-C. Butty, M. Peter, A. L. McCormack, J. R. Yates, D. G. Drubin and G. Barnes (1999). Coronin Promotes the Rapid Assembly and Cross-linking of Actin Filaments and May Link the Actin and Microtubule Cytoskeletons in Yeast. *The Journal of Cell Biology* 144(1): 83-98.
- Gordon-Weeks, P. R. (2016). The role of the drebrin/EB3/Cdk5 pathway in dendritic spine plasticity, implications for Alzheimer's disease. *Brain Research Bulletin* 126, Part 3: 293-299.
- Goslin, K., E. Birgbauer, G. Banker and F. Solomon (1989). The role of cytoskeleton in organizing growth cones: a microfilament-associated growth cone component depends upon microtubules for its localization. *The Journal of Cell Biology* 109(4): 1621-1631.

- Gotlieb, A. I., L. Subrahmanyam and V. I. Kalnins (1983). Microtubule-organizing centers and cell migration: effect of inhibition of migration and microtubule disruption in endothelial cells. *The Journal of Cell Biology* 96(5): 1266-1272.
- Grabham, P. W., G. E. Seale, M. Bennechib, D. J. Goldberg and R. B. Vallee (2007). Cytoplasmic Dynein and LIS1 Are Required for Microtubule Advance during Growth Cone Remodeling and Fast Axonal Outgrowth. *The Journal of Neuroscience* 27(21): 5823-5834.
- Griffith, L. M. and T. D. Pollard (1982). The interaction of actin filaments with microtubules and microtubule-associated proteins. *Journal of Biological Chemistry* 257(15): 9143-9151.
- Grintsevich, E. E. and E. Reisler (2014). Drebrin inhibits cofilin-induced severing of F-actin. *Cytoskeleton* 71(8): 472-483.
- Groden, J., A. Thliveris, W. Samowitz, M. Carlson, L. Gelbert, H. Albertsen, G. Joslyn, J. Stevens, L. Spirio, M. Robertson, et al. (1991). Identification and characterization of the familial adenomatous polyposis coli gene. *Cell* 66(3): 589-600.
- Harigaya, Y., M. Shoji, T. Shirao and S. Hirai (1996). Disappearance of actin-binding protein, drebrin, from hippocampal synapses in alzheimer's disease. *Journal of Neuroscience Research* 43(1): 87-92.
- Hayashi, K., R. Ishikawa, L.-H. Ye, X.-L. He, K. Takata, K. Kohama and T. Shirao (1996). Modulatory Role of Drebrin on the Cytoskeleton within Dendritic Spines in the Rat Cerebral Cortex. *The Journal of Neuroscience* 16(22): 7161-7170.
- Heidemann, S. R., J. M. Landers and M. A. Hamborg (1981). Polarity orientation of axonal microtubules. *The Journal of Cell Biology* 91(3): 661-665.
- Heisler, F. F., S. Loebrich, Y. Pechmann, N. Maier, A. R. Zivkovic, M. Tokito, T. J. Hausrat, M. Schweizer, R. Bähring, E. L. F. Holzbaur, et al. (2011). Muskelein Regulates Actin Filament- and Microtubule-Based GABAA Receptor Transport in Neurons. *Neuron* 70(1): 66-81.
- Hell, S. W. (2007). Far-Field Optical Nanoscopy. *Science* 316(5828): 1153-1158.
- Henty-Ridilla, J. L., A. Rankova, J. A. Eskin, K. Kenny and B. L. Goode (2016). Accelerated actin filament polymerization from microtubule plus ends. *Science* 352(6288): 1004-1009.
- Huang, B., H. Babcock and X. Zhuang (2010). Breaking the Diffraction Barrier: Super-Resolution Imaging of Cells. *Cell* 143(7): 1047-1058.
- Huang, J.-D., S. T. Brady, B. W. Richards, D. Stenoiien, J. H. Resau, N. G. Copeland and N. A. Jenkins (1999). Direct interaction of microtubule- and actin-based transport motors. *Nature* 397(6716): 267-270.

References

- Hubbert, C., A. Guardiola, R. Shao, Y. Kawaguchi, A. Ito, A. Nixon, M. Yoshida, X.-F. Wang and T.-P. Yao (2002). HDAC6 is a microtubule-associated deacetylase. *Nature* 417(6887): 455-458.
- Hwang, E., J. Kusch, Y. Barral and T. C. Huffaker (2003). Spindle orientation in *Saccharomyces cerevisiae* depends on the transport of microtubule ends along polarized actin cables. *The Journal of Cell Biology* 161(3): 483-488.
- Ikeda, K., T. Shirao, M. Toda, H. Asada, S. Toya and K. Uyemura (1995). Effect of a neuron-specific actin-binding protein, drebrin A, on cell-substratum adhesion. *Neuroscience Letters* 194(3): 197-200.
- Ishikawa, R., K. Hayashi, T. Shirao, Y. Xue, T. Takagi, Y. Sasaki and K. Kohama (1994). Drebrin, a development-associated brain protein from rat embryo, causes the dissociation of tropomyosin from actin filaments. *Journal of Biological Chemistry* 269(47): 29928-29933.
- Ishikawa, R., K. Katoh, A. Takahashi, C. Xie, K. Oseki, M. Watanabe, M. Igarashi, A. Nakamura and K. Kohama (2007). Drebrin attenuates the interaction between actin and myosin-V. *Biochemical and Biophysical Research Communications* 359(2): 398-401.
- Jaworski, J., L. C. Kapitein, S. M. Gouveia, B. R. Dortland, P. S. Wulf, I. Grigoriev, P. Camera, S. A. Spangler, P. Di Stefano, J. Demmers, et al. (2009). Dynamic Microtubules Regulate Dendritic Spine Morphology and Synaptic Plasticity. *Neuron* 61(1): 85-100.
- Jefferson, J. J., C. L. Leung and R. K. H. Liem (2004). Plakins: Goliaths that link cell junctions and the cytoskeleton. *Nat Rev Mol Cell Biol* 5(7): 542-553.
- Jiménez-Mateos, E. M., G. Paglini, C. González-Billault, A. Cáceres and J. Avila (2005). End binding protein-1 (EB1) complements microtubule-associated protein-1B during axonogenesis. *Journal of Neuroscience Research* 80(3): 350-359.
- Jordan, M. A. and L. Wilson (2004). Microtubules as a target for anticancer drugs. *Nat Rev Cancer* 4(4): 253-265.
- Kaech, S., B. Ludin and A. Matus (1996). Cytoskeletal Plasticity in Cells Expressing Neuronal Microtubule-Associated Proteins. *Neuron* 17(6): 1189-1199.
- Kalebic, N., S. Sorrentino, E. Perlas, G. Bolasco, C. Martinez and P. A. Heppenstall (2013). α TAT1 is the major α -tubulin acetyltransferase in mice. *Nature Communications* 4: 1962.
- Kanchanawong, P., G. Shtengel, A. M. Pasapera, E. B. Ramko, M. W. Davidson, H. F. Hess and C. M. Waterman (2010). Nanoscale architecture of integrin-based cell adhesions. *Nature* 468(7323): 580-584.

- Kapitein, L. C. and C. C. Hoogenraad (2015). Building the Neuronal Microtubule Cytoskeleton. *Neuron* 87(3): 492-506.
- Kaverina, I., O. Krylyshkina and J. V. Small (1999). Microtubule Targeting of Substrate Contacts Promotes Their Relaxation and Dissociation. *The Journal of Cell Biology* 146(5): 1033-1044.
- Kawasaki, Y., R. Sato and T. Akiyama (2003). Mutated APC and Asef are involved in the migration of colorectal tumour cells. *Nat Cell Biol* 5(3): 211-215.
- Kawasaki, Y., T. Senda, T. Ishidate, R. Koyama, T. Morishita, Y. Iwayama, O. Higuchi and T. Akiyama (2000). Asef, a Link Between the Tumor Suppressor APC and G-Protein Signaling. *Science* 289(5482): 1194-1197.
- Ketschek, A., M. Spillane, X.-P. Dun, H. Hardy, J. Chilton and G. Gallo (2016). Drebrin coordinates the actin and microtubule cytoskeleton during the initiation of axon collateral branches. *Developmental Neurobiology* 76(10): 1092-1110.
- Kirschner, M. and T. Mitchison (1986). Beyond self-assembly: From microtubules to morphogenesis. *Cell* 45(3): 329-342.
- Kitagawa, D., I. Vakonakis, N. Olieric, M. Hilbert, D. Keller, V. Olieric, M. Bortfeld, M. C. Erat, I. Flückiger, P. Gönczy, et al. (2011). Structural Basis of the 9-Fold Symmetry of Centrioles. *Cell* 144(3): 364-375.
- Kollman, J. M., A. Merdes, L. Mourey and D. A. Agard (2011). Microtubule nucleation by γ -tubulin complexes. *Nat Rev Mol Cell Biol* 12(11): 709-721.
- Komarova, Y., G. Lansbergen, N. Galjart, F. Grosveld, G. G. Borisy and A. Akhmanova (2005). EB1 and EB3 Control CLIP Dissociation from the Ends of Growing Microtubules. *Molecular Biology of the Cell* 16(11): 5334-5345.
- Komuro, H. and E. Yacubova (2003). Recent advances in cerebellar granule cell migration. *Cell Mol Life Sci* 60(6): 1084-1098.
- Komuro, H., E. Yacubova, E. Yacubova and P. Rakic (2001). Mode and Tempo of Tangential Cell Migration in the Cerebellar External Granular Layer. *The Journal of Neuroscience* 21(2): 527-540.
- Konishi, Y. and M. Setou (2009). Tubulin tyrosination navigates the kinesin-1 motor domain to axons. *Nat Neurosci* 12(5): 559-567.
- Krause, M., E. W. Dent, J. E. Bear, J. J. Loureiro and F. B. Gertler (2003). Ena/VASP Proteins: Regulators of the Actin Cytoskeleton and Cell Migration. *Annual Review of Cell and Developmental Biology* 19(1): 541-564.

References

- Kwiatkowski, A. V., D. A. Rubinson, E. W. Dent, J. Edward van Veen, J. D. Leslie, J. Zhang, L. M. Mebane, U. Philippar, E. M. Pinheiro, A. A. Burds, et al. Ena/VASP Is Required for Neuritogenesis in the Developing Cortex. *Neuron* 56(3): 441-455.
- Kwon, M., M. Bagonis, G. Danuser and D. Pellman (2015). Direct Microtubule-Binding by Myosin-10 Orients Centrosomes toward Retraction Fibers and Subcortical Actin Clouds. *Developmental Cell* 34(3): 323-337.
- Laan, L., N. Pavin, J. Husson, G. Romet-Lemonne, M. van Duijn, M. P. López, R. D. Vale, F. Jülicher, S. L. Reck-Peterson and M. Dogterom (2012). Cortical Dynein Controls Microtubule Dynamics to Generate Pulling Forces that Position Microtubule Asters. *Cell* 148(3): 502-514.
- Lansbergen, G. and A. Akhmanova (2006). Microtubule Plus End: A Hub of Cellular Activities. *Traffic* 7(5): 499-507.
- Lantz, V. A. and K. G. Miller (1998). A Class VI Unconventional Myosin Is Associated with a Homologue of a Microtubule-binding Protein, Cytoplasmic Linker Protein-170, in Neurons and at the Posterior Pole of Drosophila Embryos. *The Journal of Cell Biology* 140(4): 897-910.
- Lee, S. and P. A. Kolodziej (2002). Short Stop provides an essential link between F-actin and microtubules during axon extension. *Development* 129(5): 1195-1204.
- Leterrier, C., H. Vacher, M.-P. Fache, S. A. d'Ortoli, F. Castets, A. Autillo-Touati and B. Dargent (2011). End-binding proteins EB3 and EB1 link microtubules to ankyrin G in the axon initial segment. *Proceedings of the National Academy of Sciences* 108(21): 8826-8831.
- Liao, G., T. Nagasaki and G. G. Gundersen (1995). Low concentrations of nocodazole interfere with fibroblast locomotion without significantly affecting microtubule level: implications for the role of dynamic microtubules in cell locomotion. *Journal of Cell Science* 108(11): 3473-3483.
- Linder, S., K. Hufner, U. Wintergerst and M. Aepfelbacher (2000). Microtubule-dependent formation of podosomal adhesion structures in primary human macrophages. *Journal of Cell Science* 113(23): 4165-4176.
- López, M. P., F. Huber, I. Grigoriev, M. O. Steinmetz, A. Akhmanova, G. H. Koenderink and M. Dogterom (2014). Actin-microtubule coordination at growing microtubule ends. *Nature Communications* 5: 4778.
- Lowery, L. A. and D. V. Vactor (2009). The trip of the tip: understanding the growth cone machinery. *Nat Rev Mol Cell Biol* 10(5): 332-343.

- Luders, J. and T. Stearns (2007). Microtubule-organizing centres: a re-evaluation. *Nat Rev Mol Cell Biol* 8(2): 161-167.
- Lupas, A., M. Van Dyke and J. Stock (1991). Predicting coiled coils from protein sequences. *Science* 252(5009): 1162-1164.
- Maccioni, R. B. and V. Cambiazo (1995). Role of microtubule-associated proteins in the control of microtubule assembly. *Physiological Reviews* 75(4): 835-864.
- Mallavarapu, A. and T. Mitchison (1999). Regulated Actin Cytoskeleton Assembly at Filopodium Tips Controls Their Extension and Retraction. *The Journal of Cell Biology* 146(5): 1097-1106.
- Mammoto, A., T. Sasaki, T. Asakura, I. Hotta, H. Imamura, K. Takahashi, Y. Matsuura, T. Shirao and Y. Takai (1998). Interactions of Drebrin and Gephyrin with Profilin. *Biochemical and Biophysical Research Communications* 243(1): 86-89.
- Maness, P. F. and M. Schachner (2007). Neural recognition molecules of the immunoglobulin superfamily: signaling transducers of axon guidance and neuronal migration. *Nat Neurosci* 10(1): 19-26.
- Marcos, S., J. Moreau, S. Backer, D. Job, A. Andrieux and E. Bloch-Gallego (2009). Tubulin Tyrosination Is Required for the Proper Organization and Pathfinding of the Growth Cone. *PLOS ONE* 4(4): e5405.
- Marsh, L. and P. C. Letourneau (1984). Growth of neurites without filopodial or lamellipodial activity in the presence of cytochalasin B. *The Journal of Cell Biology* 99(6): 2041-2047.
- Mattson, M., P. Dou and S. Kater (1988). Outgrowth-regulating actions of glutamate in isolated hippocampal pyramidal neurons. *The Journal of Neuroscience* 8(6): 2087-2100.
- McCartney, B. M., D. G. McEwen, E. Grevenkoed, P. Maddox, A. Bejsovec and M. Peifer (2001). Drosophila APC2 and Armadillo participate in tethering mitotic spindles to cortical actin. *Nat Cell Biol* 3(10): 933-938.
- Medeiros, N. A., D. T. Burnette and P. Forscher (2006). Myosin II functions in actin-bundle turnover in neuronal growth cones. *Nat Cell Biol* 8(3): 216-226.
- Merriam, E. B., M. Millette, D. C. Lumbard, W. Saengsawang, T. Fothergill, X. Hu, L. Ferhat and E. W. Dent (2013). Synaptic Regulation of Microtubule Dynamics in Dendritic Spines by Calcium, F-Actin, and Drebrin. *The Journal of Neuroscience* 33(42): 16471-16482.
- Mikati, M. A., E. E. Grintsevich and E. Reisler (2013). Drebrin-Induced Stabilization of Actin Filaments. *Journal of Biological Chemistry*.

References

- Mimori-Kiyosue, Y., N. Shiina and S. Tsukita (2000). Adenomatous Polyposis Coli (APC) Protein Moves along Microtubules and Concentrates at Their Growing Ends in Epithelial Cells. *The Journal of Cell Biology* 148(3): 505-518.
- Mitchison, T. and M. Kirschner (1984). Dynamic instability of microtubule growth. *Nature* 312(5991): 237-242.
- Mitchison, T. and M. Kirschner (1988). Cytoskeletal dynamics and nerve growth. *Neuron* 1(9): 761-772.
- Mitchison, T. J. and L. P. Cramer (1996). Actin-Based Cell Motility and Cell Locomotion. *Cell* 84(3): 371-379.
- Mizui, T., N. Kojima, H. Yamazaki, M. Katayama, K. Hanamura and T. Shirao (2009). Drebrin E is involved in the regulation of axonal growth through actin–myosin interactions. *Journal of Neurochemistry* 109(2): 611-622.
- Mizui, T., Y. Sekino, H. Yamazaki, Y. Ishizuka, H. Takahashi, N. Kojima, M. Kojima and T. Shirao (2014). Myosin II ATPase Activity Mediates the Long-Term Potentiation-Induced Exodus of Stable F-Actin Bound by Drebrin A from Dendritic Spines. *PLOS ONE* 9(1): e85367.
- Moore, C. A., M. Perderiset, F. Francis, J. Chelly, A. Houdusse and R. A. Milligan (2004). Mechanism of Microtubule Stabilization by Doublecortin. *Molecular Cell* 14(6): 833-839.
- Morgan, J. L., A. Dhingra, N. Vardi and R. O. Wong (2006). Axons and dendrites originate from neuroepithelial-like processes of retinal bipolar cells. *Nat Neurosci* 9(1): 85-92.
- Morrison, E. E., P. M. Moncur and J. M. Askham (2002). EB1 identifies sites of microtubule polymerisation during neurite development. *Molecular Brain Research* 98(1–2): 145-152.
- Murphy, D. A. and S. A. Courtneidge (2011). The 'ins' and 'outs' of podosomes and invadopodia: characteristics, formation and function. *Nat Rev Mol Cell Biol* 12(7): 413-426.
- Nager, A. R., J. S. Goldstein, V. Herranz-Pérez, D. Portran, F. Ye, J. M. Garcia-Verdugo and M. V. Nachury (2017). An Actin Network Dispatches Ciliary GPCRs into Extracellular Vesicles to Modulate Signaling. *Cell* 168(1–2): 252-263.e214.
- Nakagawa, H., K. Koyama, Y. Murata, M. Morito, T. Akiyama and Y. Nakamura (2000). EB3, a novel member of the EB1 family preferentially expressed in the central nervous system, binds to a CNS-specific APC homologue. *Oncogene* 19: 210–216.
- Namba, T., Y. Funahashi, S. Nakamuta, C. Xu, T. Takano and K. Kaibuchi (2015). Extracellular and Intracellular Signaling for Neuronal Polarity. *Physiol Rev* 95(3): 995-1024.

- Ning, W., Y. Yu, H. Xu, X. Liu, D. Wang, J. Wang, Y. Wang and W. Meng (2016). The CAMSAP3-ACF7 Complex Couples Noncentrosomal Microtubules with Actin Filaments to Coordinate Their Dynamics. *Developmental Cell* 39(1): 61-74.
- Noctor, S. C., V. Martinez-Cerdeno, L. Ivic and A. R. Kriegstein (2004). Cortical neurons arise in symmetric and asymmetric division zones and migrate through specific phases. *Nat Neurosci* 7(2): 136-144.
- Obino, D., F. Farina, O. Malbec, P. J. Sáez, M. Maurin, J. Gaillard, F. Dingli, D. Loew, A. Gautreau, M.-I. Yuseff, et al. (2016). Actin nucleation at the centrosome controls lymphocyte polarity. *Nature Communications* 7: 10969.
- Oegema, K., C. Wiese, O. C. Martin, R. A. Milligan, A. Iwamatsu, T. J. Mitchison and Y. Zheng (1999). Characterization of Two Related Drosophila γ -tubulin Complexes that Differ in Their Ability to Nucleate Microtubules. *The Journal of Cell Biology* 144(4): 721-733.
- Ozer, R. S. and S. Halpain (2000). Phosphorylation-dependent Localization of Microtubule-associated Protein MAP2c to the Actin Cytoskeleton. *Molecular Biology of the Cell* 11(10): 3573-3587.
- Perez, F., G. S. Diamantopoulos, R. Stalder and T. E. Kreis (1999). CLIP-170 Highlights Growing Microtubule Ends In Vivo. *Cell* 96(4): 517-527.
- Pollard, T. D. and G. G. Borisy (2003). Cellular Motility Driven by Assembly and Disassembly of Actin Filaments. *Cell* 112(4): 453-465.
- Powell, S. K., R. J. Rivas, E. Rodriguez-Boulan and M. E. Hatten (1997). Development of polarity in cerebellar granule neurons. *Journal of Neurobiology* 32(2): 223-236.
- Prota, A. E., M. M. Magiera, M. Kuijpers, K. Bargsten, D. Frey, M. Wieser, R. Jaussi, C. C. Hoogenraad, R. A. Kammerer, C. Janke, et al. (2013). Structural basis of tubulin tyrosination by tubulin tyrosine ligase. *The Journal of Cell Biology* 200(3): 259-270.
- Rickard, J. E. and T. E. Kreis (1990). Identification of a novel nucleotide-sensitive microtubule-binding protein in HeLa cells. *The Journal of Cell Biology* 110(5): 1623-1633.
- Riedl, J., A. H. Crevenna, K. Kessenbrock, J. H. Yu, D. Neukirchen, M. Bista, F. Bradke, D. Jenne, T. A. Holak, Z. Werb, et al. (2008). Lifeact: a versatile marker to visualize F-actin. *Nat Meth* 5(7): 605-607.
- Rochlin, M. W., K. M. Wickline and P. C. Bridgman (1996). Microtubule Stability Decreases Axon Elongation but Not Axoplasm Production. *The Journal of Neuroscience* 16(10): 3236-3246.

References

- Rodriguez, O. C., A. W. Schaefer, C. A. Mandato, P. Forscher, W. M. Bement and C. M. Waterman-Storer (2003). Conserved microtubule-actin interactions in cell movement and morphogenesis. *Nat Cell Biol* 5(7): 599-609.
- Rosin-Arbesfeld, R., G. Ihrke and M. Bienz (2001). Actin-dependent membrane association of the APC tumour suppressor in polarized mammalian epithelial cells. *The EMBO Journal* 20(21): 5929-5939.
- Rothenberg, M. E., S. L. Rogers, R. D. Vale, L. Y. Jan and Y.-N. Jan (2003). Drosophila Pod-1 Crosslinks Both Actin and Microtubules and Controls the Targeting of Axons. *Neuron* 39(5): 779-791.
- Sakakibara, A., T. Sato, R. Ando, N. Noguchi, M. Masaoka and T. Miyata (2013). Dynamics of Centrosome Translocation and Microtubule Organization in Neocortical Neurons during Distinct Modes of Polarization. *Cerebral Cortex* 24(5): 1301-1310.
- Sanchez-Soriano, N., M. Travis, F. Dajas-Bailador, C. Gonçalves-Pimentel, A. J. Whitmarsh and A. Prokop (2009). Mouse ACF7 and Drosophila Short stop modulate filopodia formation and microtubule organisation during neuronal growth. *Journal of Cell Science* 122(14): 2534-2542.
- Sanford, S. D., J. C. Gatlin, T. Hökfelt and K. H. Pfenninger (2008). Growth cone responses to growth and chemotropic factors. *European Journal of Neuroscience* 28(2): 268-278.
- Sapir, T., A. Shmueli, T. Levy, T. Timm, M. Elbaum, E.-M. Mandelkow and O. Reiner (2008). Antagonistic Effects of Doublecortin and MARK2/Par-1 in the Developing Cerebral Cortex. *The Journal of Neuroscience* 28(48): 13008-13013.
- Sasaki, Y., K. Hayashi, T. Shirao, R. Ishikawa and K. Kohama (1996). Inhibition by Drebrin of the Actin-Bundling Activity of Brain Fascin, a Protein Localized in Filopodia of Growth Cones. *Journal of Neurochemistry* 66(3): 980-988.
- Schaefer, A. W., N. Kabir and P. Forscher (2002). Filopodia and actin arcs guide the assembly and transport of two populations of microtubules with unique dynamic parameters in neuronal growth cones. *The Journal of Cell Biology* 158(1): 139-152.
- Schwamborn, J. C. and A. W. Puschel (2004). The sequential activity of the GTPases Rap1B and Cdc42 determines neuronal polarity. *Nat Neurosci* 7(9): 923-929.
- Sekino, Y., S. Tanaka, K. Hanamura, H. Yamazaki, Y. Sasagawa, Y. Xue, K. Hayashi and T. Shirao (2006). Activation of N-methyl-d-aspartate receptor induces a shift of drebrin distribution: Disappearance from dendritic spines and appearance in dendritic shafts. *Molecular and Cellular Neuroscience* 31(3): 493-504.

- Shi, S.-H., T. Cheng, L. Y. Jan and Y.-N. Jan (2004). APC and GSK-3 β Are Involved in mPar3 Targeting to the Nascent Axon and Establishment of Neuronal Polarity. *Current Biology* 14(22): 2025-2032.
- Shi, S.-H., L. Y. Jan and Y.-N. Jan (2003). Hippocampal Neuronal Polarity Specified by Spatially Localized mPar3/mPar6 and PI 3-Kinase Activity. *Cell* 112(1): 63-75.
- Shim, K. S. and G. Lubec (2002). Drebrin, a dendritic spine protein, is manifold decreased in brains of patients with Alzheimer's disease and Down syndrome. *Neuroscience Letters* 324(3): 209-212.
- Shirao, T., K. Hayashi, R. Ishikawa, K. Isa, H. Asada, K. Ikeda and K. Uyemura (1994). Formation of Thick, Curving Bundles of Actin by Drebrin A Expressed in Fibroblasts. *Experimental Cell Research* 215(1): 145-153.
- Shirao, T., N. Kojima, Y. Nabeta and K. Obata (1989). Two Forms of Drebrins, Developmentally Regulated Brain Proteins, in Rat. *Proceedings of the Japan Academy, Series B* 65(7): 169-172.
- Shirao, T. and K. Obata (1985). Two Acidic Proteins Associated with Brain Development in Chick Embryo. *Journal of Neurochemistry* 44(4): 1210-1216.
- Shoukimas, G. M. and J. W. Hinds (1978). The development of the cerebral cortex in the embryonic mouse: An electron microscopic serial section analysis. *The Journal of Comparative Neurology* 179(4): 795-830.
- Sonego, M., M. Oberoi, J. Stoddart, S. Gajendra, R. Hendricusdottir, F. Oozeer, D. C. Worth, C. Hobbs, B. J. Eickholt, P. R. Gordon-Weeks, et al. (2015). Drebrin Regulates Neuroblast Migration in the Postnatal Mammalian Brain. *PLOS ONE* 10(5): e0126478.
- Song, Y. and S. T. Brady (2015). Post-translational modifications of tubulin: pathways to functional diversity of microtubules. *Trends in Cell Biology* 25(3): 125-136.
- Stepanova, T., J. Slemmer, C. C. Hoogenraad, G. Lansbergen, B. Dortland, C. I. De Zeeuw, F. Grosveld, G. van Cappellen, A. Akhmanova and N. Galjart (2003). Visualization of Microtubule Growth in Cultured Neurons via the Use of EB3-GFP (End-Binding Protein 3-Green Fluorescent Protein). *The Journal of Neuroscience* 23(7): 2655-2664.
- Stiess, M., N. Maghelli, L. C. Kapitein, S. Gomis-Rüth, M. Wilsch-Bräuninger, C. C. Hoogenraad, I. M. Tolić-Nørrelykke and F. Bradke (2010). Axon Extension Occurs Independently of Centrosomal Microtubule Nucleation. *Science* 327(5966): 704-707.
- Strasser, G. A., N. A. Rahim, K. E. VanderWaal, F. B. Gertler and L. M. Lanier (2004). Arp2/3 Is a Negative Regulator of Growth Cone Translocation. *Neuron* 43(1): 81-94.

References

- Straube, A. and A. Merdes (2007). EB3 Regulates Microtubule Dynamics at the Cell Cortex and Is Required for Myoblast Elongation and Fusion. *Current Biology* 17(15): 1318-1325.
- Swiech, L., M. Blazejczyk, M. Urbanska, P. Pietruszka, B. R. Dortland, A. R. Malik, P. S. Wulf, C. C. Hoogenraad and J. Jaworski (2011). CLIP-170 and IQGAP1 Cooperatively Regulate Dendrite Morphology. *The Journal of Neuroscience* 31(12): 4555-4568.
- Tapia, M., F. Wandosell and J. J. Garrido (2010). Impaired Function of HDAC6 Slows Down Axonal Growth and Interferes with Axon Initial Segment Development. *PLOS ONE* 5(9): e12908.
- Trivedi, N., D. R. Stabley, B. Cain, D. Howell, C. Laumonnerie, J. S. Ramahi, J. Temirov, R. A. Kerekes, P. R. Gordon-Weeks and D. J. Solecki (2017). Drebrin-mediated microtubule–actomyosin coupling steers cerebellar granule neuron nucleokinesis and migration pathway selection. *Nature Communications* 8: 14484.
- Tsvetkov, A. S., A. Samsonov, A. Akhmanova, N. Galjart and S. V. Popov (2007). Microtubule-binding proteins CLASP1 and CLASP2 interact with actin filaments. *Cell Motility and the Cytoskeleton* 64(7): 519-530.
- Vale, R. D. (2003). The Molecular Motor Toolbox for Intracellular Transport. *Cell* 112(4): 467-480.
- Van Goor, D., C. Hyland, A. W. Schaefer and P. Forscher (2012). The Role of Actin Turnover in Retrograde Actin Network Flow in Neuronal Growth Cones. *PLOS ONE* 7(2): e30959.
- Votin, V., W. J. Nelson and A. I. M. Barth (2005). Neurite outgrowth involves adenomatous polyposis coli protein and β -catenin. *Journal of Cell Science* 118(24): 5699-5708.
- Watabe-Uchida, M., K. A. John, J. A. Janas, S. E. Newey and L. Van Aelst (2006). The Rac Activator DOCK7 Regulates Neuronal Polarity through Local Phosphorylation of Stathmin/Op18. *Neuron* 51(6): 727-739.
- Waterman-Storer, C. M., R. A. WorthyLake, B. P. Liu, K. Burrige and E. D. Salmon (1999). Microtubule growth activates Rac1 to promote lamellipodial protrusion in fibroblasts. *Nat Cell Biol* 1(1): 45-50.
- Willmes, C. G., T. G. A. Mack, J. Ledderose, D. Schmitz, C. Wozny and B. J. Eickholt (2017). Investigation of hippocampal synaptic transmission and plasticity in mice deficient in the actin-binding protein Drebrin. *Scientific Reports* 7: 42652.
- Witte, H., D. Neukirchen and F. Bradke (2008). Microtubule stabilization specifies initial neuronal polarization. *The Journal of Cell Biology* 180(3): 619-632.
- Witte, H., D. Neukirchen and F. Bradke (2008). Microtubule stabilization specifies initial neuronal polarization. *J Cell Biol* 180(3): 619-632.

- Woodruff, J. B., O. Wueseke and A. A. Hyman (2014). Pericentriolar material structure and dynamics. *Philosophical Transactions of the Royal Society B: Biological Sciences* 369(1650).
- Worth, D. C., C. N. Daly, S. Geraldo, F. Oozeer and P. R. Gordon-Weeks (2013). Drebrin contains a cryptic F-actin–bundling activity regulated by Cdk5 phosphorylation. *The Journal of Cell Biology* 202(5): 793-806.
- Wu, X., A. Kodama and E. Fuchs (2008). ACF7 Regulates Cytoskeletal-Focal Adhesion Dynamics and Migration and Has ATPase Activity. *Cell* 135(1): 137-148.
- Xu, K., H. P. Babcock and X. Zhuang (2012). Dual-objective STORM reveals three-dimensional filament organization in the actin cytoskeleton. *Nat Meth* 9(2): 185-188.
- Yamada, K. M., B. S. Spooner and N. K. Wessells (1970). AXON GROWTH: ROLES OF MICROFILAMENTS AND MICROTUBULES. *Proceedings of the National Academy of Sciences* 66(4): 1206-1212.
- Zakhireh, B. and H. L. Malech (1980). The effect of colchicine and vinblastine on the chemotactic response of human monocytes. *The Journal of Immunology* 125(5): 2143-2153.
- Zheng, Y., M. L. Wong, B. Alberts and T. Mitchison (1995). Nucleation of microtubule assembly by a [γ]-tubulin-containing ring complex. *Nature* 378(6557): 578-583.
- Zhou, F.-Q., J. Zhou, S. Dedhar, Y.-H. Wu and W. D. Snider (2004). NGF-Induced Axon Growth Is Mediated by Localized Inactivation of GSK-3 β and Functions of the Microtubule Plus End Binding Protein APC. *Neuron* 42(6): 897-912.
- Zmuda, J. F. and R. J. Rivas (1998). The Golgi apparatus and the centrosome are localized to the sites of newly emerging axons in cerebellar granule neurons in vitro. *Cell Motility and the Cytoskeleton* 41(1): 18-38.
- Zolessi, F. R., L. Poggi, C. J. Wilkinson, C.-B. Chien and W. A. Harris (2006). Polarization and orientation of retinal ganglion cells in vivo. *Neural Development* 1(1): 2.
- Zou, Y. and A. I. Lyuksyutova (2007). Morphogens as conserved axon guidance cues. *Current Opinion in Neurobiology* 17(1): 22-28.

References

9. Appendix

9.1 Abbreviation List

+TIPs	plus-end tracking protein
ADFH	actin-depolymerizing factor homology
ADP	adenosine diphosphate
AIS	axon initial segment
APC	adenomatous polyposis coli
aPKC	atypical protein kinase C
Arp2/3	actin-Related Protein 2 and 3
ATP	adenosine triphosphate
BIM1	binding to microtubules1
C domain	central domain
CAMs	cell adhesion molecules
CC domain	coiled-coil domain
Cdc42	cell division cycle 42
Cdk5	cyclin-dependent kinases 5
Cep120	centrosomal protein of 120kDa
CGC	cerebellar granule cell
CLASPs	CLIP-associated proteins ()
CLIP-170	cytoplasmic linker protein 170
CP	cortical plate
CRMP-2	collapsin response mediator protein-2
Dcx	Doublecortin
Dock7	dedicator of cytokinesis 7
EB	microtubule end binding protein
ECM	extracellular matrix
EGL	external granular layer

Appendix

Ena/VASP	Enabled/ vasodilator-stimulated phosphoprotein
FA	focal adhesions
F-actin	filamentous actin
G-actin	globular actin
GDP	guanosine diphosphate
GSK-3 β	glycogen synthase kinase 3 β
GTP	guanosine triphosphate
HDAC6	histone deacetylase 6
ILM	inner limiting membrane
IPL	inner plexiform layer
IQGAP1	Ras GTPase-activating-like protein
IZ	intermediate zone
KIF	kinesin superfamily
LIS1	lissencephaly-associated protein 1
MACF	microtubule–actin cross-linking factor
MAP	microtubule binding protein
mDia1	mouse diaphanous homolog 1
ML	molecular layer
MP	multipolar
MT	microtubule
MTOC	microtubule organizing center
NGF	nerve growth factor
OLM	outer limiting membrane
P domain	peripheral domain
p140Cap/SNIP	p130cas-associated protein, p140Cap/ SNAP25-interacting protein
Par3	partition defective 3
PC	cortical pyramidal cell
PCM	pericentriolar matrix
PI3K	phosphatidylinositol 3-kinase

PP	proline-rich region
PTM	post-translational modification
RBC	Retinal bipolar cells
RGC	radial glial cell
RGC	Retinal ganglion cells
ROCK	Rho-associated protein kinase
Smurf1	Smad Ubiquitin Regulatory Factor 1
T zone	transitional zone
TTL	tubulin tyrosine ligase
VZ	ventricular zone
WASp/Scar	Wiskott-Aldrich syndrome protein
γ TuRC	γ -tubulin ring complex
γ TuSC	γ -tubulin small complex

9.2 List of hazardous substances

Substance	GHS symbol	Hazard statements	Precautionary statements
Boric acid		H303, H360	P201, P202, P280, P312, P405, P501
Dimethyl sulfoxide (DMSO)	none	H227	none
Ethanol		H225, H319	P210, P233, P240, P241, P242, P243, P264, P280, P303 + P361 + P353, P305 + P351 + P338, P337 + P313, P370 + P378, P403 + P235, P501
HEPES	none	none	none
Nitric Acid		H272, H290, H314	P210, P220, P234, P264, P280, P301 + P330 + P331, P303 + P361 + P353, P304 + P340 + P310, P305 + P351 + P338 + P310, P363, P370 + P378, P390, P405, P501
Nocodazole		H341, H361d	P281
Papain		H303, H315, H319, H334, H335	P261, P305 + P351 + P338, P342 + P311
Paraformaldehyde (PFA)		H228, H302 + H332, H315, H317, H318, H335, H351, H402	P210, P261, P280, P305 + P351 + P338
Sodium pyruvate	none	none	none
Taxol (Paclitaxel)		H303, H315, H317, H318, H334, H335, H341, H361, H370	P260, P280, P305 + P351 + P338, P307 + P311
Triton X-100		H302, H313, H315, H318, H401, H410	P264, P270, P273, P280, P301 + P312 + P330, P302 + P352, P305 + P351 + P338 + P310, P312, P332 + P313, P391, P501

9.3 List of publications

Zhao, B.* , D. P. Meka* , R. Scharrenberg, T. König, B. Schwanke, O. Kobler, S. Windhorst, M. R. Kreutz, M. Mikhaylova and F. Calderon de Anda (2017). Microtubules Modulate F-actin Dynamics during Neuronal Polarization. *Scientific Reports* 7(1): 9583.

Xiaogang Du* , Bing Zhao* , Jinyao Li, Xiaohan Cao, Mingkun Diao, Haibo Feng, Xiaobing Chen, Zhiyu Chen, Xianyin Zeng. Astragalus polysaccharides enhance immune responses of HBV DNA vaccination via promoting the dendritic cell maturation and suppressing Treg frequency in mice. *Int Immunopharmacol.*, DOI: <http://dx.doi.org/10.1016/j.intimp.2012.09.006>

Xiaogang Du* , Xiaobing Chen* , Bing Zhao* , Yao Lv, Huaiyu Zhang, Hanmei Liu, Zhiyu Chen, Yanger Chen, Xianyin Zeng. Astragalus polysaccharides enhance the humoral and cellular immune responses of hepatitis B surface antigen vaccination through inhibiting the expression of transforming growth factor β and the frequency of regulatory T cells. *FEMS Immunology & Medical Microbiology* Nov 2011, 63 (2) 228-235; DOI: 10.1111/j.1574-695X.2011.00845.x

* Shared authorship

Acknowledgement

“The road is long, with many winding turns...”, totally no idea why this lyrics line is haunting in my mind while I am facing this section. Yes, it is a long road, which is still extending ahead. Right now while I am taking the last step of the current phase of my life, I look back and retrieve all the fragments of memory related to this period. How could I be not grateful after realizing it is not a lonely journey thanks to all the companions along my side?

My supervisor Froy (Dr. Calderon de Anda), thank you for showing me how an enthusiastic scientist should be like, how to conceive an idea and tackle a question, how to “observe but not only see”, how to “work smart”. Thank you for tolerating my occasional naivety, stupidity and mistakes. Also thank you for giving me stress and anxiety, which makes me stronger.

My first supervisor Wolfram (Prof. Brune), in whose lab I spent the first two years, during which I got training and the initial sense about science. Thank you for opening me the door to a totally different world, also for giving me the challenge to allow me to know myself and to make me grow.

Praveen, the closest work partner, who is smart and diligent, thank you for having been through so many difficulties with me during the time of this project and also for sharing me your experience in doing science. Birgit, our excellent technician, who can always keep the preps in the safe side, thank you for teaching me the experimental methods and sharing the work load. Robin, who is “einfach genial”, thank you for tackling so many hard questions with your talent. Also to Melanie, who is always generous to offer help and contribute opinions; to Anne, with whom I had so much time of fun inside and outside of the lab; to Ole, who is truly friendly and always willing to share his language expertise. To the “happy hour” and all the beers I have tasted, which simply adds colors to my life.

Acknowledgement

Thanks to all my collaborators Marina Mikhaylova, Michael R. Kreutz, Oliver Kobler, Sabine Windhorst, Dennis Eggert, who unfolded the question from other dimensions and added more interpretations to the answer.

Thanks to Prof. Kneussel, Prof. Bradke and Prof. Gordon-Weeks, who are generous to share their equipments and reagents, allowing the smooth run of my project.

Also thanks to all my former lab members Jiajia, Patricia, Leila, Doris, Antonio, Eva, Tim, Eleonore, Julia, Sebastian, Wiebke, Florian, Rebeca, Martina, Gabi and Christina, who are so kind and offered me help from all aspects.

To people of Peter's and Kent's lab, who are always willing to share opinions in the joint meeting, to help make this project better.

And to all the friends in the Chinese community: Xiaoyan, Shuting, Chun, Meilan, Denan, Shaobo, Lingzhen, Xiaosong, Jiajia, Rong, Xiaxia, Lin, Xuejun, Shanting, Yangwei, Wenchao, Maiwulanjiang and Jiawei, who are holding up the community firmly. Together with them I had so much unforgettable time.

At last deep gratitude to my fiancée Bin, who supports me heart and soul all the time. You are the motivation for me to strive for our future. To my parents and sisters, who always stand behind me and give me unconditional support whenever I need.

Declaration on oath

Hiermit versichere ich an Eides statt, die vorliegende Dissertation selbst verfasst und keine anderen als die angegebenen Hilfsmittel benutzt zu haben. Die eingereichte schriftliche Fassung entspricht der auf dem elektronischen Speichermedium. Ich versichere, dass diese Dissertation nicht in einem früheren Promotionsverfahren eingereicht wurde.

Date:

Signature: